# Southeastern Geology: Volume 29, No. 1 September 1988

Edited by: S. Duncan Heron, Jr.

**Abstract**

Academic journal published quarterly by the Department of Geology, Duke University.

# SOUTHEASTERN GEOLOGY

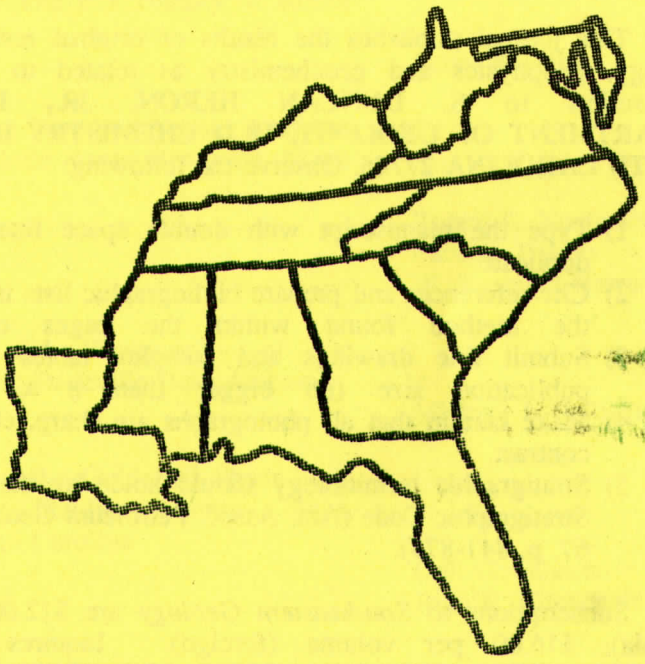

LISHED AT DUKE UNIVERSITY DURHAM, NORTH CAROLINA

OL. 29, NO. 1 SEPTEMBER 1988

# SOUTHEASTERN GEOLOGY

PUBLISHED QUARTERLY

AT

DUKE UNIVERSITY

Editor in Chief:
S. Duncan Heron, Jr.

Managing Editor:
James W. Clarke


This journal publishes the results of original research on all phases o geology, geophysics and geochemistry as related to the Southeast. Sen manuscripts to **S. DUNCAN HERON, JR., DUKE UNIVERSITY DEPARTMENT OF GEOLOGY, OLD CHEMISTRY BUILDING, DURHAM NORTH CAROLINA 27706**. Observe the following:

1) Type the manuscript with double space lines and submit in duplicate.
2) Cite references and prepare bibliographic lists in accordance with the method found within the pages of this journal.
3) Submit line drawings and complex tables reduced to final publication size (no bigger than 8 x 5 1/8 inches).
4) Make certain that all photographs are sharp, clear, and of good contrast.
5) Stratigraphic terminology should abide by the North American Stratigraphic Code (Am. Assoc. Petroleum Geologists Bulletin, v. 67, p. 841-875).

Subscriptions to *Southeastern Geology* are $12.00 per volume (US an Canada), $16.00 per volume (foreign). Inquires should be sent to **SOUTHEASTERN GEOLOGY, DUKE UNIVERSITY, DEPARTMENT O GEOLOGY, OLD CHEMISTRY BUILDING, DURHAM, NORTH CAROLIN 27706**. Make checks payable to: *Southeastern Geology*.

# SOUTHEASTERN GEOLOGY

**Table of Contents**

Vol. 29, No. 1

September, 1988

# MINERAL CHEMICAL VARIATIONS IN THE LAKE CHATUGE MAFIC-ULTRABASIC COMPLEX NORTH CAROLINA-GEORGIA: THE P-T HISTORY OF ROCKS IN THE BLUE RIDGE

JAMES K. MEEN

*Department of Geology*
*University of North Carolina*
*Chapel Hill, NC 27514*

## ABSTRACT

A metamorphosed mafic-ultrabasic complex occurs in the Blue Ridge province on the North Carolina-Georgia state line at Lake Chatuge. This complex may be exposed at the margins of a window through the Hayesville thrust fault. Mineral chemical variations indicate that the complex owes its origin to nepheline-normative picritic magma ponding at 35-40 km depth, plausibly at the continental Moho. The magma crystallized voluminous olivine to form dunites. Most residual magma apparently left the chamber, possibly to be erupted as alkali basalt, but some crystallized the olivine, plagioclase, and clinopyroxene of troctolites and olivine gabbros. The last liquids crystallized as an alkali gabbro.

During cooling, plagioclase and olivine reacted to form two pyroxenes and spinel. High temperature reactions produced granular crystals that rim relict igneous minerals. Secondary minerals formed at low temperatures were fine-grained symplectites. Clinopyroxene exsolved orthopyroxene; two pyroxene thermometry indicates T<~ 650° C, demonstrating that these minerals remained in equilibrium to relatively low temperatures. Minerals in the alkali gabbros reacted to produce garnet granulites. The cores of minerals in granulites record a PT of 840° C, 11 kbar whereas their rims indicate ~ 650° C, 7 kbar. Hydrous fluids rendered rocks near the margins of the complex amphibolites. The presence of significant amphibole along grain boundaries and coronas in all other parts of the complex indicate that the fluids penetrated all parts of the complex. A later greenschist facies event affected these rocks.

The protoliths of the amphibolites included both ultramafic and mafic rocks and the zoning of the complex with amphibolites on the outside of the body does not indicate that the complex originally demonstrated some zonation. Rather, the distribution of rock types within the protoliths of the complex was irregular, suggesting that the complex was emplaced tectonically rather than having crystallized in situ. Emplacement was contemporary with or preceded Taconic activity as amphibolites and country rocks have parallel Taconic foliations.

## INTRODUCTION

The southern Appalachian Mountains consist of northeast trending belts, apparently emplaced on the continent by Paleozoic thrusting (Cook and others, 1979). These belts are complex mosaics of blocks that plausibly had separate histories prior to amalgamation. Elucidation of pressure-temperature histories of these individual blocks is critical to understanding the evolution of the orogen.

This paper investigates the PT information provided by the mineral chemistry of a metabasic body in the Blue Ridge geologic province (BRG).

The BRG consists of a series of thrust sheets emplaced in at least two major episodes (Hatcher, 1978; Hatcher and Butler, 1979). The most easterly sheets in southern North Carolina lie east of the Hayesville fault (Figure 1). Activity on the Hayesville Fault predated Taconic metamorphism and the fault itself is complexly deformed. The Hayesville fault may be a suture zone as it separates terranes with distinct histories (Hatcher, 1978; Hatcher and Butler, 1979).

The thermal maximum of Taconic and Acadian metamorphism, in which rocks are at upper amphibolite to lower granulite facies (Absher and McSween, 1985), is east of the Hayesville fault. Metamorphic grade decreases westward to lower greenschist facies (Hadley and Nelson, 1971; Rankin and others, 1972; Hatcher and Butler, 1979). Retrograde metamorphism is widespread, particularly along zones of late Paleozoic motion. Minor bodies of mafic and ultrabasic igneous rocks that experienced variable metamorphism occur east of the Hayesville fault. Hatcher and others (1987) inferred that the metaigneous complexes occur at the base of the thrust sheet. Hatcher (1978) and Eggers (1983) suggest an ophiolitic origin for some bodies. One metamorphosed mafic-ultrabasic occurs at Lake Chatuge on the North Carolina-Georgia state line. This paper presents the results of a mineral chemical study of this body and uses the results to suggest the nature of the magma that crystallized to this body and the PT history of these rocks. Specifically, I reject an ophiolitic origin for the Lake Chatuge mafic-ultrabasic complex (LCC), preferring a model in which the protoliths crystallized at the base of the continental crust.

## GEOLOGICAL SETTING

The BRG in North Carolina and Georgia is a complexly deformed anticlinorum, bounded on the southeast by the Brevard Zone. The entire province was apparently thrust northwestward over younger sedimentary rocks in the Valley and Ridge province. Interpretations of seismic sections suggest that the BRG is a 6-15 km thick stack of thrust sheets with a basal decollement that extends to the east (Harris and Boyer, 1979; Cook and others, 1979; Boyer and Elliott, 1982).

The oldest rocks in the BRG are amphibolite to granulite facies gneisses and plutonic rocks, metamorphosed during the Grenville orogeny. Some rocks are at least 1.8 b.y. old (Rodgers, 1970; Hatcher and Butler, 1979; Monrad and Gulley 1983). The Toxaway Gneiss (Hatcher, 1977), exposed east of Lake Chatuge, has a whole rock Rb-Sr age of 1200 m.y. (Fullagar and others, 1979). Toxaway and correlative rocks are overlain by the Tallulah Falls Formation (Hatcher and Butler 1979) of metagraywacke, pelitic schists, and mafic volcanic rocks, and by gneisses schists, and quartzites of the Coweeta Group. Supracrustal rocks northwest of the

**Figure 1. Geological map of Lake Chatuge mafic-ultrabasic complex and surrounding areas, largely after Hartley (1973). Numbered arrows indicate the localities from which samples were collected. Small inset shows location of the LCC and other mafic-ultrabasic complexes in the Blue Ridge of North Carolina and Georgia. Large inset shows the disposition of various faults in the Blue Ridge (after Hatcher, 1978).**

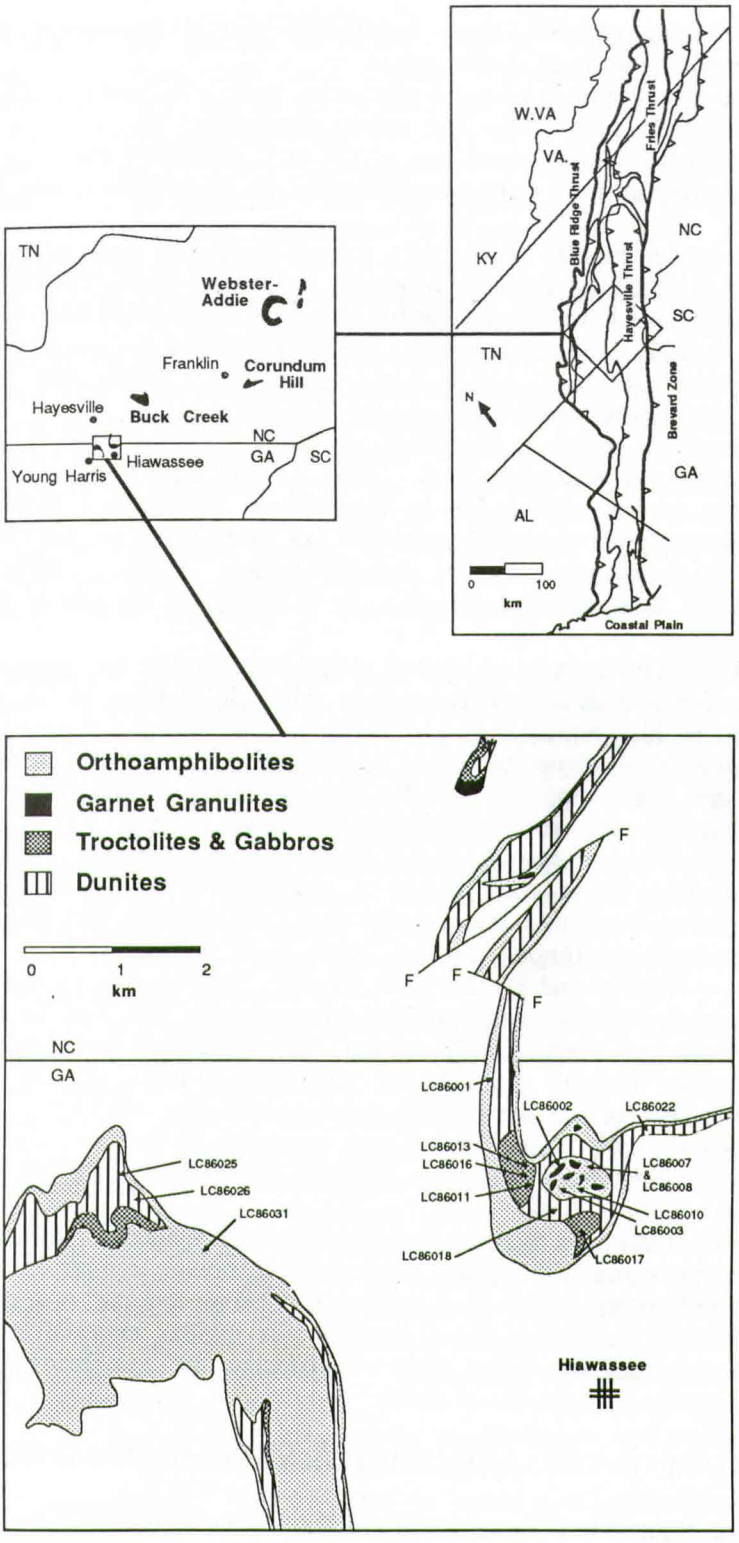
TN
Webster-
Addie
Franklin
Corundum
Hill
Hayesville
Buck Creek
NC
Young Harris
Hiawassee
GA
SC
W.VA
VA.
KY
TN
NC
SC
GA
AL
Blue Ridge Thrust
Fries Thrust
Hayesville Thrust
Brevard Zone
N
0
100
km
Coastal Plain
Orthoamphibolites
Garnet Granulites
Troctolites & Gabbros
Dunites
0
1
2
km
NC
GA
F
F
F
F
LC86001
LC86002
LC86022
LC86013
LC86016
LC86011
LC86007
&
LC86008
LC86010
LC86003
LC86018
LC86017
LC86025
LC86026
LC86031
Hiawassee

Hayesville fault are the Ocoee Supergroup that is dominantly composed of metasedimentary rocks of clastic origin.

The Bakersville metabasic intrusions form a coherent northeast-trending suite that cut the older rocks and is best represented west of Asheville. These rocks yield a Rb-Sr whole rock age of 734 m.y. (Goldberg and others, 1986) and were apparently intruded during inception of Late Proterozoic rifting of the Iapetus Ocean.

Numerous granite bodies with a great variety of sizes occur in the BRG southwest of Asheville and were originally mapped by Keith (1907b) as Whiteside granite. The suite is very heterogeneous and was divided into five units by Hadley and Nelson (1971). Miller and Kish (1980) showed that the granitoids belong to a regional suite of low-K peraluminous granitoids. Miller and others (1983) suggested that these rocks were intruded 390-460 m.y. ago.

Ultrabasic bodies in the BRG are traditionally included in a chain from Newfoundland to Alabama (Hess, 1955). Misra and Keller (1978) reviewed occurrences of ultrabasic bodies in the southern Appalachian Mountains, noting they are strongly concentrated in the BRG of North Carolina and Georgia, where Hunter (1941) documented more than 275 bodies. Figure 1 shows some larger bodies in this area. Most ultrabasic rocks in this region are east of the Hayesville fault.

All ultrabasic rocks are altered. Most small bodies are completely replaced by serpentine and other low-temperature minerals. Larger bodies contain areas dominated by high-temperature assemblages. Dunite is the commonest rock type in lesser altered ultrabasic bodies. Carpenter and Phyfer (1975) showed that some dunites are dominated by olivine that is $Fo_{92}$. Harzburgite, lherzolite, orthopyroxenite, amphibole peridotite, troctolite, gabbro, and anorthosite also occur; websterite occurs only in the Webster-Addie complex. Some ultramafic complexes have thick outer zones of amphibolites suggested to be hydrated equivalents of associated mafic rocks (e.g., the Chunky Gal amphibolite/Buck Creek peridotite — Hadley, 1949). Some mafic complexes (e.g., Kimsey Bald complex — Hatcher and Butler, 1979; Eggers, 1983) contain no ultrabasic rocks.

The nature of contact relations of complexes and host rocks is unclear. Some authors (e.g., Hartley, 1973, on the LCC) argued that complexes are intrusive whereas other authors (e.g., Kuntz and Hedge, 1981, on the Chunky Gal amphibolite) suggested that bodies were tectonically emplaced. Macroscopic compositional bands in the Buck Creek peridotite (Sailor and Kuntz, 1973) are discordant to foliation in wall rocks, although concordant to it in the LCC (Hartley, 1973).

Current versions of maps of the site of the Appalachian ultradeep core hole (Hatcher and others, 1987) place some mafic-ultrabasic complexes at the base of the Hayesville thrust sheet. Such bodies do not represent part of a pervasive layer at the base of the thrust sheet, however, as similar material is not exposed continuously along the thrust fault. Apparently, the complexes form localized bodies at the base of the thrust sheet.

## GEOLOGY OF THE LAKE CHATUGE MAFIC-ULTRAMAFIC COMPLEX

The Nantahala Folio of Keith (1907a) shows ultrabasic rocks and amphibo-

lites within schists and gneisses in North Carolina. Kellberg (1943, 1947) described ultrabasic rocks near Lake Chatuge. Hartley (1973) undertook a detailed study of the LCC and its host rocks. Jones and others (1973) reported $^{87}Sr/^{86}Sr$ for 15 samples from the LCC (14 whole rocks and an olivine separate) and 4 samples of country rock. Dallmeyer (1974) presented whole rock and mineral chemistry of garnetiferous rocks from the LCC. Shaw and Wasserburg (1984) gave the Sr-Nd isotopic composition of an orthoamphibolite.

The petrography of the LCC is well described by Hartley (1973). Dunite in the center of LCC is partially serpentinized; much is intensely altered. Olivine grains, 0.5-4 mm across, are fractured and veined with alteration products — dominantly antigorite (determined by X-ray diffraction) and magnetite. A few 2-5 mm chromite grains occur in dunites. Troctolites contain olivine grains, 1-5 mm across and less altered than in dunites, and twinned 2-10 mm plagioclase grains. Some troctolites are compositionally banded. Alternating layers, 3-20 mm thick, are composed of either plagioclase or olivine. Magnesian clinopyroxenes[1], present in small amounts in troctolites, are round, 0.5-3 mm across, and twinned. Most contain sub-micron exsolution lamellae of orthopyroxene. Olivine gabbros are gradational into troctolites; gabbros differ only in containing more than 10% primary clinopyroxene according to the nomenclature scheme of Streckeisen (1976).

The ultramafic portions of LCC have the assemblage olivine-plagioclase-clinopyroxene. This assemblage is not stable under hydrous conditions at temperatures below ~900° C (Spear, 1981) and was not affected by the hydrous metamorphism reflected by mineral assemblages in the enclosing metapelitic rocks. These assemblages are considered to be preserved from the magmatic protoliths and were not produced by metamorphism. This is supported by the observation of alternating layers of olivine and plagioclase in the LCC. Although the assemblages are relict, the minerals apparently changed compositions (by exsolution or exchange) during cooling to maintain thermodynamic equilibrium. These grains are relict despite textural and chemical modification, however, having formed in a magmatic environment.

Relict grains in troctolites and gabbros have coronas of secondary minerals. Olivine crystals are surrounded by 50-500 μm granular orthopyroxene and clinopyroxene grains. Clinopyroxene crystals are rimmed by 50-350 μm orthopyroxene grains. Most of the boundaries of the anhydrous minerals are occupied by stringers of bluish green amphibole. Broad (200 μm-2 mm) zones separating plagioclase and olivine grains are composed of intergrowths of amphibole and green spinel. Amphibole grains between clinopyroxene and plagioclase grains are <50 μm and contain no spinel. Bands of olivine and plagioclase in troctolites are separated by coronitic zones similar to those in unlayered rocks. Grains of the same mineral in the layers (either olivine or plagioclase) are not separated by secondary minerals and interfacial angles between these grains are typically ~120°. Subsolidus recrystallization apparently obliterated any original magmatic fabric.

Primary and secondary clinopyroxenes are similar in composition and are

---

[1]The term "clinopyroxene" will be used to refer to Ca-rich clinopyroxenes throughout.

distinguished on the basis of size and textural relations. Secondary clinopyroxenes occur in coronas and few are larger than 500 μm. Some primary clinopyroxenes are very large (Hartley, 1973, described crystals 5 cm long; grains 2-10 mm are more common) and possess partial rims of smaller orthopyroxene grains.

Orthoamphibolite constitutes the outer sheath of the LCC. The resistant amphibolite forms high areas around the lake and outcrops are common. Few contacts between amphibolite and wall rocks are exposed. Rocks a few centimeters from the presumed contact, however, appear identical to those meters from the contact. Foliation of amphibolites, where present, parallels that in country rocks. Amphibolites are dominated by bytownite to andesine plagioclase and pargasitic amphibole that vary considerably in modal amounts and chemical compositions. Some are more than 90% plagioclase; others more than 90% amphibole. Clinozoisite replacing amphibole is ubiquitous. Quartz, rutile, pyrrhotite, ilmenite, and sphene are accessory minerals.

Lenses of garnet granulite in LCC (Figure 1) form hills because of their greater resistance to erosion. They contain garnet, clinopyroxene, plagioclase, rutile, apatite, and quartz with secondary amphibole, sphene, clinozoisite, and

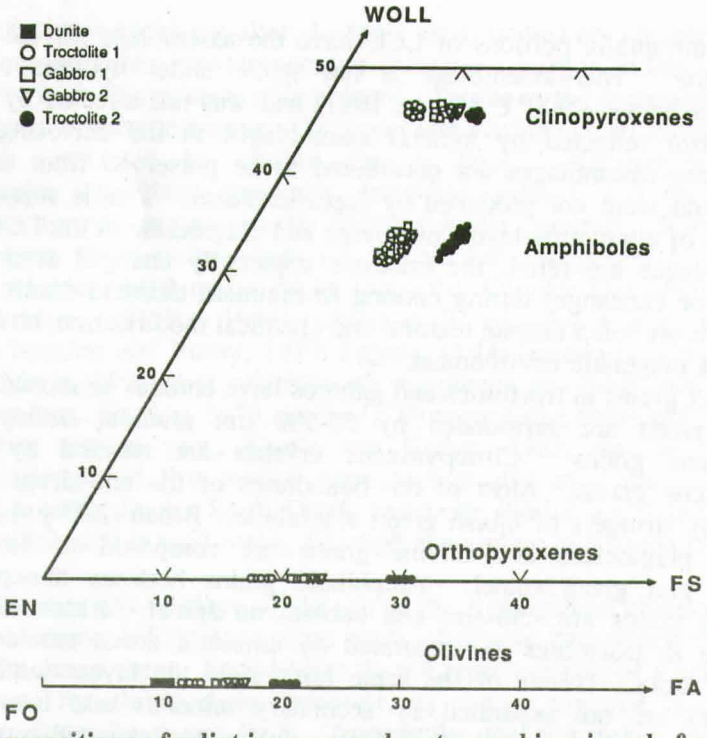


**Figure 2. Compositions of relict igneous and metamorphic minerals from ultrabasic rocks in the LCC. Rocks as defined in Table 1. Compositions of olivine shown in terms of forsterite (FO) and fayalite (FA) components; those of pyroxenes in terms of wollastonite (WOLL), enstatite (EN), and ferrosilite (FS) components. Amphibole compositions are expressed in terms of Ca-, Mg-, and Fe-endmembers on the pyroxene quadrilateral.**

ilmenite. Garnet and lamellae-free clinopyroxene form 2-10 mm grains separated by 50 μm-2 mm trains of secondary amphibole. Small crystals of quartz, plagioclase, rutile, and clinopyroxene occur in garnet grains. Unprotected rutile grains are partially replaced by sphene intergrown with amphibole. This assemblage is, itself, locally replaced by clinozoisite and ilmenite.

Outcrops of garnet granulite are rare. The hills noted above are strewn with 1-5 m boulders with garnet-rich cores that grade outward into amphibolite. Garnet-rich zones are discoidal and have long axes of 0.5-2 m. Garnetiferous cores pass into narrow (5-20 cm) garnet-free zones of clinopyroxene and plagioclase that are partly replaced by amphibole. Relict clinopyroxenes in these zones and some in the granulites are strongly deformed, having complexly folded cleavages. Foliation in amphibolites that surround granulites wraps around discoidal granulites in all three dimensions but fades through transition zones. Granulites are unfoliated and garnets show no deformation fabric.

The dominant host rock of the LCC is garnet biotite gneiss, composed of quartz, plagioclase, garnet, and two micas. Poikiloblastic garnets have been rotated. Hartley (1973) described kyanite- and sillimanite-bearing variants. Garnet mica schists occur in probable windows through the Hayesville thrust sheet (Hatcher and others, 1987).

## ANALYTICAL TECHNIQUES

Thin-sections were examined petrographically and analyzed by the MAC-5 electron microprobe at UNC-Chapel Hill using a wavelength-dispersive system and natural minerals as standards. A 15 kV accelerating potential, 20 namp specimen current, and ~2 μm beam size were employed. All data were analyzed by on-line computer using reduction factors of Albee and Ray (1970).

## ANALYTICAL RESULTS

Averages and ranges of compositions of minerals of the LCC are given in Tables 1 and 2. Relict igneous minerals in dunites, troctolites, and gabbros are homogeneous in a single outcrop although there is marked variation across LCC. Four different samples of dunite contain olivine close to $Fo_{91}$ (Figure 2) and with ~3000 ppm Ni. Olivine in gabbros and troctolites, however, has lower contents of magnesium (Figure 2) and nickel, although correlation of compositional parameters and location in the complex is poor.

Plagioclase is homogeneous on the outcrop scale (excluding rims adjacent to amphiboles) but varies across the complex from $An_{82}$ to $An_{73}$ (Table 1). Decrease of anorthite content of plagioclase accompanies a decrease in forsterite content of coexisting olivine. Plagioclase and olivine in banded troctolites demonstrate little variation in composition in a single outcrop.

Clinopyroxenes are unzoned and homogeneous on the outcrop scale. Their variation in Mg# (atomic $100*Mg/[Mg+Fe^{2+}]$) parallels that in coexisting olivine (Figure 2). Pyroxenes contain 45-48% wollastonite in terms of pyroxene quadrilateral components (Figure 2). Other components are minor — in addition to minor Cr-diopside, aegirine, and Ti-bearing endmembers, Ca-tschermak's molecule is 4-6% of the formula unit. Unzoned clinopyroxenes rimming larger

## Table 1. Averages and ranges of compositions of relic igneous minerals in Lake Chatuge Complex

| | Dunite[1] | Troctolite 1[2] | | | Gabbro 1[3] | | | Gabbro 2[4] | | | Troctolite 2[5] | | |
|---|---|---|---|---|---|---|---|---|---|---|---|---|---|
| | Ol[6] | Ol | Pl[6] | Cpx[6] | Ol | Pl | Cpx | Ol | Pl | Cpx | Ol | Pl | Cpx |
| n[7] | 26 | 20 | 18 | 17 | 18 | 25 | 20 | 22 | 28 | 25 | 19 | 27 | 21 |
| $SiO_2$ | 40.9 ±0.8 | 40.3 ±0.7 | 47.6 ±0.9 | 52.5 ±1.2 | 39.8 ±0.8 | 48.0 ±1.2 | 51.5 ±0.9 | 39.6 ±0.8 | 48.8 ±0.9 | 51.3 ±1.3 | 38.8 ±0.9 | 49.4 ±1.0 | 51.1 ±0.8 |
| $TiO_2$ | n.d. | 0.02±0.02 | 0.04±0.02 | 0.48±0.08 | 0.02±0.02 | 0.03±0.02 | 0.63±0.06 | n.d. | 0.02±0.02 | 0.67±0.08 | n.d. | n.d. | 0.84±0.06 |
| $Al_2O_3$ | n.d. | n.d. | 33.4 ±0.8 | 3.94±0.17 | n.d. | 33.2 ±1.0 | 4.55±0.22 | n.d. | 32.8 ±0.8 | 4.97±0.19 | n.d. | 32.7 ±0.7 | 5.08±0.23 |
| $Cr_2O_3$ | n.d. | n.d. | n.d. | 0.54±0.05 | n.d. | n.d. | 0.35±0.04 | n.d. | n.d. | 0.14±0.04 | n.d. | n.d. | 0.08±0.04 |
| FeO | 8.82±0.22 | 11.5 ±0.6 | 0.08±0.03 | 4.64±0.12 | 15.1 ±0.7 | 0.03±0.03 | 6.28±0.17 | 16.2 ±0.6 | 0.04±0.03 | 6.88±0.21 | 18.4 ±0.3 | 0.06±0.04 | 7.88±0.19 |
| MnO | 0.15±0.05 | 0.19±0.07 | n.d. | 0.20±0.06 | 0.14±0.05 | n.d. | 0.29±0.08 | 0.19±0.05 | n.d. | 0.32±0.09 | 0.18±0.06 | n.d. | 0.42±0.07 |
| MgO | 49.9 ±0.7 | 47.6 ±0.8 | 0.02±0.02 | 15.4 ±0.3 | 44.7 ±0.9 | 0.01±0.02 | 14.0 ±0.4 | 44.0 ±0.9 | 0.02±0.02 | 13.5 ±0.3 | 41.7 ±0.4 | n.d. | 12.9 ±0.4 |
| NiO | 0.31±0.06 | 0.20±0.05 | n.d. | 0.03±0.02 | 0.17±0.04 | n.d. | n.d. | 0.14±0.04 | n.d. | n.d. | 0.12±0.03 | n.d. | n.d. |
| CaO | 0.10±0.04 | 0.08±0.04 | 16.6 ±0.4 | 23.1 ±0.6 | 0.04±0.03 | 16.1 ±0.3 | 22.9 ±0.7 | n.d. | 15.7 ±0.5 | 22.9 ±0.6 | n.d. | 15.3 ±0.3 | 22.4 ±0.7 |
| $Na_2O$ | n.d. | n.d. | 1.99±0.12 | 0.38±0.09 | n.d. | 2.32±0.16 | 0.52±0.12 | n.d. | 2.59±0.10 | 0.59±0.11 | n.d. | 2.71±0.15 | 0.76±0.14 |
| $K_2O$ | n.d. | n.d. | 0.04±0.02 | n.d. | n.d. | 0.04±0.02 | n.d. | n.d. | 0.05±0.02 | n.d. | n.d. | 0.05±0.02 | n.d. |
| Total | 100.2 | 99.9 | 99.8 | 101.2 | 100.0 | 99.7 | 101.0 | 100.1 | 100.2 | 101.3 | 99.2 | 100.2 | 101.5 |
| Si | 0.997 | 0.997 | 2.19 | 1.90 | 1.00 | 2.20 | 1.89 | 0.999 | 2.23 | 1.88 | 0.999 | 2.25 | 1.88 |
| Ti | -- | -- | 0.001 | 0.013 | -- | 0.001 | 0.017 | -- | 0.001 | 0.018 | -- | -- | 0.023 |
| Al | -- | -- | 1.81 | 0.168 | -- | 1.80 | 0.196 | -- | 1.77 | 0.215 | -- | 1.76 | 0.220 |
| Cr | -- | -- | -- | 0.015 | -- | -- | 0.010 | -- | -- | 0.004 | -- | -- | 0.002 |
| $Fe_{II}$ | 0.180 | 0.238 | 0.003 | 0.131 | 0.317 | 0.001 | 0.169 | 0.342 | 0.002 | 0.182 | 0.396 | 0.002 | 0.208 |
| $Fe_{III}$[8] | | | | 0.010 | | | 0.023 | | | 0.029 | | | 0.034 |
| Mn | 0.003 | 0.004 | -- | 0.006 | 0.003 | -- | 0.009 | 0.004 | -- | 0.010 | 0.004 | -- | 0.013 |
| Mg | 1.81 | 1.76 | 0.001 | 0.832 | 1.67 | 0.001 | 0.764 | 1.65 | 0.001 | 0.737 | 1.600 | -- | 0.706 |
| Ni | 0.006 | 0.004 | -- | 0.001 | 0.003 | -- | -- | 0.003 | -- | -- | 0.002 | -- | -- |
| Ca | 0.003 | 0.002 | 0.817 | 0.897 | 0.001 | 0.792 | 0.899 | -- | 0.773 | 0.899 | -- | 0.746 | 0.881 |
| Na | -- | -- | 0.177 | 0.027 | -- | 0.206 | 0.037 | -- | 0.233 | 0.042 | -- | 0.239 | 0.054 |
| K | -- | -- | 0.002 | -- | -- | 0.002 | -- | -- | 0.003 | -- | -- | 0.003 | -- |
| Total | 3.00 | 3.00 | 5.00 | 4.01 | 3.00 | 5.00 | 4.01 | 3.00 | 5.01 | 4.01 | 3.00 | 5.00 | 4.02 |

[1]Average from four separate dunites -- LC86-018, LC86-022, LC86-025, LC86-026. [2]Sample LC86-016. [3]Sample LC86-011. [4]Sample LC86-017. [5]Sample LC86-013. [6]Abbreviations used: Ol -- olivine; Pl -- plagioclase; Cpx -- Ca-rich clinopyroxene. [7]Number of data points used in calculating averages. [8]Amount of ferric iron calculated from stoichiometry for pyroxenes only. Cation structural formulae calculated assuming 4 oxygens for olivine, 8 for feldspar, 6 for pyroxene.

## Table 2. Averages and ranges of composition of metamorphic minerals in Lake Chatuge Complex

| | Troctolite 1[1] | | | Gabbro[2] | | | Troctolite 2[3] | | | | | | |
|---|---|---|---|---|---|---|---|---|---|---|---|---|---|
| | Opx[9] | Amp[9] | Spinel | Opx | Amp | Spinel | Opx | Amp | Spinel | Cpx[9]Core[10] | Cpx Rim[10] | Gt[9]Core[10] | Gt Rim[10] |
| n[14] | 13 | 22 | 15 | 15 | 17 | 12 | 15 | 19 | 13 | | | | |
| $SiO_2$ | 54.7 ±0.7 | 45.8 ±0.5 | 0.03±0.03 | 54.0 ±1.2 | 45.3 ±0.6 | 0.09±0.04 | 53.0 ±1.1 | 44.1 ±0.5 | 0.05±0.9 | 50.3 | 52.5 | 39.0 | 38.7 |
| $TiO_2$ | 0.05±0.02 | 0.04±0.04 | 0.09±0.04 | 0.04±0.03 | 0.02±0.02 | 0.08±0.05 | 0.04±0.03 | n.d. | 0.12±0.06 | 0.45 | 0.22 | 0.05 | 0.14 |
| $Al_2O_3$ | 3.77±0.16 | 17.6 ±1.0 | 65.0 ±0.5 | 4.12±0.17 | 17.6 ±1.2 | 64.9 ±0.7 | 4.67±0.20 | 17.7 ±1.4 | 64.4 ±0.9 | 6.34 | 3.86 | 22.2 | 22.5 |
| $Cr_2O_3$ | 0.04±0.02 | n.d. | n.d. | n.d. | n.d. | n.d. | n.d. | n.d. | n.d. | 0.10 | 0.10 | 0.03 | 0.03 |
| FeO | 11.1 ±0.6 | 6.17±0.34 | 17.6 ±0.3 | 12.9 ±0.8 | 6.31±0.41 | 18.3 ±0.4 | 17.1 ±0.6 | 8.98±0.5 | 20.9 ±0.06 | 6.96 | 5.56 | 20.4 | 23.2 |
| MnO | 0.32±0.06 | 0.10±0.03 | 0.13±0.04 | 0.40±0.06 | 0.14±0.05 | 0.18±0.07 | 0.53±0.09 | 0.30±0.04 | 0.22±0.03 | 0.15 | 0.10 | 0.75 | 1.15 |
| MgO | 29.8 ±0.9 | 15.0 ±1.2 | 16.3 ±0.5 | 28.3 ±1.1 | 14.5 ±1.3 | 15.1 ±0.8 | 24.6 ±0.9 | 12.8 ±1.0 | 14.5 ±0.6 | 13.1 | 14.5 | 8.41 | 6.30 |
| NiO | 0.30±0.04 | 0.01±0.01 | 0.16±0.06 | 0.18±0.06 | n.d. | 0.10±0.03 | 0.07±0.02 | n.d. | 0.08±0.03 | n.d. | n.d. | n.d. | n.d. |
| CaO | 0.31±0.03 | 11.9 ±0.05 | n.d. | 0.40±0.04 | 12.1 ±0.06 | n.d. | 0.49±0.07 | 12.3 ±0.1 | n.d. | 20.3 | 21.6 | 8.29 | 8.47 |
| $Na_2O$ | 0.07±0.03 | 2.76±0.09 | n.d. | 0.11±0.04 | 2.95±0.11 | n.d. | 0.16±0.03 | 2.99±0.09 | n.d. | 1.06 | 0.61 | n.d. | n.d. |
| $K_2O$ | n.d. | 0.16±0.03 | n.d. | n.d. | 0.17±0.02 | n.d. | n.d. | 0.17±0.02 | n.d. | n.d. | n.d. | n.d. | n.d. |
| Total | 100.5 | 99.5 | 99.3 | 100.5 | 99.1 | 98.8 | 100.7 | 99.3 | 100.3 | 98.7 | 99.1 | 99.1 | 100.5 |
| Si | 1.92 | 6.35 | 0.001 | 1.91 | 6.33 | 0.002 | 1.91 | 6.24 | 0.001 | 1.88 | 1.94 | 2.99 | 2.97 |
| Ti | 0.001 | 0.004 | 0.002 | 0.001 | 0.002 | 0.002 | 0.001 | -- | 0.002 | 0.013 | 0.006 | 0.003 | 0.008 |
| Al | 0.156 | 2.88 | 1.99 | 0.172 | 2.90 | 2.00 | 0.198 | 2.95 | 1.98 | 0.279 | 0.168 | 2.01 | 2.04 |
| Cr | 0.001 | -- | -- | -- | -- | -- | -- | -- | -- | 0.003 | 0.003 | 0.002 | 0.002 |
| $Fe_{II}$ | 0.324 | 0.715 | 0.381 | 0.376 | 0.737 | 0.400 | 0.515 | 1.06 | 0.456 | 0.200 | 0.172 | 1.31 | 1.49 |
| $Fe_{III}$[15] | 0.002 | | | 0.007 | | | -- | | | 0.017 | -- | | |
| Mn | 0.010 | 0.012 | 0.003 | 0.012 | 0.017 | 0.004 | 0.016 | 0.036 | 0.005 | 0.005 | 0.003 | 0.049 | 0.075 |
| Mg | 1.56 | 3.10 | 0.630 | 1.50 | 3.02 | 0.588 | 1.32 | 2.70 | 0.563 | 0.729 | 0.799 | 0.961 | 0.721 |
| Ni | 0.008 | 0.001 | 0.003 | 0.005 | -- | 0.002 | 0.002 | -- | 0.002 | -- | -- | -- | -- |
| Ca | 0.012 | 1.77 | -- | 0.015 | 1.81 | -- | 0.019 | 1.87 | -- | 0.812 | 0.855 | 0.681 | 0.697 |
| Na | 0.005 | 0.742 | -- | 0.008 | 0.799 | -- | 0.011 | 0.820 | -- | 0.077 | 0.044 | -- | -- |
| K | -- | 0.024 | -- | -- | 0.030 | -- | -- | 0.031 | -- | -- | -- | -- | -- |
| Total | 4.00 | 15.59 | 3.01 | 4.00 | 15.64 | 3.00 | 3.99 | 15.71 | 3.01 | 4.01 | 3.99 | 8.00 | 8.00 |

[1]Sample LC86-016. [2]Samples LC86-011 and LC86-017. [3]Sample LC86-013. [4]Samples LC86-002, LC86-008, and LC86-010. [5]Sample LC86-007 - zone transitional between amphibolite and granulite. [6]Sample LC86-003. [7]Sample LC86-031. [8]Sample LC86-001. [9]Abbreviations used: Opx - orthopyroxene; Cpx - Ca-rich clinopyroxene; Gt - garnet; Pl - plagioclase; AF - alkali feldspar; Amp - amphibole. [10]Core and rim compositions of garnet and clinopyroxene in granulite. These are best estimates and number of data points and ranges are not given. [11]Composition of inclusions in garnet and pyroxene. [12]Cores and rims of granular feldspars. [13]Interstitial alkali feldspar. [14]Number of data points used in calculating averages. [15]Amount of ferric iron calculated from stoichiometry for pyroxenes only. Cation structural formulae calculated assuming 6 oxygens for pyroxene, 8 for feldspar, 12 for garnet, 23 for amphibole, 4 for spinel.

## Table 2. Continued

| Granulite[4] | | | | Amphibolite 1[5] | | | | Amphibolite 2[6] | | Amphibolite 3[7] | | Amphibolite 4[8] | |
|---|---|---|---|---|---|---|---|---|---|---|---|---|---|
| Pl[9] ic[11] | Pl core[12] | Pl rim[12] | AF[9] is[13] | Amp | Cpx | Pl | Amp | Pl | Amp | Pl | Amp | Pl | Amp |
| 20 | 19 | 25 | 17 | 19 | 22 | 20 | 19 | 20 | 25 | 18 | 23 | 22 | 19 |
| 58.2 ±0.4 | 56.2 ±0.7 | 59.9 ±0.8 | 65.5 ±1.1 | 45.0 ±3.2 | 52.2 ±0.3 | 56.8 ±0.8 | 45.7 ±0.2 | 53.7 ±0.9 | 48.6 ±1.0 | 59.3 ±1.2 | 46.0 ±0.8 | 49.9 ±0.8 | 46.6 ±0.6 |
| n.d. | 0.02±0.02 | n.d. | 0.02±0.02 | 0.77±0.13 | 0.55±0.06 | n.d. | 0.83±0.04 | 0.02±0.01 | 0.33±0.06 | n.d. | 0.66±0.08 | n.d. | 0.48±0.09 |
| 26.6 ±0.3 | 27.3 ±0.7 | 24.7 ±0.9 | 20.7 ±0.9 | 15.6 ±3.2 | 5.06±0.27 | 26.7 ±0.5 | 13.7 ±0.5 | 30.0 ±1.2 | 15.3 ±0.7 | 25.4 ±0.9 | 14.2 ±0.6 | 32.8 ±0.8 | 14.3 ±0.5 |
| n.d. | n.d. | n.d. | n.d. | 0.03±0.03 | 0.06±0.02 | n.d. | 0.04±0.04 | n.d. | n.d. | n.d. | 0.05±0.02 | n.d. | n.d. |
| 0.19±0.06 | 0.16±0.03 | 0.21±0.04 | 0.05±0.02 | 12.3 ±1.3 | 7.55±0.16 | 0.07±0.02 | 12.6 ±0.2 | 0.16±0.02 | 4.18±0.12 | 0.11±0.04 | 13.2 ±0.5 | 0.05±0.04 | 10.1 ±0.2 |
| n.d. | n.d. | n.d. | n.d. | 0.19±0.09 | 0.23±0.04 | n.d. | 0.17±0.05 | n.d. | 0.10±0.03 | n.d. | 0.16±0.02 | n.d. | 0.23±0.04 |
| n.d. | 0.01±0.01 | 0.03±0.01 | n.d. | 10.6 ±1.3 | 12.6 ±0.3 | 0.01±0.01 | 10.9 ±0.2 | 0.01±0.01 | 17.2 ±0.3 | 0.03±0.01 | 11.1 ±0.3 | n.d. | 13.3 ±0.3 |
| n.d. | n.d. | n.d. | n.d. | n.d. | n.d. | n.d. | n.d. | n.d. | n.d. | n.d. | n.d. | n.d. | n.d. |
| 8.26±0.23 | 9.21±0.18 | 6.37±0.27 | 1.54±0.13 | 12.4 ±0.7 | 22.1 ±0.4 | 9.46±0.26 | 12.2 ±0.2 | 12.5 ±0.3 | 11.7 ±0.4 | 7.12±0.28 | 11.8 ±0.5 | 14.6 ±0.3 | 11.7 ±0.2 |
| 6.90±0.18 | 6.24±0.11 | 7.69±0.24 | 6.93±0.26 | 2.05±0.37 | 0.87±0.12 | 6.27±0.14 | 1.87±0.10 | 4.42±0.21 | 1.34±0.21 | 7.37±0.22 | 1.75±0.12 | 3.18±0.10 | 1.55±0.30 |
| 0.06±0.01 | 0.09±0.02 | 0.37±0.08 | 5.37±0.19 | 0.04±0.04 | n.d. | 0.11±0.02 | 0.10±0.01 | 0.05±0.02 | 0.12±0.03 | 0.19±0.05 | 0.21±0.03 | 0.05±0.01 | 0.19±0.02 |
| 100.2 | 99.2 | 99.3 | 100.1 | 99.0 | 101.2 | 99.4 | 98.1 | 100.9 | 98.9 | 99.5 | 99.1 | 100.6 | 98.5 |
| 2.60 | 2.54 | 2.69 | 2.92 | 6.46 | 1.91 | 2.57 | 6.62 | 2.41 | 6.66 | 2.66 | 6.60 | 2.26 | 6.62 |
| -- | 0.001 | -- | 0.001 | 0.083 | 0.015 | -- | 0.090 | 0.001 | 0.034 | -- | 0.071 | -- | 0.051 |
| 1.40 | 1.46 | 1.31 | 1.09 | 2.64 | 0.218 | 1.42 | 2.34 | 1.59 | 2.47 | 1.34 | 2.40 | 1.75 | 2.40 |
| -- | -- | -- | -- | 0.003 | 0.002 | -- | 0.005 | -- | -- | -- | 0.006 | -- | -- |
| 0.007 | 0.006 | 0.008 | 0.002 | 1.48 | 0.231 | 0.003 | 1.53 | 0.006 | 0.479 | 0.004 | 1.583 | 0.002 | 1.20 |
| | | | | | -- | | | | | | | | |
| -- | -- | -- | -- | 0.023 | 0.007 | -- | 0.021 | -- | 0.012 | -- | 0.019 | -- | 0.028 |
| -- | 0.001 | 0.002 | -- | 2.27 | 0.687 | 0.001 | 2.35 | 0.001 | 3.51 | 0.002 | 2.37 | -- | 2.82 |
| -- | -- | -- | -- | -- | -- | -- | -- | -- | -- | -- | -- | -- | -- |
| 0.395 | 0.446 | 0.306 | 0.074 | 1.91 | 0.866 | 0.458 | 1.89 | 0.601 | 1.72 | 0.342 | 1.81 | 0.709 | 1.78 |
| 0.597 | 0.547 | 0.669 | 0.599 | 0.570 | 0.062 | 0.549 | 0.525 | 0.384 | 0.356 | 0.640 | 0.487 | 0.279 | 0.427 |
| 0.003 | 0.005 | 0.021 | 0.305 | 0.007 | -- | 0.006 | 0.018 | 0.003 | 0.021 | 0.011 | 0.038 | 0.003 | 0.034 |
| 5.00 | 5.01 | 5.00 | 4.99 | 15.43 | 4.00 | 5.00 | 15.39 | 4.99 | 15.26 | 5.00 | 15.39 | 5.01 | 15.36 |

[1]Sample LC86-016. [2]Samples LC86-011 and LC86-017. [3]Sample LC86-013. [4]Samples LC86-002, LC86-008, and LC86-010. [5]Sample LC86-007 - zone transitional between amphibolite and granulite. [6]Sample LC86-003. [7]Sample LC86-031. [8]Sample LC86-001. [9]Abbreviations used: Opx - orthopyroxene; Cpx - Ca-rich clinopyroxene; Gt - garnet; Pl - plagioclase; AF - alkali feldspar; Amp - amphibole. [10]Core and rim compositions of garnet and clinopyroxene in granulite. These are best estimates and number of data points and ranges are not given. [11]Composition of inclusions in garnet and pyroxene. [12]Cores and rims of granular feldspars. [13]Interstitial alkali feldspar. [14]Number of data points used in calculating averages. [15]Amount of ferric iron calculated from stoichiometry for pyroxenes only. Cation structural formulae calculated assuming 6 oxygens for pyroxene, 8 for feldspar, 12 for garnet, 23 for amphibole, 4 for spinel.

minerals are compositionally similar to large clinopyroxenes. Homogeneous orthopyroxenes in coronas are close to enstatite-ferrosilite and contain even less minor components than do clinopyroxenes (Table 2). Coexisting pyroxenes record $T <\sim 650°C$ using the formulation of Lindsley (1983). Errors on temperature estimates are plausibly worse than $\pm 50°C$ because of steep slopes on solvus limbs at low temperatures (Lindsley, 1983).

Spinels in symplectic intergrowth with amphibole are also homogeneous over wide areas, although Mg# varies with (and is consistently less than) that of coexisting mafic silicate minerals. These simple Mg-Fe-Al spinels have low contents of Cr and Ti (Table 2) and no stoichiometric requirement for ferric iron.

Amphibole compositions, conversely, vary significantly according to the neighboring mineral as illustrated in Figure 3. Amphibole adjacent to plagioclase is enriched in $Al_2O_3$ and, possibly, $K_2O$ and depleted in MgO relative to that bordering olivine. CaO and $Na_2O$ contents of amphiboles appear insensitive to the nature of neighboring grains. Plagioclase rims adjacent to amphiboles are enriched in anorthite ($An_{96-98}$), i.e., their $Na_2O$ contents are ~25% of that in the rest of the grain. Neighboring amphibole is not enriched in $Na_2O$. These zoned regions may be 10-15 μm wide but may be absent against wide amphibole-spinel intergrowths.

Clinopyroxenes and garnets in granulites are chemically zoned (Table 2), unlike the minerals in the ultramafic rocks. Homogeneous garnet cores are surrounded by thin rims depleted in CaO and MgO and enriched in FeO (Figures 4 and 5). Clinopyroxenes are broadly zoned and have no region of constant composition. Rims of pyroxenes are enriched in CaO and MgO and depleted in FeO, $Al_2O_3$, $TiO_2$, and $Na_2O$ relative to cores. Deformed clinopyroxenes are compositionally homogeneous and enriched in CaO and FeO compared with cores of granular clinopyroxenes (Figure 4). Orthopyroxene is absent from granulites.

Two generations of plagioclase crystals occur in the granulites (Table 2). Small homogeneous plagioclase inclusions ($An_{40}$) occur in garnet and clinopyroxene and display no compositional differences according to their host mineral. Large (up to 5 mm) grains of plagioclase also occur unarmored by other minerals. Within granulites, these have cores of $An_{40-45}$ and more sodic rims that merge into interstitial alkali feldspar (~ $Ab_{60}Or_{30}$). Large anhedral plagioclase crystals in zones transitional to amphibolites are similar in composition to those in the amphibolites (see below).

Amphiboles in granulites demonstrate marked chemical variation according to the neighboring mineral, as noted for amphiboles in troctolites and gabbros. Amphiboles adjacent to garnets are enriched in $Al_2O_3$ and FeO and depleted in CaO and MgO relative to those bordering pyroxenes. Some clinopyroxene grains, particularly in transition zones, are replaced by edenitic amphibole. Although margins and cores of clinopyroxene grains are in optical continuity, different regions contrast in color, birefringence, and chemical composition. In particular, contents of CaO, MgO, and $SiO_2$ are lower, and those of $Al_2O_3$, FeO, and $Na_2O$ are higher in outer zones — stages transitional to formation of amphibole.

Amphibole and plagioclase in amphibolites are variable in composition, although grains are relatively homogeneous on the outcrop scale. Plagioclase is $An_{83}$ in one amphibolite that contains more than 85% modal plagioclase; $An_{35}$ in an amphibolite dominated by amphibole. Mg# of amphiboles (i.e., essentially

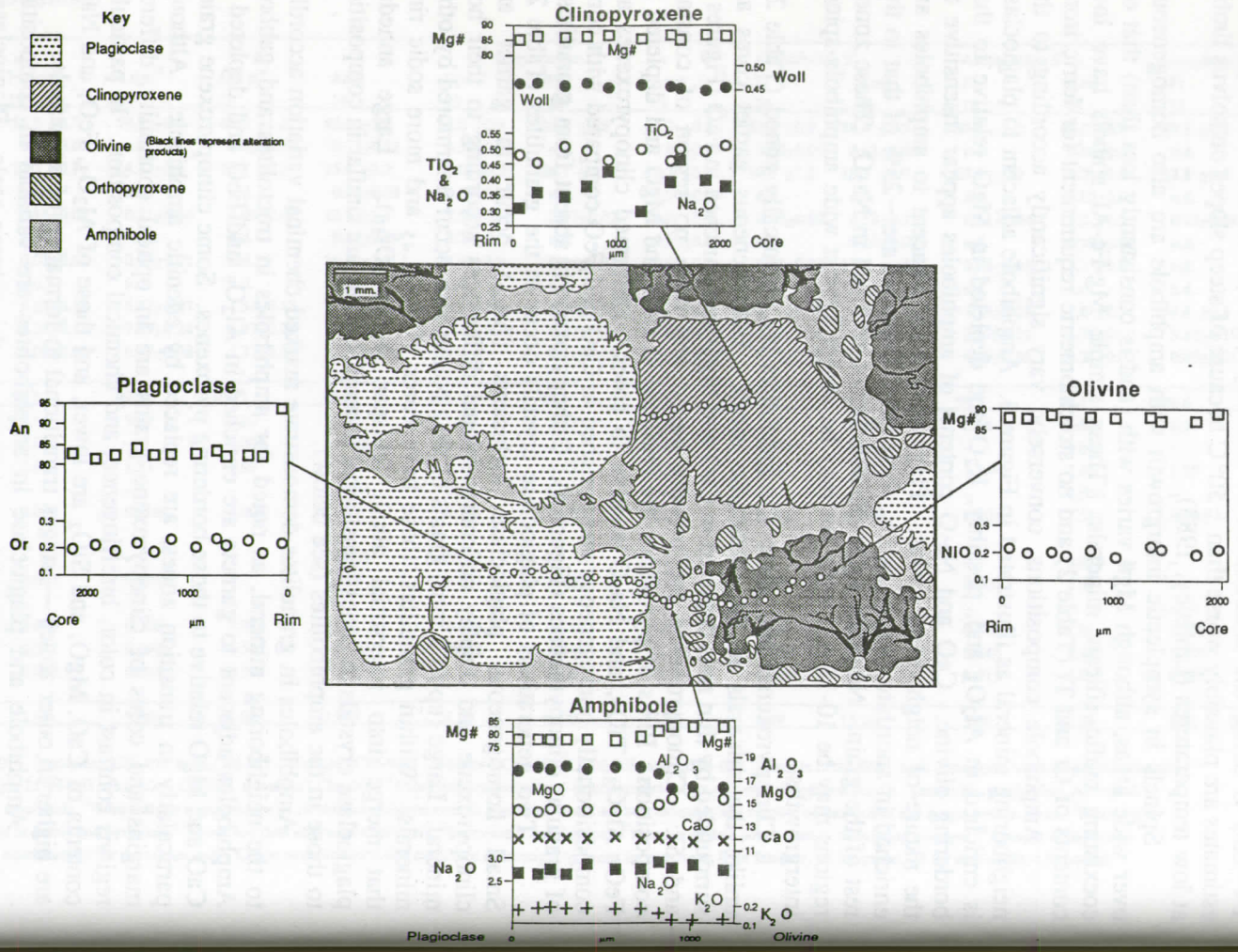
Key
Plagioclase
Clinopyroxene
Olivine
(Black lines represent alteration products)
Orthopyroxene
Amphibole
Clinopyroxene
Mg#
Wo II
TiO2
Na2O
Rim
Core
µm
1 mm.
Plagioclase
An
Or
Olivine
NiO
Amphibole
Al2O3
MgO
CaO
K2O

that of the whole rock) is 90-60. Magnesian amphiboles are poor in CaO, $Na_2O$, and $Al_2O_3$ although some are in amphibolites dominated by calcic plagioclase. Iron- rich amphiboles have higher contents of $K_2O$, $Na_2O$, and $TiO_2$.

## DISCUSSION

### Estimation of PT history of Lake Chatuge complex

PT histories of mineral assemblages may be estimated by use of the petrogenetic grid and geothermobarometers based on partitioning of elements between coexisting phases. The petrogenetic grid employs knowledge of phase relations of materials of appropriate chemical composition in the appropriate PT regime. Dallmeyer (1974) gave analyses of garnet granulites that are similar to those of alkali basalts (Table 3). Green and Ringwood (1967) determined phase relations of a material with similar composition (Table 3). Although no bulk-rock analyses are available for olivine gabbros, they are probably well modeled by the most mafic compositions (Mg#~90) studied by Green and Ringwood (Table 3).

The arguments presented below are based on the assumption that secondary assemblages formed in equilibrium, although they re-equilibrated during cooling. The dominant reactions in the ultramafic rocks were formation of pyroxene and spinel by reaction between olivine and plagioclase and exsolution of one pyroxene from the other. The large size of cumulate phases and the slow pace of solid state diffusion through the coronas left much of the high-temperature assemblage unaltered. Exsolution does not require reaction and only ceased when temperatures were too low to allow nucleation and growth of the exsolving phase.

Plagioclase and olivine in the finer grained, unlayered gabbros reacted thoroughly to form garnet. Clinopyroxene did not exsolve orthopyroxene in these silica-undersaturated rocks, but changed composition by cation exchange with garnet. The observed metamorphic assemblage in these rocks was established during cooling and reflects an equilibrium paragenesis.

The following observations are pertinent to the environment of formation of LCC:

1. Plagioclase and olivine crystallized from magmas that formed the LCC, as shown by magmatic olivine-plagioclase banding of troctolites.
2. Garnet did not form in rocks with Mg#>75.

**Figure 3. Map of part of a thin-section of troctolite LC86016 showing the appearance of large relict and secondary coronitic grains. Many small grains of pyroxenes, amphibole, and spinel are not shown for the sake of clarity. Similarly, late stage clinozoisite and ilmenite are not shown and amphibole is shown as a homogeneous mass whereas it is composed of many separate grains.**

**Open circles represent points of microprobe analysis shown in the accompanying analytical traverses from core to rim or, in the case of the amphibole, from grains bordering olivine to those bordering plagioclase. The relict igneous grains are homogeneous except for a thin alteration rind of plagioclase. Amphibole grains show a compositional dependence upon the neighboring relict igneous phase. Thus, amphibole bordering olivine is enriched in MgO and depleted in $Al_2O_3$ and $K_2O$ relative to that bordering plagioclase.**

Table 3. Analyses and norms of Lake Chatuge Complex granulites and of materials used in experimental studies.

| | D[1] | | | G&R[2] | |
|---|---|---|---|---|---|
| | UM-1 | UM-7 | UM-8 | AOB | MT |
| $SiO_2$ | 46.8 | 46.2 | 45.5 | 45.4 | 51.4 |
| $TiO_2$ | 1.92 | 1.60 | 1.42 | 2.52 | 2.20 |
| $Al_2O_3$ | 13.2 | 14.0 | 13.8 | 14.7 | 14.3 |
| $Cr_2O_3$ | 0.04 | 0.03 | 0.03 | -- | -- |
| $Fe_2O_3$ | 2.11 | 1.91 | 1.88 | 1.61 | 0.71 |
| FeO | 11.4 | 10.7 | 10.1 | 12.7 | 5.28 |
| MnO | 0.24 | 0.23 | 0.11 | 0.18 | 0.16 |
| MgO | 7.00 | 7.57 | 7.62 | 10.4 | 12.9 |
| CaO | 13.5 | 13.5 | 14.6 | 9.14 | 11.1 |
| $Na_2O$ | 2.63 | 2.87 | 2.93 | 2.62 | 1.90 |
| $K_2O$ | 1.36 | 1.20 | 1.22 | 0.78 | 0.08 |
| $P_2O_5$ | 0.26 | 0.30 | 0.16 | 0.02 | -- |
| $H_2O$ | 0.05 | 0.12 | 0.14 | -- | -- |
| Total | 100.7 | 100.3 | 99.9 | 100.0 | 100.0 |
| Mg#[3] | 52.3 | 55.8 | 57.5 | 59.4 | 81.4 |
| Or | 7.21 | 6.30 | 6.56 | 3.64 | 0.47 |
| Ab | 8.21 | 6.34 | 1.57 | 13.9 | 16.1 |
| An | 18.1 | 19.4 | 19.0 | 20.6 | 30.2 |
| Ne | 6.38 | 8.25 | 11.4 | 2.00 | -- |
| Di | 33.4 | 31.6 | 37.6 | 12.4 | 19.7 |
| Wo | 16.9 | 16.0 | 19.1 | 6.33 | 10.4 |
| En | 8.50 | 8.46 | 10.4 | 3.57 | 7.91 |
| Fs | 8.02 | 7.11 | 8.08 | 2.50 | 1.42 |
| Hy | -- | -- | -- | -- | 27.6 |
| En | -- | -- | -- | -- | 23.4 |
| Fs | -- | -- | -- | -- | 4.21 |
| Ol | 20.5 | 22.4 | 17.9 | 41.8 | 0.67 |
| Fo | 10.0 | 11.6 | 9.64 | 23.6 | 0.56 |
| Fa | 10.4 | 10.8 | 8.27 | 18.2 | 0.11 |
| Mt | 2.74 | 2.46 | 2.47 | 1.85 | 1.03 |
| Il | 3.27 | 2.70 | 2.45 | 3.78 | 4.18 |
| Cm | 0.06 | 0.04 | 0.04 | -- | -- |
| Ap | 0.55 | 0.63 | 0.34 | 0.04 | -- |

[1]Analyses of garnet granulites from Dallmeyer (1974), employing his sample numbers.
[2]Analyses of starting materials from Green and Ringwood (1967); AOB is alkali olivine basalt; MT is magnesian tholeiite. [3]Atomic $100*Mg/(Mg+Fe^{2+})$.
$Fe_2O_3/FeO$ calculated assuming a temperature of $1100^{\circ}C$ with oxygen fugacity on the quartz-fayalite-magnetite buffer according to the algorithm of Sack and others (1980).

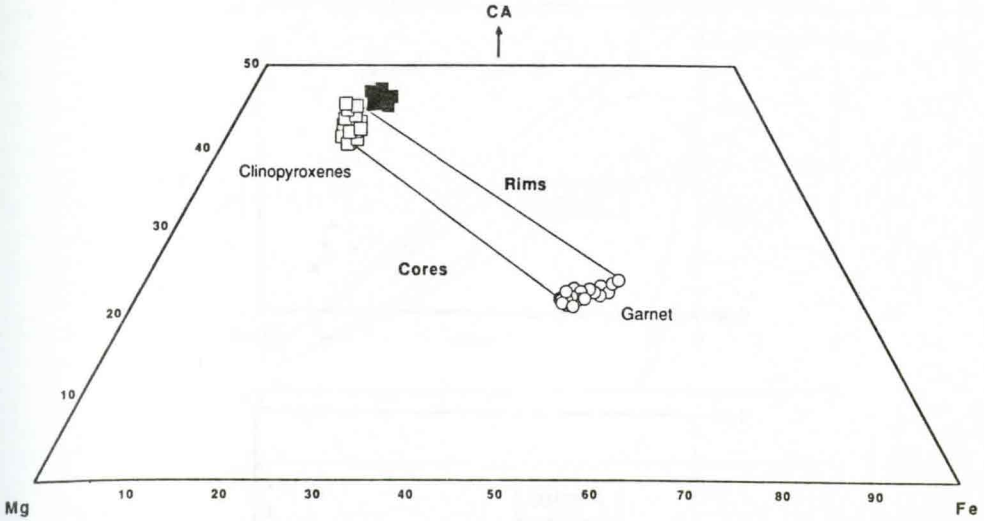


**Figure 4. Compositions of clinopyroxenes and garnets from the granulites in terms of their Ca-, Mg- and Fe-endmembers. Tie lines between cores of garnets and pyroxenes and between their rims highlight the zoning of these minerals. Deformed clinopyroxenes from the granulites and neighboring amphibolites are also shown. These are considerably richer in Ca than the other pyroxenes.**

3. Garnet was stable with respect to olivine+plagioclase in granulites (Mg#<60). Plagioclase was stable, however, as shown by its occurrence as inclusions in garnet and clinopyroxene.

Figure 6a is a PT diagram for mafic-ultramafic compositions from Green and Ringwood. The assemblage olivine-plagioclase-clinopyroxene in ultramafic rocks (Mg#~90) forms granulites by reactions:
olivine+anorthite=spinel+pyroxene (AB) and anorthite+spinel+pyroxene=garnet (EF). The magma crystallized olivine and plagioclase, so P<13 kbar (Figure 6a). Absence of garnet from coronas in gabbros shows they did not cross EF.

Reaction of plagioclase and olivine to form garnet in rocks with Mg#<60 occurs at CD; plagioclase disappears along GH to leave eclogite. Granulite protoliths crossed CD to form plagioclase+garnet+clinopyroxene. $P_{reaction}$ depends upon assumed $T_{reaction}$. If T>700° C, then P>7 kbar, so that $P_{crystallization}$ must have been 10±3 kbar. Furthermore, the LCC cooled between EF and CD after formation of garnet.

Partitioning of Fe and Mg between coexisting garnet and pyroxene has been calibrated as a geothermometer. Essene (1982) reviewed different thermodynamic formulations of the geothermometer and suggested use of that of Ellis and Green (1979) for granulites. Newton and Perkins (1982) suggested using coexisting garnet, clinopyroxene, plagioclase, and quartz to estimate $P_{equilibration}$ of mafic granulites. Garnet granulites in LCC contain this assemblage.

Compositions of cores of garnet and pyroxene were used to obtain $T_{crystallization}$ for the garnetiferous assemblage — 837° C. As shown below, this temperature can only reflect cooling if the rate of that cooling was extremely slow. This temperature is, therefore, taken as the temperature at which garnet formed,

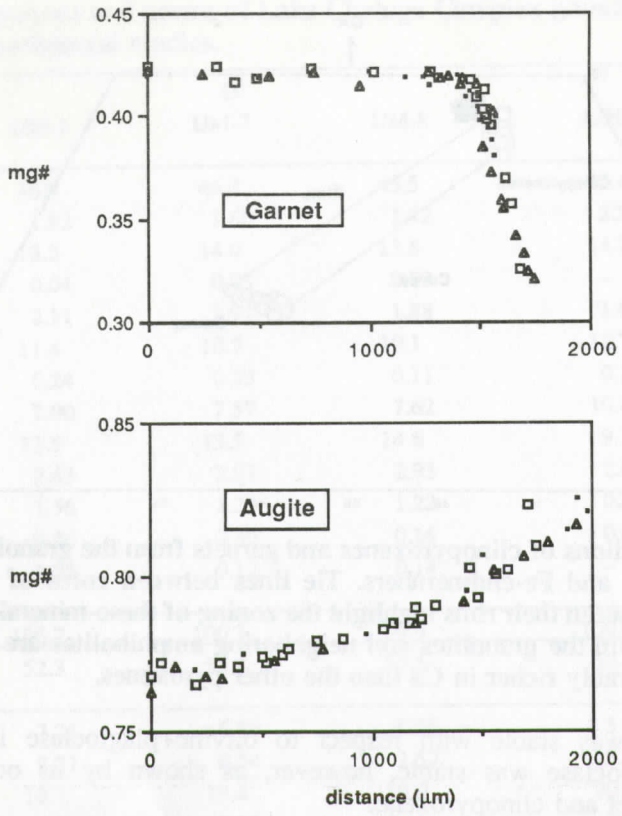


**Figure 5. Zonation of magnesium numbers (mg#; atomic Mg/[Mg+Fe]*100) of clinopyroxenes and garnets from granulites from cores to rims. Cores of garnets are homogeneous and surrounded by 200-300 μm rinds that are strongly zoned to iron-rich compositions. Clinopyroxenes exhibit broad zonation with rims more magnesian than the cores.**

in equilibrium with clinopyroxene, from olivine and plagioclase. Estimation of $P_{crystallization}$ requires knowledge of the composition of plagioclase in equilibrium with garnet and pyroxene cores. Inclusions of plagioclase occur in both minerals and are unlikely to have reequilibrated during cooling as compositions of all inclusions are similar ($An_{40}$). Pyroxene presumably did not lose $CaAlAlSiO_6$ to plagioclase inclusions during cooling because of the lack of free $SiO_2$ (required to form anorthite from Ca-tschermak's molecule) in the inclusions. The estimated pressure of formation of the granulite is 10.9 kbar. The PT estimate for granulite formation is marked on Figure 6a as "Y".

Original garnet-clinopyroxene boundaries are occupied by amphibole. Some amphibole stringers are thin and the total amount of garnet and pyroxene replaced was small. Compositions of the rims of these grains are assumed to be similar to those of original rims. The PT estimate for the rims assumes equilibrium with cores of plagioclase interstitial to garnet and pyroxene ($An_{45}$). This estimate is 646° C, 7.2 kbar — marked on Figure 6a as "Z".

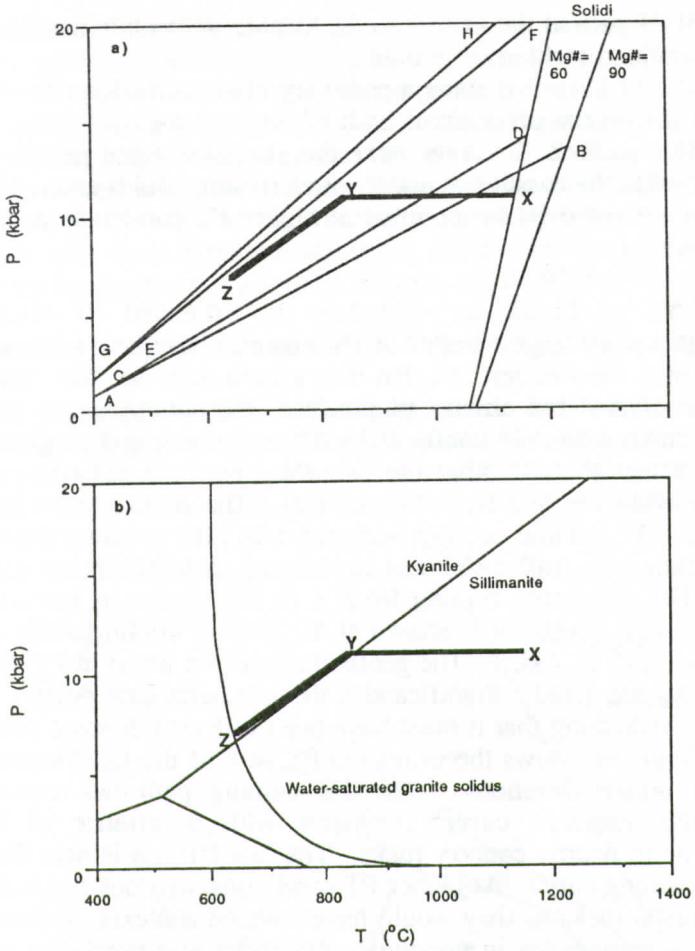


Figure 6. Estimated pressure-temperature history of Lake Chatuge garnet granulites superimposed on relevant reactions. The cooling path of the LCC is shown as XYZ. The point X is conjectural — the pressure at which the magma crystallized was less than 13 kbar as olivine and plagioclase both crystallized from the melt. The point Y is the PT recorded by the cores of minerals in the granulites and records the establishment of the granulite mineralogy. The point Z is the PT recorded by the rims of the minerals in the granulites.

a) PT path of the LCC with the reactions that result in the gabbro-granulite-eclogite transformation (Green and Ringwood, 1967).

AB — olivine+plagioclase= 2 pyroxenes+spinel ('olivine out')

EF — spinel+plagioclase+pyroxene=garnet (mg#=90) ('garnet in/ plagioclase out')

CD — spinel+plagioclase+pyroxene=garnet (mg#=60) ('garnet in/ spinel out')

GH — plagioclase+pyroxene=garnet (mg#=60) ('plagioclase out')

During cooling, the ultrabasic rocks crossed AB but not EF; the granulites crossed CD but not GH. The LCC path between EF and CD is thus consistent with this diagram.

b) PT path of the LCC with the kyanite-sillimanite reaction and the curve for water-saturated melting of granite.

The LCC cooled along a path very close to the kyanite-sillimanite reaction, consistent with the presence of both minerals in the host rocks of the complex.

The point Z lies very near the water-saturated granite solidus and may correspond to the conditions under which hydrous fluids entered the complex. Such fluids could not exist in the crust at higher PT conditions as they would induce anatexis.

XYZ on Figure 6a represents the estimated PT history of granulites. Although a very large number of PT histories may be envisioned for the LCC, I have chosen the simplest one that is in accord with the data. The protoliths of the granulite crystallized olivine, plagioclase, and clinopyroxene at T>~ 1100° C and P<13 kbar (because ultramafic rocks contain olivine and plagioclase — Figure 6a) and no lower than 11 kbar (so that the protoliths did not experience pressure increase while cooling from the solidus). The estimated PT of crystallization is shown as "X". Initial cooling occurred with little pressure decrease until thermal equilibrium with wall rocks was established, possibly in the garnet stability field ("Y"). For simplicity, cooling from X to Y is shown as isobaric and intersection with the local geotherm is shown at Y. Further cooling along YZ occurred with uplift to ~650° C, 7 kbar. The geotherm is shown linear in PT space although only two points are fixed. Significantly, the geotherm extrapolates to 275° C at zero pressure, indicating that it must have been inflected at some point.

Figure 6b shows the estimated PT path of the LCC superimposed on some relevant crustal reactions. The YZ cooling path lies close to the kyanite-sillimanite transition curve, consistent with occurrence of both kyanite and sillimanite in nearby country rocks. The low PT end is near the water- saturated granite melting curve. At higher PT conditions, hydrous fluids did not exist in the felsic crustal rocks as they would have induced anatexis. Influx of fluids to form secondary amphiboles in previously dry rocks was precluded until the crust had cooled through this curve.

The geothermal gradient determined by Kittelson and McSween (1987) for metasediments northeast of the LCC is similar to the low PT portion of YZ. The hydrous metasedimentary assemblages apparently yield conditions similar to those recorded by cooling of anhydrous granulites in LCC.

Mineral zonation in granulites is attributed to the slow kinetics of diffusional exchange between clinopyroxene and garnet — dominantly because of the slow Fe-Mg binary diffusion in pyroxene. Analysis of zonation patterns in coexisting minerals has been treated by Lasaga (1983) who showed that the temperatures recorded by cores of a pair of minerals of a given size are dependent on the cooling rate. Following his analysis for the garnet-clinopyroxene pairs in the granulite (using the diffusion data of Lasaga and others, 1977, for garnet, and of Brady and McCallister, 1983 for clinopyroxene), the temperature recorded by the cores of the garnet and clinopyroxene would be a cooling temperature if the cooling rate were ~0.01° C/m.y. If the garnet and clinopyroxene had existed at a higher temperature and cooled at a faster rate, their cores would record a higher temperature (1060° C for cooling at 10° C/m.y.; 905° C for 0.1° C/m.y.).

A cooling rate of 0.01° C/m.y. is extraordinarily slow — it represents,

assuming a geothermal gradient of 30° C/km, an uplift rate of ~ 30 cm/m.y. Furthermore, the granulites would have taken 19 b.y. to cool from 840° C (cores) to 650° C (rims)! I conclude, therefore, that the temperature recorded by the cores of the garnet and clinopyroxene is the temperature at which these minerals formed by reaction of olivine and plagioclase. The fact that point "Y" on Figure 6a does not lie on the line CD is presumably a reflection of the fact that the composition of the granulite is not exactly the same as the composition used by Green and Ringwood (1967), combined with their experimental errors and in errors on data presented here and in the thermodynamic analysis of Newton and Perkins (1983).

## Nature of Magmatic Precursors of Lake Chatuge Complex

Magmatic precursors of LCC crystallized olivine and spinel, followed by olivine+plagioclase+clinopyroxene. The granulite protoliths were probably composed of clinopyroxene, plagioclase, olivine (replaced by garnet), apatite, Fe-Ti oxide (replaced by rutile), and, possibly, other phases. Phase relations are

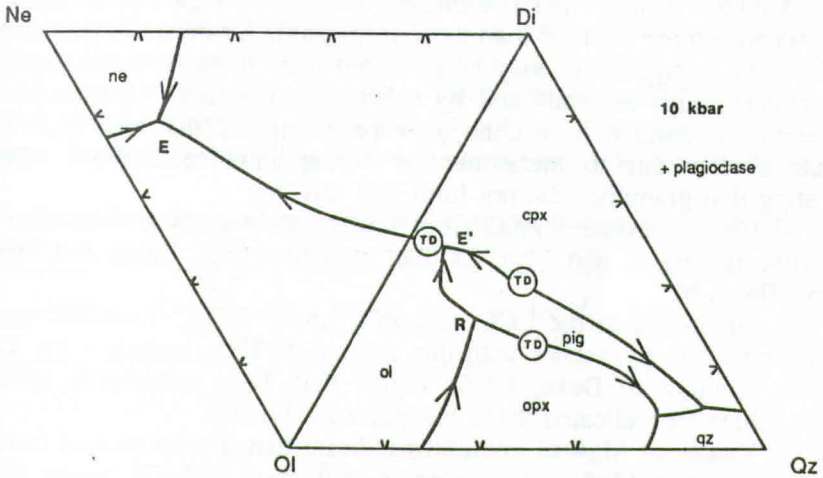


**Figure 7. Projection of phase relations at 10 kbar from pl onto the plane *ol-di-qz-ne* as inferred by Meen (1987a). Pseudounivariant lines are marked with arrows showing direction of decreasing temperature. The thermal divides that have been calculated from compositions of mineral phases coexisting with melts in this system are shown by circles marked "TD". Some pseudoinvariant points are lettered. E is L(*ol,cpx,pl,ne*); E' is L(*ol,pig,cpx,pl*); R is L(*ol,pig,opx,pl*) and is the point at which *opx* is replaced by *pig* in equilibrium with melt, olivine, and plagioclase.**

**A tholeiitic liquid on the *qz*-side of the thermal divide defined by compositions of coexisting olivine, clinopyroxene, and plagioclase will evolve to E'. With increasing $K_2O$ content, E' moves to more *qz*-rich compositions and *opx* replaces *pig* as the crystallizing low-Ca pyroxene. An alkaline or transitional liquid on the *ne* side of that thermal divide will evolve to E, where it crystallizes nepheline.**

**Abbreviations employed: *ol* - olivine; *cpx* - Ca-rich clinopyroxene; *opx* - orthopyroxene; *pig* - pigeonite; *pl* - plagioclase; *qz* - quartz; *ne* - nepheline.**

approximated by nepheline-olivine-clinopyroxene-plagioclase-quartz (*ne-ol-cpx-pl-qz*), and are shown in projection in Figure 7 for contents of $K_2O$ in the melt less than ~1.5% and at a pressure of 10 kbar (taken from the analysis of Meen, 1987a). At conditions relevant to crystallization of magmas parental to the LCC (P=10-13 kbar), orthopyroxene (*opx*) and pigeonite (*pig*) melt congruently. *Ol*-normative melts that are silica-saturated (i.e., on the *qz* side of the critical plane of silica-saturation, *ol-cpx-pl*) will crystallize to the pseudoinvariant point L(*ol,opx/pig,cpx,pl*) (E' on Figure 7). Melts on the other side of the critical plane do not precipitate a low-Ca pyroxene but evolve along L(*ol,cpx,pl*) to L(*ol,cpx,pl,ne*) (E).

Ultrabasic rocks contain relict olivine, plagioclase, and clinopyroxene with no primary low-Ca pyroxene. Variations in Mg# and contents of compatible elements in mafic silicate minerals imply that melts experienced considerable fractionation. Lack of low-Ca pyroxene from even the most iron-rich rocks is strong evidence that melts were on the *ne*-side of the critical plane of silica-saturation.

Analyses of granulites (Dallmeyer, 1974) have Mg#[2]=52-57 and crystallized from magmas more evolved than those responsible for most ultrabasic rocks in the LCC. Rock compositions may be modified from those of crystallizing melts by entrained cumulus minerals and by subsolidus alteration. Dallmeyer suggested that granulites formed from clinopyroxene grains and that high $K_2O$ contents of granulites were due to metasomatism during amphibolitization. Observations indicating that granulites did not form this way are:

1. Clinopyroxene crystallizing from basalt magma at ~ 10 kbar have less normative ne and Al and more Ca than granulites (e.g., Baker and Eggler, 1987; Meen, 1987a, b).

2. Granulites in the LCC contain ~ 1.65% $TiO_2$. Tholeiitic magmas that would crystallize pyroxenes with this amount of $TiO_2$ contain ~ 4% $TiO_2$ (using partition relations of Duke, 1976), higher than $TiO_2$ contents in most magmas. Lower values are indicated if the magma was alkaline.

3. Values of Mg# of granulites indicate that if they formed from magmas, the magmas had Mg# ~ 32 (using $K_D^{px/liq(Fe/Mg)}$=0.40), lower than typical basaltic values.

4. Granulites contain 0.2-0.3% $P_2O_5$ and apatite is included in garnet and pyroxene so $P_2O_5$ was not all introduced metasomatically. Apatite may have crystallized from the original magma.

5. Amphiboles in granulites contain <0.10 $K_2O$, so not all $K_2O$ in these rocks is contained in their 10-20% amphibole, as also indicated by their significant contents of alkali feldspar. Furthermore, amphiboles in ultrabasic rocks surrounding the granulites contain 0.1-0.2% $K_2O$, so these rocks contain only 0.02-0.05% $K_2O$. If all the $K_2O$ in the granulites was introduced metasomatically, it was carried through the surrounding ultrabasic without affecting them and most of the $K_2O$ stabilized in the granulite is in alkali feldspar rather than in amphibole. Most $K_2O$ in the granulite was presumably present before influx of hydrous fluids and formation of amphibole.

---

[2]Recalculated using $FeO/Fe_2O_3$ calculated by algorithm of Sack and others (1980)

6. Desilicification may accompany amphibole formation. $SiO_2$ contents of granulites must, however, have been lowered from ~50% to ~46% (with respect to 100% total) if protoliths were *hy*-normative. The limited amount of amphibole in these rocks and the low alkali contents of the rocks is not compatible with extensive desilicification.

Granulites have compositions that are similar to those of many primitive alkali basalts (Table 3). I consider that granulite protoliths formed from alkali basaltic magmas trapped in the cumulate pile.

Experimental and natural systems have yielded data on partitioning of elements between basaltic magma and cumulate phases, allowing estimation of certain chemical parameters of a magma by analysis of cumulate phases. Parameters calculated from compositions of minerals in Table 1 are listed in Table 4. Dunites crystallized from very mafic magmas (Mg#~75; ~300 ppm Ni). The constancy of composition of olivine in dunites in the LCC indicates that the magma body was large enough that crystallization of olivine did not significantly affect its composition. Melts that crystallized gabbros and troctolites were more evolved than those that crystallized dunites. Mass balance calculations based on Mg# and assuming a picritic primary magma indicate that melts crystallized 10-15% olivine to evolve to the most mafic troctolite-precipitating magma. If Mg# of the melts decreased monotonically with evolution, troctolites and gabbros did not succeed each other simply (Table 4). Either plagioclase or clinopyroxene may have been the second mineral to crystallize although plagioclase was volumetrically domi-

**Table 4. Estimated chemical parameters of magmas that crystallized Lake Chatuge Complex**

| | Dunite[1] | Troctolite 1[1] | Gabbro 1[1] | Gabbro 2[1] | Troctolite 2[1] | Granulite[2] |
|---|---|---|---|---|---|---|
| Mg#[3] | 75 | 69 | 61 | 59 | 55 | 55 |
| $TiO_2$[4,5] | -- | 1.07 | 1.40 | 1.49 | 1.87 | 1.65 |
| $K_2O$[4,6] | -- | 0.24 | 0.24 | 0.30 | 0.30 | 1.26 |
| Ni[7,8] | 305 | 200 | 165 | 140 | 120 | -- |
| Cr[7,9] | -- | 185 | 120 | 48 | 27 | -- |

[1]Samples as listed in footnote to Table 1. [2]Averages of compositions given by Dallmeyer (1974). [3]Atomic 100*Mg/(Mg+$Fe^{2+}$). Estimated from compositions of olivine in samples using partitioning relationship of (Fe/Mg) between olivine and liquid as given by Roeder and Emslie (1970). [4]In weight percent. [5]Estimated from compositions of clinopyroxenes using partition coefficient of 0.45 for $TiO_2$ between clinopyroxene and liquid (Duke, 1976). [6]Estimated from compositions of plagioclase using partition coefficient of 0.17 for $K_2O$ between plagioclase and liquid (Arth, 1976). [7]In parts per million. [8]Estimated from compositions of olivine using partition coefficient of 8 for Ni between olivine and liquid. This value was obtained by Duke (1976) for more mafic liquids. [9]Estimated from compositions of clinopyroxenes using partition coefficient of 12 for Cr between clinopyroxene and liquid (Duke, 1976).

Note that $K_2O$ contents of melts are minimum estimates. Plagioclase may have exsolved small amounts of alkali feldspar during cooling and thus relict grains have lower $K_2O$ contents than the original magmatic feldspars.

nant over clinopyroxene. The marked change in Mg# of gabbros and troctolites may have resulted from crystallization from small bodies of magma separate from the extensive magma body that had previously crystallized only olivine. I have used the average granulite composition (Table 3) of Dallmeyer (1974) as the most evolved melt composition.

## HISTORY OF THE LAKE CHATUGE COMPLEX

Mineral parageneses produced in the LCC are summarized in Table 5. Arguments presented above indicate that the LCC owes its existence to formation of a chamber containing mildly ne-normative picritic magma at 10-13 kbar, possibly at the base of continental crust. Density contrasts between mafic magmas and continental crust are sufficient that rising mafic magmas will be trapped at the Moho unless their velocity is great (Sparks and others, 1980; Stolper and Walker, 1980).

**Table 5. Mineral parageneses produced during history of Lake Chatuge Complex**

| | Crystallization | Isochemical Cooling | Taconic (?) Metm. | Upper Pz. Metm. |
|---|---|---|---|---|
| Dunites | Olivine | Recrystallized | | |
| Gabbros and Troctolites | Olivine plagioclase clinopyroxene | Olivine and plagioclase react to 2 pyroxenes & spinel<br>Clinopyroxenes exsolve orthopyroxene | Secondary amphiboles and sphene | |
| | | | Some rocks reconstituted to amphibolites | Clinozoisite and ilmenite |
| Granulites | Olivine plagioclase clinopyroxene with apatite and iron-titanium oxides | Olivine and plagioclase react to form garnet and quartz<br>Oxides form rutile. | | |

Melts crystallized olivine and, later, plagioclase and clinopyroxene. Magmas crystallizing olivine, plagioclase, and clinopyroxene are close to the minimum density attained during evolution (Sparks and others, 1980; Stolper and Walker, 1980) and are likely to have risen. Troctolites and gabbros may have crystallized from trapped residual liquid rather than from the main body as indicated by considerable variation of Mg#. Final liquids crystallized to alkali gabbros containing olivine, clinopyroxene, plagioclase, apatite, and, probably, Fe-Ti oxide, nepheline, and alkali feldspar.

Initial cooling was presumably accompanied by little uplift until the local geotherm was attained. Olivine and plagioclase in ultrabasic rocks reacted to form orthopyroxene, clinopyroxene, and spinel. The large crystal size of relict phases prevented complete reaction. Furthermore, olivine and plagioclase in some troctolites occur in layers. Reactions occurred only at the contact between these layers. In consequence, potentially reactant olivine and plagioclase were separated by coronas of pyroxenes and spinel. Clinopyroxene and orthopyroxene in the ultramafic rocks remained in equilibrium to ~650° C, presumably continuing

mutual exsolution to these low temperatures.

The finer grained and unlayered alkali gabbros recrystallized completely to form granulites. Olivine was consumed in reaction with plagioclase to form garnet and quartz. Oxide reacted to form rutile — Fe was incorporated in garnet. Geothermobarometric estimates from granulites indicate that mineral cores were "frozen" in at 840° C, ~11 kbar and an analysis of the kinetics of Fe-Mg exchange indicates that this is the temperature of formation rather than of cooling unless the cooling rate was inordinately slow. Rims of minerals record cooling to 650° C, ~7 kbar. These estimates are consistent with the petrogenetic grid established for similar rocks and with mineral assemblages in country rocks.

Isochemical cooling terminated near the solidus of water-saturated granite when hydrous fluids entered the LCC. Fluids may have been freed by crystallization of migmatites or their influx may have accompanied tectonic intercalation of LCC metabasites and metasediments. This event probably occurred during or after the Taconic orogeny.

The fluids formed amphibole along almost all grain boundaries in the LCC indicating that penetration was pervasive. Coronas in ultrabasic rocks were especially prone to attack, presumably because of their small grain size, and are extensively replaced by amphibole. Pyroxenes in symplectic intergrowth with spinel were totally replaced by amphibole although spinels are unaltered. Large relict minerals were peripherally replaced by amphiboles. Minerals in granulites are replaced by amphibole that are inhomogeneous and have compositions dependent upon the replaced mineral. Hydration was apparently sufficiently rapid to allow retention of compositional heterogeneities.

The cumulate rocks are surrounded by a sheath of amphibolites. The modal assemblages and mineral chemistry of LCC amphibolites shows that they probably formed from a wide variety of rock types. Values of Mg# of amphibolites are 90-60. If Mg# was altered little during metamorphism, protoliths had a range in Mg# similar to that of less altered rocks. Consequently, the LCC is not simply zoned with a hydrated, mafic sheath and an ultrabasic core. Rather, the complex includes both basic and ultrabasic rocks that are variably hydrated as a consequence of their relative proximity to the contact with country rocks.

A greenschist facies event is indicated by replacement of amphibole and sphene by clinozoisite and ilmenite. This may have been the local response to Acadian or Alleghanian activity, possibly accompanying emplacement of the BRG on the continent.

The LCC has been transported from the base of the continental crust (35-40 km) to the surface. Initial cooling and uplift may have occurred by simple erosion. Most uplift must, however, result from tectonic activity. The time at which the LCC and its host rocks were juxtaposed is unknown. If juxtaposition occurred prior to tectonic exhumation, the host metasediments were once deep crustal rocks, presumably at granulite facies. Present-day mineral parageneses, in this case, reflect retrograde metamorphism during the Paleozoic. Alternatively, metabasites and metasediments were brought into tectonic contact during Taconic thrusting and their Precambrian histories are discrete. This situation suggests that the area east of the Hayesville thrust includes several thrust sheets with separate histories.

## ACKNOWLEDGMENTS

I am grateful to J.R. Butler and S. Swanson for reviews that greatly improved this manuscript. I am also indebted to J.R. Butler, P.D. Fullagar, J.J.W. Rogers, and S.A. Goldberg for spending time on discussions with me. The author and the research were supported by the Department of Geology, University of North Carolina, Chapel Hill.

## REFERENCES CITED

Absher, B.S. and McSween, H.Y., 1985, Granulites at Winding Stair Gap, North Carolina: The thermal axis of Paleozoic metamorphism in the southern Appalachians: Geological Society of America Bulletin, v. 96, p. 588- 599.

Albee, A.L. and Ray, L., 1970, Correction factors for electron probe microanalysis of silicates, oxides, carbonates, phosphates, and sulfates: Analytical Chemistry, v. 80, p. 1408-1414.

Arth, J.G., 1976, Behavior of trace elements during magmatic processes — a summary of theoretical models and their applications: Journal of Research U.S. Geological Survey, v. 4, p. 41-47.

Baker, D.R. and Eggler, D.H., 1987, Compositions of anhydrous and hydrous melts coexisting with plagioclase, augite, and olivine or low-calcium pyroxene from one atmosphere to 8 kbar: Application to the Aleutian volcanic center of Atka: American Mineralogist, v. 72, p. 12-28.

Boyer, S.E. and Elliott, D., 1982, Thrust systems: American Association of Petroleum Geologists Bulletin, v. 66, p. 1196-1230.

Brady, J.B. and McCallister, R.H., 1983, Diffusion data for clinopyroxenes from homogenization and self-diffusion experiments: American Mineralogist, v. 68, p. 95-105.

Carpenter, J.R. and Phyfer, D.W., 1975, Olivine compositions from southern Appalachian ultramafics: Southeastern Geology, v. 16, p. 169-172.

Cook, F.A., Albaugh, D.S., Brown, L.D., Kaufman, S., Oliver, J.E., and Hatcher, R.D., Jr., 1979, Thin-skinned tectonics in the crystalline southern Appalachians, COCORP seismic-reflection profiling of the Blue Ridge and Piedmont: Geology, v. 7, p. 563-567.

Dallmeyer, R.D., 1974, Eclogite inclusions in an alpine peridotite sill, Georgia-North Carolina: Their chemistry and petrogenetic evolution: American Journal of Science, v. 274, p. 356-377.

Duke, J.M., 1976, Distribution of the period four transition elements among olivine, calcic clinopyroxene and mafic silicate liquid: Experimental Results: Journal of Petrology, v. 17, p. 499-521.

Eggers, M.B., 1983, Geology of the Kimsey Bald mafic body, southwest North Carolina: Geological Society of America Abstracts with Programs, v. 15, p. 51.

Ellis, D.J. and Green, D.H., 1979, An experimental study of the effect of Ca upon garnet-clinopyroxene exchange equilibria: Contributions to Mineralogy and Petrology, v. 71, p. 13-22.

Essene, E.J., 1982, Geological thermometry and barometry: In: Ferry, J.M. (ed.), Characterization of Metamorphism through Mineral Equilibria, Minera-

logical Society of America Reviews in Mineralogy, v. 10, p. 153-206.
Fullagar, P.D., Hatcher, R.D., Jr., and Merschat, C.E., 1979, 1200 m.y.-old gneisses in the Blue Ridge province of North and South Carolina: Southeastern Geology, v. 20, p. 69-77.
Goldberg, S.A., Butler, J.R., and Fullagar, P.D., 1986, The Bakersville dike swarm: Geochronology and petrogenesis of Late Proterozoic basaltic magmatism in the Southern Appalachian Blue Ridge: American Journal of Science, v. 286, p. 403-430.
Green, D.H. and Ringwood, A.E., 1967, An experimental investigation of gabbro to eclogite transformation and its petrological applications: Geochimica Cosmochima Acta, v. 31, p. 767-833.
Hadley, J.B., 1949, Preliminary report on corundum deposits in the Buck Creek peridotite, Clay County, North Carolina: U.S. Geological Survey Bulletin. 948-E, p. 103-128.
Hadley, J.B. and Nelson, A.E., 1971, Geological map of the Knoxville quadrangle, North Carolina, Tennessee, and South Carolina: U.S. Geological Survey Miscellaneous Investigations Map I-654.
Harris, L.D. and Boyer, K.C., 1979, Sequential development of the Appalachian orogen above a master decollement — a hypothesis: Geology, v. 7, p. 568-572.
Hartley, M.E., 1973, Ultramafic and related rocks in the vicinity of Lake Chatuge: Geological Survey of Georgia Bulletin, v. 85, 61 p.
Hatcher, R.D., Jr., 1977, Macroscopic polyphase folding illustrated by the Toxaway dome, eastern Blue Ridge, South Carolina-North Carolina: Geological Society of America Bulletin, v. 88, p. 1678-1688.
Hatcher, R.D., Jr., 1978, Tectonics of the western Piedmont and Blue Ridge, Southern Appalachians: Review and speculation: American Journal of Science, v. 278, p. 276-304.
Hatcher, R.D., Jr. and Butler, J.R., 1979, Guidebook for Southern Appalachian field trip in the Carolinas, Tennessee, and northeastern Georgia: International Geological Correlation Project, Caledonide Orogen Project, 117 p.
Hatcher, R.D., Jr., Hopson, J.L., Edelman, S.H., Liu, A., McLennan, E.A., and Stieve, A.L., 1987, Geology of the Appalachian Ultradeep Core Hole (ADCOH) site area: Detailed map and cross-sections of a major part the crystalline Southern Appalachians.: Geological Society of America Abstracts with Programs, v. 19, p. 89.
Hess, H.H., 1955, Serpentines, orogeny, and epeirogeny: Geological Society of America Special Paper 62, p. 391-408.
Hunter, C.E., 1941, Forsterite olivine deposits of North Carolina and Georgia: North Carolina Division Mineral Resources Bulletin 41, 117 p.
Jones, L.M., Hartley, M.E., and Walker, R.L., 1973, Strontium isotopic composition of alpine-type ultramafic rocks in the Lake Chatuge district, Georgia-North Carolina: Contributions to Mineralogy and Petrology, v.38, p. 321-327.
Keith, A., 1907a, Nantahala Folio: U.S. Geological Survey Geological Atlas of the United States Folio 143.
Keith, A., 1907b, Pisgah Folio: U.S. Geological Survey Geological Atlas of the

United States Folio 147.
Kellberg, J.M., 1943, Basic intrusives in the Chatuge Reservoir: Tennessee Valley Authority Report.
Kellberg, J.M., 1947, Basic intrusives in the Chatuge Reservoir in North Carolina and Georgia: Geological Society of America Abstracts, Annual Meeting, Ottawa, p. 1199.
Kittelson, R.C. and McSween, H.Y., 1987, The amphibolite to granulite facies transition in the Blue Ridge, Macon County, N.C.: Geological Society of America Abstracts with Programs, v. 19, p. 93.
Kuntz, M.A. and Hedge, C.E., 1981, Petrology and major-element, minor-element, and Rb-Sr geochemistry of the ophiolite complex at Buck Creek, North Carolina: EOS (Transactions of the American Geophysical Union), v. 62, p. 1088.
Lasaga, A.C., 1983, Geospeedometry: An extension of geothermometry: In: Saxena, S.K. (ed.), Kinetics and Equilibrium in Mineral Reactions, Advances in Physical Chemistry, v. 3, Springer-Verlag, New York, p. 81-114.
Lasaga, A.C., Richardson, S.M., and Holland, H.D., 1977, The mathematics of cation diffusion and exchange between silicate minerals during retrograde metamorphism: In: Saxena, S.K. and Bhattachanji, S. (ed.) Energetics of Geologicl Processes, Springer-Verlag, New York, p. 353-388.
Lindsley, D.H., 1983, Pyroxene thermometry: American Mineralogist, v. 68, p. 477-493.
Meen, J.K., 1987a, Experimental evidence for production of $K_2O$-enrichment without $SiO_2$-enrichment by fractional crystallization of dry basaltic magma at 10-15 kbar: Geological Society of America Abstracts with Programs v. 19, p. 769.
Meen, J.K., 1987b, Formation of shoshonites from calcalkaline basalt magmas: Geochemical and experimental constraints from the type locality: Contributions to Mineralogy and Petrology, v. 97, p. 333-351.
Miller, C.F. and Kish, S.A., 1980, Peraluminous trondhjemite, Whiteside pluton, North Carolina: Geological Society of America Abstracts with Programs, v.12, p. 201.
Miller, C.F., Sando, T.W., Fullagar, P.D. and Kish, S.A., 1983, Low potassium plutonism in the Blue Ridge of North Carolina and northern Georgia: Geological Society of America Abstracts with Programs, v. 15, p. 46.
Misra, K.C. and Keller, F.B., 1978, Ultramafic bodies in the southern Appalachians: American Journal of Science, v. 278, p. 389-418.
Monrad, J.R. and Gulley, G.L., 1983, Age and P-T conditions during metamorphism of granulite-facies gneisses, Roan Mountain, NC-TN: Carolina Geological Society Field Trip Guidebook, Carolina Geological Society Society Article IV.
Newton, R.C. and Perkins, D. III, 1982, Thermodynamic calibration of geobarometers based on the assemblages garnet-plagioclase-orthopyroxene (clinopyroxene)-quartz: American Mineralogist, v. 67, p. 203-222.
Rankin, D.W., Espenshade, G.H., and Neuman, R.D., 1972, Geologic map of the western half of the Winston-Salem quadrangle, North Carolina, Virginia,

Rodgers, J., 1970, The tectonics of the Appalachians: Wiley-Interscience, New York, 271 p.

Roeder, P.L. and Emslie, R.F., 1970, Olivine-liquid equilibria: Contributions to Mineralogy and Petrology, v. 29, p. 275-289.

Sack, R.O., Carmichael, I.S.E., Rivers, M. and Ghiorso, M.S., 1980, Ferric-ferrous equilibria in natural silicate liquids at 1 bar: Contributions to Mineralogy and Petrology, v. 75, p. 369-376.

Sailor, R.V. and Kuntz, M.A., 1973, Petrofabric and textural evidence for syntectonic recrystallization of the Buck Creek dunite, North Carolina: Geological Society of America Abstracts with Programs, v. 5, p. 791-792.

Shaw, H.F. and Wasserburg, G.J., 1984, Isotopic constraints on the origin of the Appalachian mafic complexes: American Journal of Science, v. 284, p. 319-349.

Sparks, R.S.J., Meyer, P., and Sigurdsson, H., 1980, Density variation amongst mid-ocean ridge basalts: Implications for magma mixing and the scarcity of primitive lavas: Earth and Planetary Science Letters, v. 46, p. 419-430.

Spear, F.S., 1981, An experimental study of hornblende stability and compositional variability in amphibolite: American Journal of Science, v. 281, p. 697-734.

Stolper, E. and Walker, D., 1980, Melt density and the average composition of basalt: Contributions to Mineralogy and Petrology, v. 74, p. 7-12.

Streckeisen, A., 1976, To each plutonic rock its proper name: Earth Science Reviews, v. 12, p. 1-33.

# SOURCE CONSTRAINTS BASED ON BIOTITE ANALYSES FOR THE 47 MA CASTLE HAYNE BENTONITE, NORTH CAROLINA

ROBERT L. NUSBAUM — *Department of Geology, College of Charleston Charleston, SC 29424*

PAUL A. THAYER
W. BURLEIGH HARRIS — *Department of Earth Sciences, University of North Carolina at Wilmington, Wilmington, NC 28403*

## ABSTRACT

Bentonite (46 Ma) forms a relatively thin (60 cm maximum thickness) lens within the mid-Eocene Castle Hayne Limestone of the North Carolina Coastal Plain. Evidence of pyroclastic origin for the bentonite includes abundant smectite, euhedral pyroclasts, and relict pyroclastic textures.

Microprobe analysis of biotite grains reveals that they: 1) are unzoned with preservation of magmatic character for 87% of the population; 2) are homogeneous with respect to grain size and composition; 3) crystallized in magma of intermediate (dacitic or trachytic?) composition; and 4) have anomalously high BaO values ($\bar{\chi}$ = 1.06 wt%). Biotite crystals could have traveled up to about 4000 km from the source area based on long diameter measurements for 200 grains ($\bar{\chi}$ = 1.95$\phi$ = 0.26 mm).

We propose that the source of Castle Hayne bentonite is the Highland County, Virginia igneous complex based on age considerations, proximity, and suitable lithologies.

## INTRODUCTION

Bentonite of demonstrable volcanic origin is rare in the Atlantic Coastal Plain (Jordan and Adams, 1962) compared to the Gulf Coastal Plain. That difference presumably reflects proximity to volcanic sources. Thayer and others (1986) described a bentonite at the Fussell Quarry that forms a thin (60 cm maximum thickness) lens within middle Eocene Castle Hayne Limestone of the North Carolina Coastal Plain (Figure 1). Evidence for a volcanic origin includes: 1) abundant smectite, presumably altered from volcanic glass; 2) medium sand- to silt-sized, unaltered biotite and apatite euhedra; and 3) relict pumice and glass shard features (columnules and honeycomb texture, respectively). These characteristics are ubiquitous among the samples studied by Thayer and others (1986). Based on age and distribution, they speculated that the origin for the volcanic ash was either the Highland County, Virginia, hypabyssal intrusive complex, or Bermuda.

This report presents biotite compositions determined by electron microprobe analysis of more than 250 spots on about 100 grains of biotite from the Castle Hayne bentonite. We also provide size characteristics for the biotite population. Data reported here provide constraints regarding: 1) the original composition of the pyroclastic air-fall material; 2) the degree of magmatic character preserved in the biotite population; and 3) the source for the pyroclastic material.

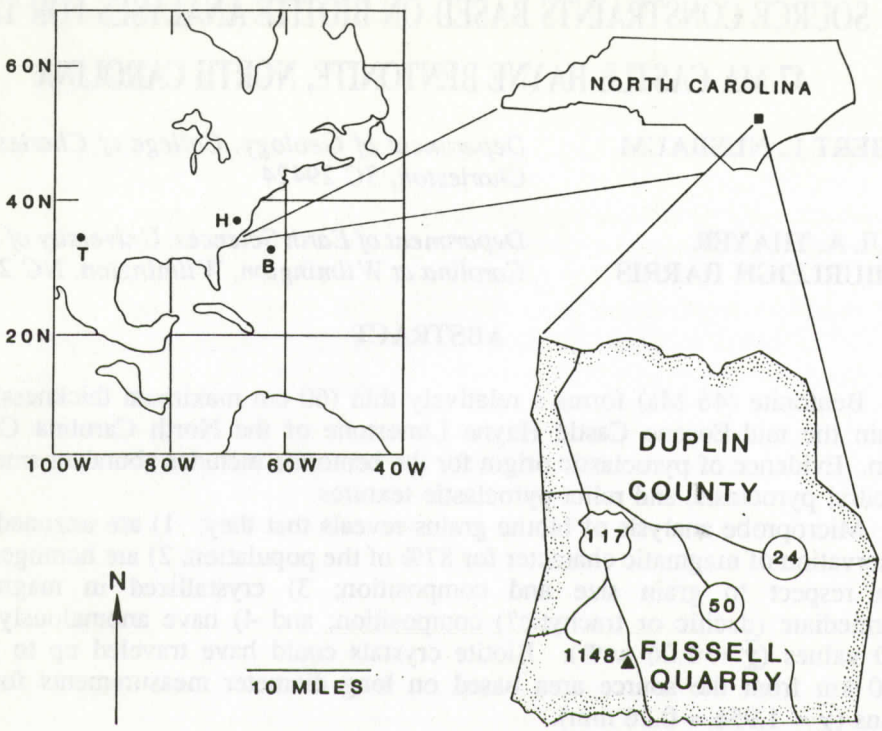


**Figure 1. Index map showing location of Fussell Quarry, Highland County hypabyssal complex (H), Trans-Pecos Igneous Province (T), and the reconstructed position of North America relative to Bermuda (B) during Claibornian time (50 Ma) (Morgan, 1983).**

## STRATIGRAPHY

Unconsolidated sandy, bryozoan biocalcarenite of Castle Hayne Limestone at the Fussell Quarry represents two middle Eocene depositional sequences that are separated by a regional unconformity (Zullo and Harris, 1987). Zullo and Harris (1987) designated the sediments that contain the bentonite lens depositional sequence 1, and on the basis of the echinoids *Protoscutella mississippiensis rosehillensis* and *Santeelampas oviformis*, a small oyster of the genus *Cubitostrea*, and calcareous nannofossils *Chiasmolithus gigas* and *C. solitus* (Worsley and Laws, 1986), correlated the sequence to Okada and Bukry's (1980) CP13b Zone or Martini's (1971) NP15 Zone. Jones (1983) studied samples from the Fussell Quarry for planktonic foraminifera, and assigned the sediments to Blow's (1969) foraminiferal zones P12-13. Therefore, using microfauna and megafauna, Zullo and Harris (1987) correlated biocalcarenite beds containing the bentonite at the Fussell Quarry to the middle Eocene (Claibornian) Lower Lisbon Formation of Alabama.

## BIOTITE GRAIN SIZE

Euhedral biotite pyroclasts (Figure 2) are ubiquitous throughout the Castle Hayne bentonite; however, they seldom comprise more than 0.3 percent of the

whole-rock volume. Scanning electron microscopy of numerous bentonite samples coupled with petrographic examination of more than 30 smear slides indicates that most biotite grains are coarser than 4.5ϕ (44 mm; U.S. #325 mesh).

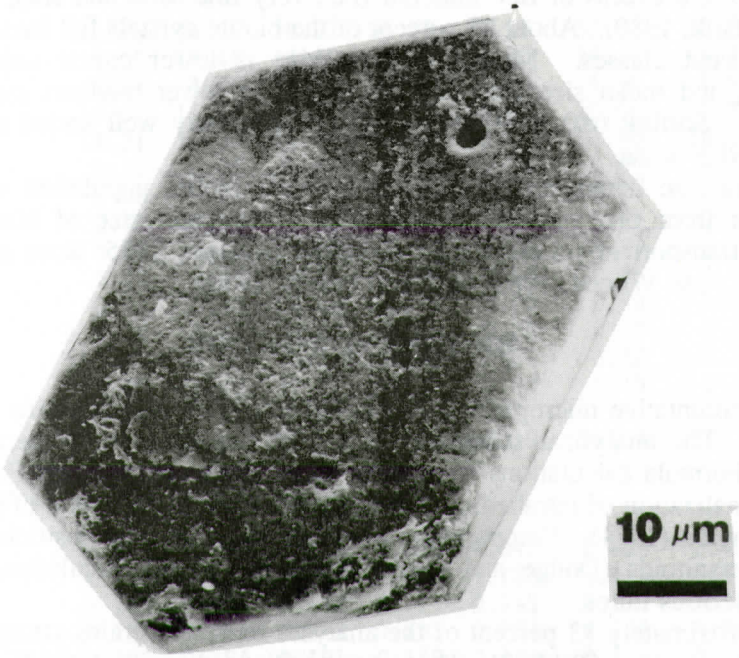


**Figure 2. Scanning electron micrograph of euhedral, pseudohexagonal biotite crystal. Grain size is very fine sand.**

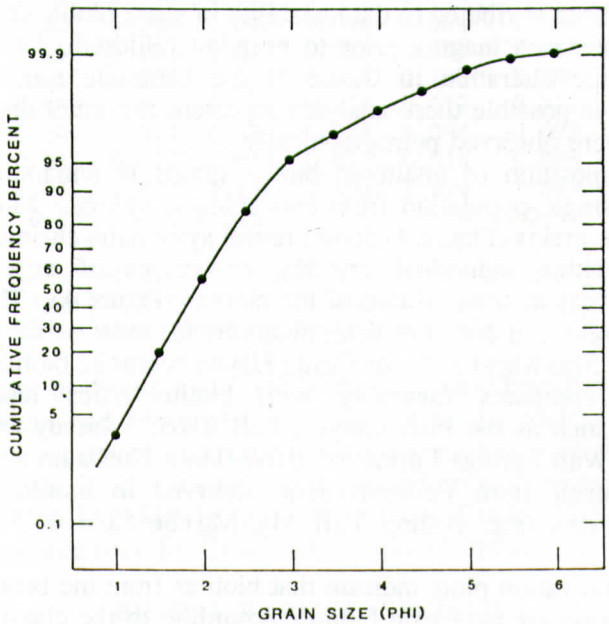


**Figure 3. Cumulative frequency curve (probability ordinate) showing grain-size distribution of biotite crystals from Castle Hayne bentonite.**

Figure 3 is a cumulative frequency curve showing maximum diameter grain-size distribution of biotite crystals from the Castle Hayne bentonite. The curve shows a slight excess of fine material (i.e., very fine sand and silt), and is fine-skewed (Folk, 1980). About 95 percent of the biotite cyrstals fall into the fine and medium sand classes. Maximum grain size is lower coarse sand (0.86$\phi$ = 0.55mm), and mean size (Mz of Folk, 1980) is lower medium sand (1.95$\phi$ = 0.26mm). Sorting ($\sigma$I) is 0.54$\phi$, which is moderately well sorted according to Folk's (1980) scale.

Grain size homogeneity indicates a single biotite population and suggests derivation from one volcanic source area. The grain size of biotite euhedra suggests transport of no more than 4000 km (Amajor, 1985; Rose and Chesner, 1987; Izett and Wilcox, 1982; Izett and others, 1970).

## BIOTITE COMPOSITION

Representative microprobe analyses for unaltered biotite grains are listed in Table 1. The analytical scheme used is that described by Solberg and Speer (1982). Formula calculations were done by methods described by Foster (1960), with normalization of tetrahedral and octahedral cations to a total of seven (7) as per Ludington (1974). Comparison to biotites of similar composition from Sierra Nevada granitoids (Dodge and others, 1969) facilitated calculation of cationic ferric to ferrous ratios.

Approximately 13 percent of the analyses represent grains strongly deficient in interlayer cations (Table 2). These compositions show depleted K and addition of Ca to twelve-fold sites, which is required to balance the overall charge. Total oxide values are lower due to an excess of water in the structure. This type of alteration has been attributed to the instability of some biotite crystals residing near the top of water-rich magma prior to eruption (Hildreth, 1977). Although the origin of biotite alteration in Castle Hayne bentonite samples is not clearly understood, it is possible these analyses represent the small detrital population of biotites that were observed petrographically.

The composition of unaltered biotite grains is remarkably homogeneous, suggesting a single population from one volcanic source. Microprobe traverses across 3 biotite grains (Figure 4) do not reveal systematic chemical zoning of oxide components within individual crystals, or groups of crystals. Minor Fe-enrichment occurs in cores of two of the biotites (Figure 4). This pattern was not observed, however, in core-rim determinations for most of the biotite population. Mean cationic $Mg/(Mg+Fe^{2+})$ for Castle Hayne bentonite biotite samples is 0.67 $\pm$ 0.01, which compares favorably with biotite ratios reported for dacitic compositions such as the Fish Canyon Tuff (0.65; Whitney and Stormer, 1985), and the Wah Wah Springs Formation (0.66-0.69); Nusbaum and Grant, in prep.). Low ratios result from Fe-enrichment observed in biotites from high silica magmatic systems (e.g. Bishop Tuff $Mg/(Mg+Fe^{2+})$ = 0.45 to 0.50; Hildreth, 1977).

Octahedral cation plots indicate that biotites from the bentonite in the Castle Hayne Limestone are magnesio-biotites according to the classification scheme of Foster (1960). We compare our data with those for tuffs and plutons studied in mineralogic and petrologic detail (Figure 5). Castle Hayne biotites overlap with

Table 1. Representative Biotite Analyses.

| | 238 | 237 | 408 | 410 | 63 | 64 | Mean + S.D. (n = 218) |
|---|---|---|---|---|---|---|---|
| $SiO_2$ | 36.65 | 36.36 | 36.81 | 36.65 | 37.16 | 37.52 | 36.23±0.55 |
| $Al_2O_3$ | 14.55 | 14.45 | 14.40 | 14.44 | 14.35 | 14.18 | 14.34±0.32 |
| $TiO_2$ | 4.75 | 4.86 | 4.89 | 4.94 | 4.58 | 4.59 | 4.87±0.20 |
| FeO* | 14.98 | 15.14 | 14.86 | 14.65 | 15.05 | 15.05 | 15.31±0.41 |
| MgO | 14.31 | 14.30 | 14.16 | 14.37 | 14.18 | 13.88 | 14.03±0.35 |
| MnO | 0.13 | 0.16 | 0.13 | 0.12 | 0.15 | 0.09 | 0.15±0.03 |
| CaO | 0.08 | 0.05 | 0.09 | 0.04 | 0.05 | 0.07 | 0.06±0.04 |
| $Na_2O$ | 0.45 | 0.59 | 0.49 | 0.57 | 0.63 | 0.57 | 0.56±0.07 |
| $K_2O$ | 8.01 | 8.08 | 8.12 | 8.04 | 8.32 | 8.29 | 8.15±0.10 |
| BaO | 1.13 | 1.14 | 0.83 | 1.23 | 0.58 | 0.66 | 1.06±0.18 |
| F | 0.42 | 0.40 | 0.38 | 0.35 | 0.40 | 0.39 | 0.44±0.08 |
| Cl | 0.24 | 0.23 | 0.26 | 0.21 | 0.13 | 0.12 | 0.19±0.07 |
| $H_2O$** | 3.77 | 3.77 | 3.78 | 3.80 | 3.81 | 3.82 | 3.74±0.05 |
| O=F+Cl | -0.23 | -0.22 | -0.22 | -0.20 | -0.20 | -0.19 | 0.23±0.03 |
| Total | 99.24 | 99.43 | 98.98 | 99.27 | 99.19 | 99.04 | 98.13±0.89 |
| Tetrahedral and octahedral cations = 7 | | | | | | | |
| Si | 2.809 | 2.792 | 2.828 | 2.814 | 2.847 | 2.885 | 2.798±0.029 |
| Al(IV) | 1.191 | 1.208 | 1.172 | 1.186 | 1.153 | 1.115 | 1.202±0.029 |
| Al(VI) | 0.123 | 0.100 | 0.132 | 0.121 | 0.143 | 0.170 | 0.103±0.028 |
| Ti | 0.274 | 0.281 | 0.283 | 0.285 | 0.264 | 0.265 | 0.283±0.011 |
| $Fe^{3+}$* | 0.192 | 0.194 | 0.191 | 0.188 | 0.193 | 0.194 | 0.198±0.006 |
| $Fe^{2+}$ | 0.768 | 0.778 | 0.764 | 0.753 | 0.771 | 0.774 | 0.791±0.022 |
| Mg | 1.635 | 1.637 | 1.622 | 1.645 | 1.619 | 1.591 | 1.165±0.037 |
| Mn | 0.008 | 0.010 | 0.008 | 0.008 | 0.010 | 0.006 | 0.009±0.002 |
| Ca | 0.006 | 0.004 | 0.007 | 0.003 | 0.004 | 0.006 | 0.005±0.003 |
| Na | 0.065 | 0.085 | 0.071 | 0.082 | 0.091 | 0.082 | 0.081±0.010 |
| K | 0.760 | 0.768 | 0.771 | 0.764 | 0.788 | 0.786 | 0.779±0.010 |
| Ba | 0.033 | 0.033 | 0.024 | 0.036 | 0.017 | 0.019 | 0.031±0.005 |
| F | 0.099 | 0.094 | 0.089 | 0.082 | 0.094 | 0.092 | 0.105±0.018 |
| Cl | 0.030 | 0.029 | 0.033 | 0.027 | 0.016 | 0.015 | 0.024±0.009 |
| OH** | 1.871 | 1.877 | 1.878 | 1.891 | 1.890 | 1.893 | 1.871±0.017 |
| $Mg/(Fe^{2+}+Mg)$ | 0.68 | 0.68 | 0.67 | 0.69 | 0.68 | 0.67 | 0.671±0.010 |

*Total Fe determined as FeO. $Fe^{3+}$ calculated by comparison to biotites of similar composition (Dodge and Others, 1969).
**OH and $H_2O$ calculated assuming 2 equivalents per formula.

analyses of biotites in dacitic rocks, while rhyolitic (and granitic) biotite analyses show Fe-enrichment and Mg-depletion compared to the dacitic biotites. Setter and Adams (1986) observed identical trends for a suite of calc-alkaline intrusive rocks of intermediate to felsic composition. Based on the comparisons illustrated in Figure 5 and the $Mg/(Mg+Fe^{2+})$ ratio for the Castle Hayne bentonite, we suggest that the source rock for these biotites was of intermediate composition.

## BIOTITE BARIUM CONTENT

Analyses of unaltered Castle Hayne biotites (Table 1) reveal a BaO content

Table 2. Representative interlayer cation deficient biotite analyses.

| | 10 | 11 | 418 | 431 | | 10 | 11 | 418 | 431 |
|---|---|---|---|---|---|---|---|---|---|
| | | | | | Tetrahedral & octahedral cations = 7 | | | | |
| $SiO_2$ | 36.36 | 36.31 | 36.45 | 35.78 | Si | 2.831 | 2.799 | 2.793 | 2.824 |
| $Al_2O_3$ | 13.95 | 14.18 | 14.35 | 13.43 | Al(IV) | 1.168 | 1.201 | 1.207 | 1.176 |
| $TiO_2$ | 4.83 | 5.06 | 5.09 | 4.95 | Al(VI) | 0.133 | 0.087 | 0.089 | 0.073 |
| FeO* | 15.36 | 15.65 | 15.10 | 18.17 | Ti | 0.283 | 0.293 | 0.293 | 0.294 |
| MgO | 13.72 | 13.93 | 14.36 | 12.04 | $Fe^{3+}$** | 0.200 | 0.202 | 0.194 | 0.240 |
| MnO | 0.16 | 0.15 | 0.16 | 0.27 | $Fe^{2+}$ | 0.800 | 0.807 | 0.744 | 0.959 |
| CaO | 1.27 | 0.66 | 1.13 | 2.52 | Mg | 1.593 | 1.601 | 1.640 | 1.416 |
| $Na_2O$ | 0.32 | 0.40 | 0.42 | 0.12 | Mn | 0.011 | 0.010 | 0.010 | 0.018 |
| $K_2O$ | 5.84 | 6.98 | 6.12 | 3.56 | Ca | 0.103 | 0.053 | 0.090 | 0.207 |
| BaO | 0.79 | 0.72 | 0.80 | 0.45 | Na | 0.047 | 0.058 | 0.061 | 0.018 |
| F | 0.48 | 0.55 | 0.42 | 0.43 | K | 0.563 | 0.666 | 0.581 | 0.349 |
| Cl | 0.16 | 0.14 | 0.28 | 0.34 | Ba | 0.023 | 0.021 | 0.023 | 0.014 |
| $H_2O$** | 3.70 | 3.71 | 3.75 | 3.61 | F | 0.115 | 0.130 | 0.099 | 0.104 |
| O=F+L | -0.24 | -0.26 | -0.24 | -0.26 | Cl | 0.020 | 0.018 | 0.035 | 0.044 |
| | | | | | CH** | 1.865 | 1.852 | 1.866 | 1.851 |
| Total | 96.70 | 98.18 | | 98.18 | 95.41 | | | | |

*Total Fe determined as FeO. $Fe^{3+}$ calculated by comparison to biotites of similar composition (Dodge and others, 1969)
**OH and $H_2O$ calculated assuming 2 equivalents per formula.

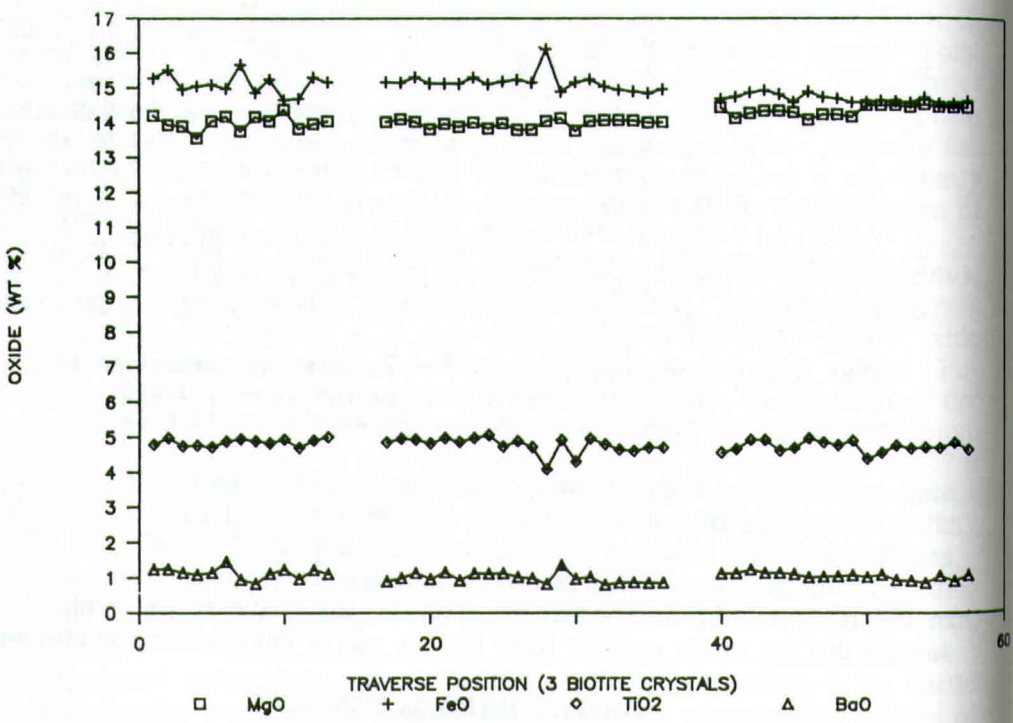


Figure 4. Oxide traverses for three separate biotite crystals from the Castle Hayne bentonite. Total Fe reported as FeO.

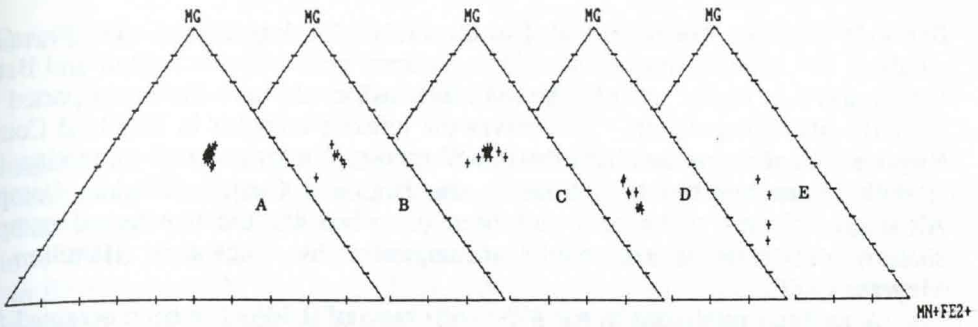


**Figure 5. Octahedral cation compositional plots for biotite analyses. (A) Castle Hayne biotite (n = 70); (B) Fish Canyon Tuff biotites (n = 8; Whitney and Stormer, 1985); (C) Wah Wah Springs Formation (n = 20; Nusbaum and others, in prep.); (D) Bishop Tuff biotites (n = 14; Hildreth, 1977); and (E) Sierra Nevada granite biotites (n = 4; Dodge and others, 1969). R3 = $Fe^{3+} + Ti^{4+} + Al(VI)^{3+}$.**

that ranges from 0.58 to 1.55 weight percent ($\bar{\chi}$ BaO=1.06). These values are markedly higher than those for samples from the Wah Wah Springs Formation ($\bar{\chi}$ BaO=0.66; Nusbaum and Grant, in prep.), and Fish Canyon Tuff ($\bar{\chi}$ BaO=0.18 wt%; Whitney and Stormer, 1985). BaO values for Bishop Tuff samples are even lower ($\bar{\chi}$ BaO=0.08 wt%; Hildreth, 1977). Because of similar ionic size, Ba substitutes for K in the interlayer sites and demonstrates compatible behavior (Mahood and Hildreth, 1983; Schnetzler and Philpotts, 1970; Higuchi and Nagasawa, 1969).

Most igneous biotites contain less than 1 weight percent BaO (Speer, 1984). We interpret the unusually high BaO content of Castle Hayne bentonite biotites as indicative of a source rock with some alkalic character. Rocks of intermediate to mafic compositions that are strongly alkalic would have much higher BaO contents (e.g., 7.32 wt% BaO in leucitite; Thompson, 1977).

## SOURCE AREA CONSTRAINTS

The biotite crystals from the bentonite in the Castle Hayne Limestone are generally unaltered and have preserved magmatic character. They crystallized in magma of intermediate composition (dacitic or trachytic?) that was enriched in BaO. Based on grain size data, the biotite crystals could have traveled up to about 4000 km from the source area. Areas that experienced this type of igneous activity coeval with the age of the Castle Hayne bentonite (46 Ma; Fullagar and Harris, 1988) include: 1) the Trans-Pecos province, Texas (Price and others, 1986); 2) the Highland County, Virginia complex (Fullagar and Bottino, 1969; Johnson and others, 1971; Kettren, 1971; Rader and others, 1986); and 3) Bermuda (Tucholke and others, 1979).

Of these possible source areas, two can be shown to be unlikely. Bentonites are generally less than 10 cm thick (Fisher and Schmincke, 1984) and thicker accumulations are thought to imply a relatively close source. Thayer and others (1986) reported that the Castle Hayne bentonite is up to 60 cm thick, and has not undergone extensive reworking. Using this argument, the Trans-Pecos province can be effectively eliminated as a likely source for the pyroclastic material.

Bermuda is closer, but it is located to the east of the depositional site. Prevailing winds at this latitude during the middle Eocene were westerlies (Dott and Batten, 1988), and it is highly unlikely that volcanic ash could have been transported to a westerly site of deposition. This leaves the igneous complex in Highland County, Virginia. Confirming this hypothesis will require further research on biotites (and apatites) from hypabyssal plutons in the Highland County, Virginia Complex. Although volcanic rocks have not been described for the hypabyssal complex, shallow plutonism is commonly accompanied by volcanism (Hamilton and Meyers, 1967).

A recently published initial 87Sr/86Sr ratio of 0.7063 has been obtained from Castle Hayne apatite pyroclasts (Fullager and Harris, 1988). This value is high compared to a range of whole rock initial 87Sr/86Sr ratios reported for the Highland County, Virginia Complex (0.7035-0.7055, Fullagar and Bottino, 1969). Nevertheless, the range of values is large indicating isotopic variability within the complex. It is conceivable that additional isotopic work in the complex would produce values comparable to those published for Castle Hayne apatite crystals.

## CONCLUSION

This study documents compositional and size characteristics of biotite crystals in the Castle Hayne bentonite. Magmatic compositions are preserved in 87% of the biotites analyzed. Unaltered biotites are unzoned and have remarkably uniform compositions with $Mg/(Mg+Fe^{2+}) = 0.67 \pm 0.01$. The composition of the original pyroclastic rock was intermediate. Castle Hayne biotites compare favorably with biotites from rocks of dacitic composition . We favor a source with mild alkalic character owing to unusually high BaO (1 wt%) in Castle Hayne biotites.

Castle Hayne biotite crystals are dominantly euhedral with maximum lengths (per crystal) ranging from silt, to coarse sand-sized. Maximum grain size is 0.86$\phi$ (0.55 mm) and the mean size for the population is 1.95$\phi$ (0.26 mm). Biotites are moderately well-sorted (0.54$\phi$). Grain size and compositional homogeneity support a single volcanic source. The thickness of the bentonite (60 cm) limits the source area to the southeastern United States.

Based on the age of the Castle Hayne bentonite and data provided herein, we propose that the source of the Castle Hayne bentonite is the Highland County, Virginia igneous complex. Volcanic rocks in the complex have not been recognized; however, they could have been denuded (Johnson and others, 1971). Given the hypabyssal nature of the complex, it is likely that coeval volcanics existed. Confirmation of this hypothesis will require acquisition of compositional data for biotites (and apatites) from the Highland County, Virginia complex.

## ACKNOWLEDGEMENTS

R. L. Nusbaum is grateful to Todd Solberg for assistance in microprobing biotite crystals. The analyses were preformed at the microprobe facility, Virginia Polytechnic Institute and State University. G. A. Izett and J. A. Speer provided helpful discussions during the course of research. J. L. Carew reviewed an earlier version of this manuscript. P. D. Fullagar provided a thorough review which

improved the manuscript. Joan Newell typed the manuscript.

## REFERENCES CITED

Amajor, L.C., 1985, Biotite grain size distribution and source area of the Lower Cretaceous Viking bentonites, Alberta, Canada: Bulletin of Canadian Petroleum Geology, v. 33, p. 471-478.

Blow, W.H., 1969, Late middle Eocene planktonic foraminiferal biostratigraphy, *in* Bronnimman, R., and Renz, H.H., eds., Proceedings of the First International Conference on Planktonic Microfossils, Geneva, 1967, v. 1: Leiden, E.J. Brill, p. 199-421.

Dodge, F.C.W., Smith, V.C., and Mays, R.W., 1969, Biotites from granitic rocks of the central Sierra Nevada Batholith, California: Journal of Petrology, v. 10, p. 250-285.

Dott, R.H., and Batten, R.L., 1988, Evolution of the Earth: New York, McGraw-Hill, 643 p.

Fisher, R.V., and Schmincke, H.U., 1984, Pyroclastic Rocks: New York, Springer-Verlag, 472 p.

Folk, R.L., 1980, Petrology of Sedimentary Rocks: Austin, Texas, Hemphill Publishing Co., 182 p.

Foster, M.D., 1960, Interpretation of the composition of trioctahedral micas: U.S. Geological Survey Professional Paper 354-B, 49 p.

Fullagar, P.D., and Harris, W.B., 1988, Middle Eocene bentonite and glauconite from the Atlantic Coastal Plain, North Carolina: Comparison of radiometric ages: Geological Society of America Abstracts with Programs, v. 20, no. 4, p. 264-265.

Fullagar, P.D., and Bottino, M.L., 1969, Tertiary felsite intrusions in the Valley and Ridge Province, Virginia: Geological Society of America Bulletin, v. 80, p. 1853-1858.

Hamilton, W., and Myers, W.B., 1967, The nature of batholiths: U.S. Geological Survey Professional Paper 554-C, p. C1-C30.

Higuchi, H., and Nagasawa, H., 1969, Partition of trace elements between rock-forming minerals and the host volcanic rocks: Earth and Planetary Science Letters, v. 7, p. 281-287.

Hildreth, E.W., 1977, The magma chamber of the Bishop Tuff: Gradients in temperature, pressure, and composition: Unpublished Ph.D. dissertation, University of California, Berkeley, 328 p.

Izett, G.A., and Wilcox, R.E., 1982, Map showing localities and inferred distributions of the Huckleberry Ridge, Mesa Falls, and Lava Creek ash beds (Pearlette Family ash beds) of Pliocene and Pleistocene age in the western United States and Canada: U.S. Geological Survey Miscellaneous Investigations Map I-325.

Izett, G.A., Wilcox, R.E., Powers, H.A., and Desborough, G.A., 1970, The Bishop ash bed, a Pleistocene marker bed in the western United States: Quaternary Research, v. 1, p. 121-132.

Johnson, R.W., Milton, C., and Dennison, J.M., 1971, Field trip to the igneous rocks of Augusta, Rockingham, Highland, and Bath Counties, Virginia: Virginia Division of Mineral Resources, Information Circular 16, 67 p.

Jones, G.D., 1983, Foraminiferal biostratigraphy and depositional history of the Coastal Plain of North Carolina: North Carolina Department of Natural Resources and Community Development, Geological Survey Section, Special Publication 8, 80 p.

Jordan, R.R., and Adams, J.K., 1962, Early Tertiary bentonite from the subsurface of central Delaware: Geological Society of America Bulletin, v. 73, p. 395-398.

Kettren, L.P., 1971, Igneous intrusions in the Monterey area, Highland County, Virginia, *in* Lowry, W.D., Tillman, C.G., Fara, M., and Kettren, L.P., eds., Guidebook to contrasting style of deformation of the southern and central Appalachians of Virginia: Virginia Polytechnic Institute and State University, Blacksburg, Virginia, p. 70-96.

Ludington, S.D., 1974, Application of fluorine-hydroxyl exchange data to natural minerals: Unpublished Ph.D. dissertation, University of Colorado, Boulder, 167 p.

Mahood, G.A., and Hildreth, W. 1983, Large partition coefficients for trace elements in high silica rhyolites: Geochimica et Cosmochimica Acta, v. 47, p. 11-30.

Martini, E., 1971, Standard Tertiary and Quaternary calcareous nannoplankton zonation; in Frainacci, A., ed., Proceedings of the Second Planktonic Conference; Roma, Edizioni Technoscienza, p. 739-785.

Morgan, W.J., 1983, Hotspot tracks and early rifting of the Atlantic: Tectonophysics, v. 94, p. 123-139.

Nusbaum, R.L., and Grant, S.K., (in prep), Homogeneous, voluminous magmatism of the mid-Oligocene outflow member of the Wah Wah Springs Formation, Utah and Nevada.

Okada, H., and Bukry, D., 1980, Supplemental modification and introduction of code numbers to the low-latitude coccolith biostratigraphic zonation (Bukry, 1973, 1975): Marine Micropaleontology, v. 5, p. 321-325.

Price, J.G., Henry, C.D., Parker, D.F., 1986, Igneous geology of Trans-Pecos, Texas, Guidebook 23: Bureau of Economic Geology, Austin, Texas, 360 p.

Rader, E.K., Gathright, T.M., and Marr, J.D., 1986, Trimble Knob basalt diatreme and associated dikes, Highland County, Virginia, *in* Neathery, T.L., ed., Southeastern Section of the Geological Society of America, Centennial Field Guide Volume 6, p. 97-100.

Rose, W.I., and Chesner, C.A., 1987, Dispersal of ash in the great Toba eruption, 75 ka: Geology, v. 15, p. 913-917.

Schnetzler, C.C., and Philpotts, J.A., 1970, Partition coefficients of rare earth elements between igneous matrix material and rock-forming mineral phenocrysts-II: Geochimica et Cosmochimica Acta, v. 34, p. 331-340.

Setter, J.R., and Adams, J.S., 1986, Petrology and geochemistry of the Quitman Mountains, Hudspeth County, Texas, *in*, Price, J.G., Henry, C.D., Parker, D.F., eds., Igneous geology of Trans-Pecos Texas, Guidebook 23: Bureau of Economic Geology, Austin, Texas, p. 178-206.

Solberg, T.N., and Speer, J.A., 1982, QALL, A 16-element analytical scheme for efficient petrologic work on an automated ARL-SEMQ: Application to mica reference samples, *in*, Heinrich, K.F., Microbeam Analysis, San Francisco Press, Inc., San Francisco, California, p. 422-426.

Speer, J.A., 1984, Micas in igneous rocks, *in*, Bailey, S.W., Reviews in

Mineralogy, Micas: Mineralogical Society of America, v. 13, p. 299-356.
Thayer, P.A., Harris, W.B., and Zullo, V.A., 1986, Bentonite from the Eocene Castle Hayne Limestone, *in* Textoris, D.A., ed., SEPM Field Trip Guidebooks, Southeastern United States, Third Annual Meeting, Raleigh, N.C., Society of Economic Paleontologists and Mineralogists, p. 307-310.
Thompson, R.N., 1977, Primary basalts and magma genesis III, Albian Hills, Roman comagmatic province, central Italy: Contributions to Mineralogy and Petrology, v. 60, p. 91-103.
Tuchoke, B.E., and others, eds., 1979, Initial Reports of the Deep Sea Drilling Project 43: Washington, U.S. Government Printing, 1115 p.
Whitney, J.A., and Stormer, J.C., 1985, Mineralogy, petrology, and magmatic conditions from the Fish Canyon Tuff, central San Juan Volcanic Field, Colorado: Journal of Petrology, v. 26, p. 726-762.
Worsley, T.M., and Laws, R.A., 1986, Calcareous nannofossil biostratigraphy of the Castle Hayne Limestone; *in* Textoris, D.A., ed., SEPM Field Trip Guidebooks, Southeastern United States, Third Annual Meeting, Raleigh, N.C., Society of Economic Paleontologists and Mineralogists, p. 289-296.
Zullo, V.A., and Harris, W.B., 1987, Sequence stratigraphy, biostratigraphy, and correlation of Eocene through lower Miocene strata in North Carolina; *in* Ross, C.A., and Haman, D., eds., Timing and depositional history of eustatic cycles: constraints on seismic stratigraphy: Cushman Foundation for Foraminiferal Research, Special Publication 24, p. 197-214.

# THE STRUCTURE AND STRATIGRAPHY OF THE TALLASSEE SYNFORM, DADEVILLE BELT, ALABAMA

MICHAEL J. NEILSON

*Dept. of Geology,*
*The University of Alabama at Birmingham*
*Birmingham, AL, 35294*

## ABSTRACT

The Tallassee synform is the dominant $F_2$ structure in the western portion of the Dadeville belt of Alabama's Inner Piedmont. The lowest structural unit, the Ropes Creek Amphibolite, consists of mafic and felsic amphibolites and hornblende schists with small amounts of clastic material. The Agricola Schist, composed of pelitic and psammitic schists and gneisses, overlies the Ropes Creek Amphibolite. Both units are intruded by tonalitic and granitic plutons, the Camp Hill and Chattasofka Creek gneisses respectively, as well as mafic and ultramafic plutons of metanorite, metagabbro, and metaorthopyroxenite.

The earliest recognizable episode of deformation, which was synchronous with prograde regional metamorphism of Acadian age, generated isoclinal folds ($F_1$) on all scales. These folds were refolded by macroscopic, moderately open $F_2$ folds that include the Tallassee synform. The Brevard fault zone truncates $F_2$ structures.

The Ropes Creek Amphibolite was deposited in a back-arc basin and was followed by clastic sedimentation (Agricola Schist) at the onset of mountain building. Magmatic activity associated with subduction generated mafic complexes, and the Camp Hill and Chattasofka Creek gneisses.

## INTRODUCTION

The northern and western boundary of Alabama's Inner Piedmont is the Brevard fault zone; in the southwest Inner Piedmont rocks are covered by the Coastal Plain onlap. To the south, the Towaliga fault separates the Inner Piedmont from the Pine Mountain block. The Inner Piedmont consists of two lithologic belts that are separated by the Stonewall line: the Dadeville belt, dominated by metaigneous rocks; and the Opelika belt, composed predominantly of metasedimentary rocks (Bentley and Neathery, 1970). Two macroscopic second generation folds occur within the Dadeville belt: the Tallassee synform, which occupies the western part of the block in Tallapoosa County (Neathery, 1968), and the Boyds Creek synform, found in southeastern Chambers County adjacent to the Stonewall line (Bentley and Neathery, 1970).

Our present knowledge of the structure, stratigraphy, and tectonic evolution of Alabama's Inner Piedmont block is heavily dependent on the work of Neathery (1968) and Bentley and Neathery (1970). The ideas expressed in these papers are incorporated in regional geologic maps (Williams, 1978) and in tectonic models for the southern Appalachians (Hatcher, 1972, 1978; Hatcher and others, 1979).

Since 1970, Alabama's Inner Piedmont has been the focus of several

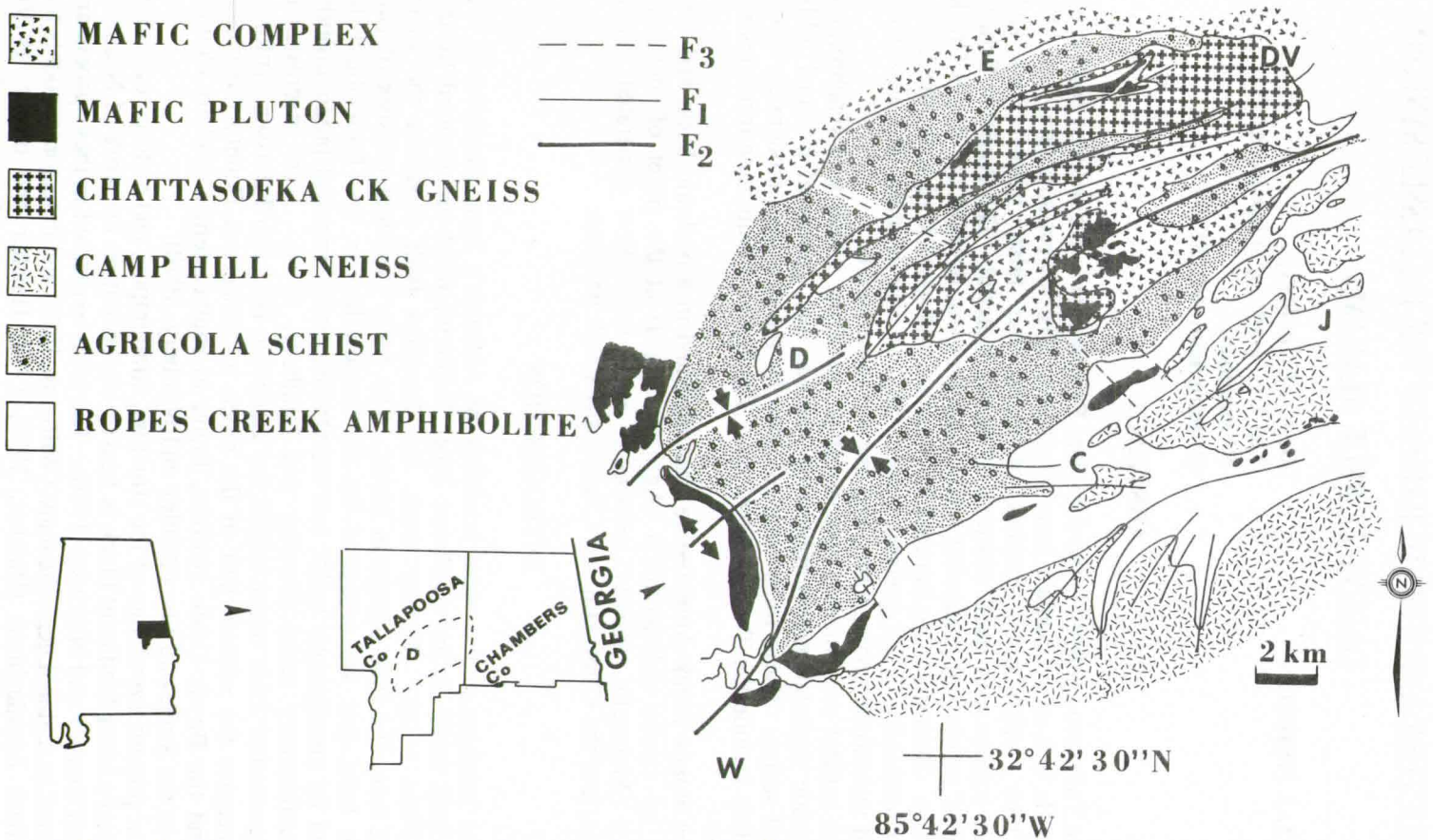


Figure 1. Geological Map of the Tallassee synform. Geology by C. Allison, J. Clark, G. Fleming, J. Monteith, T. Neathery, M. Neilson, A. Nunan, J. Robinson, J. Wilson. Localities: C = Camp Hill, D = Dadeville, DV = Dudleyville, J = Judson, W = Walnut Hill

research projects. Sears and others (1981) published results of their investigations in the southeastern part of the belt near Opelika, Alabama. Bittner and Cook (1987) have presented their mapping in the area between the Boyds Creek synform and the Tallassee synform. Clark (973) mapped the Seroyer Branch complex within the Tallassee synform. My students are I have mapped some 400 $km^2$ of the Dadeville belt within the Tallassee synform (Fleming and others 1980, Allison and Neilson, 1981; Neilson, 1983). This paper summarizes the results of our mapping, together with a comparison with the geology of the Inner Piedmont elsewhere in the southern Appalachians.

## GEOLOGY OF THE TALLASSEE SYNFORM

The geologic map of the Tallassee synform is shown in Figure 1. This map is a compilation of mapping by several people: acknowledgement is given in the caption to Figure 1.

### Stratigraphy

**The Ropes Creek Amphibolite:** This unit includes both the Ropes Creek Amphibolite of Bentley and Neathery (1970) and the Waverly Gneiss of Bentley and others (in press). The Ropes Creek Amphibolite crops out throughout much of southern Tallapoosa and Chambers Counties as well as in the northwestern portion of Lee County. Although Bentley and others (in press) are able to separate the more felsic Waverly Gneiss from the Ropes Creek Amphibolite on a map scale in Lee County, felsic and mafic units are intercalated on an outcrop scale in the Tallassee synform (Fleming and others, 1980) and, thus, are grouped as a single unit in this paper.

As described by Stow and others (1984), a typical mafic member of this unit has a tholeiitic basaltic composition and occurs as an equigranular, fine-grained amphibolite which displays a conspicuous lineation and foliation defined by hornblende. Compositional banding is observed on a 5 to 10 cm scale. The felsic members are leucocratic, have a far more obvious, thicker gneissic banding and contain appreciable quartz. Massive, coarse-grained amphibolite occurs sporadically throughout the Ropes Creek Amphibolite. These rocks are considered to be the completely metamorphosed representatives of the Doss Mountain metanorite (see Mafic Complexes). Clastic material occurs sporadically and in small volume throughout the Ropes Creek Amphibolite in the Tallassee synform. Clark (1973) described garnet quartzites and quartzites as restricted horizons within the Ropes Creek Amphibolite 5 km to the east of Camp Hill.

**The Agricola Schist:** The Agricola Schist (Agricola schist-gneiss of Bentley and Neathery, 1970) is best exposed in the core of the Tallassee synform near Dadeville. This unit mainly consists of interlayered pelitic and quartzofeldspathic mica schists and gneisses. The schistose units are typically biotite- and muscovite-rich and weather to a light to medium red-brown saprolite. The gneisses are leucocratic, contain muscovite in excess of biotite, occasionally are kyanite- or sillimanite-rich, and display compositional banding in the range of 3 to 10 mm. Minor lithologies include amphibolite and micaceous quartzite.

**The Camp Hill Gneiss:** Intrusive into both the Agricola Schist and the Ropes Creek Amphibolite is the Camp Hill gneiss (Neilson, 1987). The gneiss is weakly foliated, coarse-grained, light gray in color, and characterized by the virtual absence of alkali feldspar, which gives this rock a tonalitic composition. Many specimens contain both biotite and primary muscovite, and some are garnet-bearing. A few samples contain hornblende in place of muscovite. Accessory minerals include sphene and epidote. Xenoliths of both the Ropes Creek Amphibolite and the Agricola Schist occur within this unit. The Camp Hill gneiss and the Chattasofka Creek gneiss are the Rock Mills-Camp Hill granite and gneiss of Bentley and Neathery (1970).

**The Chattasofka Creek Gneiss:** A second felsic gneiss occurs throughout the Tallassee synform. This gneiss is granitic in composition (Neilson, 1987). It is distinguished from the Camp Hill gneiss by the presence of abundant microcline and contains muscovite as a ubiquitous mineral. Xenoliths of both the Agricola Schist and Ropes Creek Amphibolite occur within the Chattasofka Creek gneiss. The relative ages of the two felsic units is unknown.

The felsic orthogneisses have many characteristics of mesozonal to catazonal intrusions (Buddington, 1959): they appear to be rootless bodies, are composed of foliated rocks, and display concordant contacts with the surrounding metasedimentary and metavolcanic sequences. No evidence of contact metamorphic effects due to these plutons has been seen.

**The Mafic Complexes:** The intimately intermixed sequence of amphibolite, metapyroxenite, metanorite, metagabbro and soapstone (the mafic complexes of Bentley and Neathery, 1970) has been examined in great detail within the Tallassee synform. Neilson and Stow (1986) considered that these complexes are plutonic and are the result of two episodes of mafic plutonic activity. Although both magmatic episodes predate the major dynamothermal event in this area, metamorphic effects are highly variable and rocks with relic igneous textures are common throughout the area.

Neilson and Stow (1986) divided these rocks into two suites: the Doss Mountain and Slaughters suites. The Doss Mountain suite consists of metaorthopyroxenite and metanorite and their foliated equivalents, actinolite schist and massive, coarse-grained amphibolite. The outcrop patterns of these rocks suggest that they occur as sills, layered intrusions and as dykes (Clark, 1973; Fleming and others, 1980; Neilson and Stow, 1986). The Slaughters suite consists of both olivine-bearing and olivine-free metagabbro. These rocks occur as small, concordant bodies that are considered to be younger than the Doss Mountain suite (Neilson and Stow, 1986). Contact metamorphic effects due to these plutons have been described by Clark (1973) and Brown and Cook (1981).

## Metamorphism

Neilson (1983) recorded evidence of two metamorphic events in these rocks. The earliest recognizable event ($M_1$) was prograde and broadly synchronous with the first regional deformational event. Distinctive assemblages such as kyanite-biotite-muscovite-garnet-plagioclase-quartz in the Agricola Schist

indicate Barrovian amphibolite facies metamorphism that was above the stability field of staurolite (Walls and Neilson, 1982). Sillimanite-bearing rocks are scattered throughout the area with kyanite and sillimanite coexisting in several samples.

A later retrograde metamorphic event ($M_2$) is recorded in some of the iron-rich pelites of the Agricola Schist. Large, helicitic porphyroblasts of chloritoid overprint a chlorite-muscovite-kyanite assemblage. The presence of chloritoid indicates upper greenschist facies of metamorphism. In addition, some metanorites of the Doss Mountain suite display a chlorite-tremolite assemblage which post-dates the hornblende foliation.

## Structure

Three episodes of folding are recognized within the Tallassee synform.

**Deformation $D_1$:** The earliest recognized deformational event generated isoclinal to tight, similar folds ($F_1$) on all scales. The mesoscopic folds are rootless, with amplitudes of less than 1 m and wavelengths in the order of 15 to 20 cm. The combined $D_1$-$M_1$ event generated the dominant structural fabric in these rocks, a well-defined foliation ($S_1$). This foliation parallels compositional banding ($S_0$) in the Agricola Schist and the Ropes Creek Amphibolite. A mineral lineation ($L_1$) is evident within the plane of the foliation. A plot of 50 $L_1$ and hinge line orientations (Figure 2a) shows a strong maximum which indicates $F_1$ axes plunging 20° to the northeast. A second concentration of fold axes with westerly to southwesterly plunges is the result of refolding of $F_1$ axes by the $D_3$ folding event.

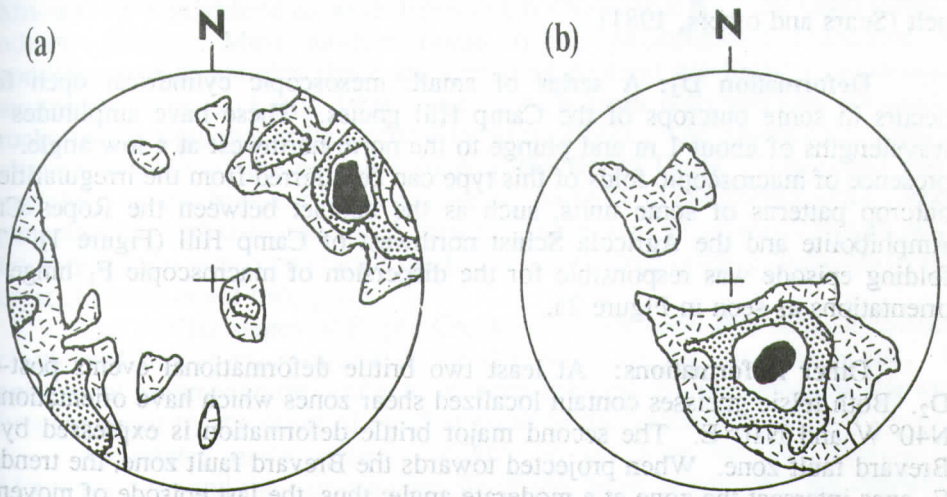


**Figure 2. Structural data from the Tallassee synform. (a) Plot of 50 $L_1$ and $F_1$ hinge line orientations: 0, 2, 4, 6% contours. (b) Plot of 248 poles to $S_1$: 0, 2, 4, 6% contours.**

Tight to isoclinal folds attributed to the $D_1$ event are seen on the map scale in the Tallassee synform. The axial traces of these folds are shown in Figure 1.

They are particularly well-developed in the area between Doss Mountain and Easton where the outcrop pattern of the Chattasofka Creek gneiss displays a series of hairpin folds (Figure 1). $F_1$ folds control the outcrop pattern in those areas where the fold geometry has not been greatly affected by later refolding; however, over most of the Tallassee synform the effects of $D_2$ and $D_3$ modify outcrop patterns to some extent.

**Deformation $D_2$:** The second deformational event generated macroscopic, moderately open folds. The trace of the axial surface of the largest of these folds, the Tallassee synform, is curved and passes through the map area from west of Walnut Hill, through Doss Mountain, to 4 km south of Dudleyville (Figure 1). Two smaller $F_2$ folds are recognized between Dadeville and Walnut Hill, but their axes cannot be traced through the Agricola Schist. A compilation of 248 poles to $S_1$ (Figure 2b) shows that the Tallassee synform has folded $S_1$. The smaller concentration of poles to $S_1$ on the NW limb of the fold is the result of limited data collection in the northwestern part of the field area. These data indicate that the synform plunges to the northeast at a low angle (10° to 20°). The effect of this folding episode on outcrop patterns is evident in the Walnut Hill area where both the Ropes Creek Amphibolite and a large sill of Doss Mountain metanorite are wrapped around the trace of the axis of the Tallassee synform (Figure 1). To the north of this area, in the vicinity of Lake Martin, the smaller $F_2$ synform and antiform also affect the outcrop pattern of the metanorite sill. The convergence of macroscopic $F_1$ fold axes about the trace of the Tallassee synform to the east of Dadeville illustrates the effect of $F_2$ on $F_1$ (Figure 1). In the Tallassee synform, $F_1$ and $F_2$ axes have subparallel orientations; thus the effect of later folding on the earlier fold axes is not as dramatic as seen in the southeastern part of the Dadeville belt (Sears and others, 1981).

**Deformation $D_3$:** A series of small, mesoscopic cylindrical open folds occurs in some outcrops of the Camp Hill gneiss. These have amplitudes and wavelengths of about 1 m and plunge to the north-northwest at a low angle. The presence of macroscopic folds of this type can be inferred from the irregularities in outcrop patterns of some units, such as the contact between the Ropes Creek Amphibolite and the Agricola Schist northwest of Camp Hill (Figure 1). This folding episode was responsible for the dispersion of macroscopic $F_1$ hinge line orientations as seen in Figure 2a.

**Other Deformations:** At least two brittle deformational events post-date $D_2$. Both felsic gneisses contain localized shear zones which have orientations of N40° W and N10° E. The second major brittle deformation is expressed by the Brevard fault zone. When projected towards the Brevard fault zone, the trends of $F_2$ axes intersect the zone at a moderate angle; thus, the last episode of movement on the Brevard fault zone appears to post-date $F_2$. Mylonitic textures are seen in many thin sections of the felsic gneisses, and members of the Ropes Creek Formation often display deformational twinning in plagioclase. These features have not been related to any of the episodes of deformation.

**Ages of Deformations:** According to regional tectonic models for the

Southern Appalachians (Hatcher and Odom, 1980; Williams and Hatcher, 1983), a series of mountain building events that included early thrusting and associated nappe formation, regional prograde metamorphism, granite magmatism, and ended with final movement along the Brevard fault zone began with the Taconic orogeny, continued through the Acadian orogeny and ended with the Alleghanian orogeny. Only K/Ar dates are available for rocks within the Dadeville belt. These give ages from 307 to 323 m.y. (Wampler and others, 1970) and probably indicate uplift. A Rb-Sr date from the Farmville pluton within the Opelika belt gives an age of 369 m.y. (Goldberg and others, 1985). This rock is an orthogneiss and has been folded by an $F_2$ fold that affects rocks within both the Dadeville and Opelika belts (Sears and others, 1981). Thus, the $D_1$-$M_1$ event is thought to be Acadian. According to Bittner and Cook (1987), $D_2$ was Alleghanian.

## DISCUSSION

### Tectonic Setting of the Dadeville Belt

As in most high grade metamorphic terrains, evidence for directions of younging is absent from the metasedimentary and metavolcanic units of the Dadeville belt. However, relative age data are available for the metaplutonic rocks. In the model of the evolution of the Dadeville belt prior to $D_1$ here proposed, the assumption is made that the Agricola Schist—which occupies the core of the Tallassee synform—is younger than the Ropes Creek Amphibolite.

The mafic members of the Ropes Creek Amphibolite have an E-MORB geochemical signature (Stow and others, 1984). Thus, the oldest rocks within the Dadeville belt record a period of rifting in which ocean floor basalts, lutites, and Mn- and Fe-rich sediments were deposited, probably in a back-arc basin (Stow and others, 1984). Most modern ocean rifting environments associated with convergent plate margins (back-arc spreading centers) are found in intra-oceanic arc-trench systems (Karig, 1974), and in such areas both volcanic and plutonic rocks of the ophiolite suite occur (Hawkins, 1977). The absence of mafic and ultramafic rocks of the ophiolite suite in the Ropes Creek Amphibolite may be explained by the back-arc basin developing partially in continental crust. Magma generated beneath the continental crust may have worked its way upwards along a fracture system which precluded the formation of large magma chambers in which crystallization could take place.

The waning stages of Ropes Creek volcanism coincided with an episode of clastic sedimentation, resulting in the deposition of the Agricola Schist. This episode of sedimentation could have been initiated by the uplift of the craton brought about by the onset of the first pulse of the Taconic orogeny.

Arc-related mafic igneous activity, in the form of the tholeiitic Doss Mountain suite and the calc-alkaline Slaughters suite, began after the cessation of Agricola sedimentation (Stow and others, 1984; Neilson and Stow, 1986). This activity generated the numerous small plutons of norite, orthopyroxenite, and gabbro now found within the Dadeville belt. Volcanic activity associated with these magmatic episodes is not preserved in the Dadeville belt. The onset of the Acadian orogeny saw the development of felsic plutonism, now represented by the Camp Hill and Chattasofka Creek gneisses.

## Comparison with the Inner Piedmont of Georgia and South Carolina

In the Inner Piedmont of South Carolina, Griffin (1971, 1974) recognized three sub-parallel zones: the northwestern flank, the Inner Piedmont core, and the southeastern flank. The boundaries between the core and its flanks were interpreted as tectonic slides. Amphibolite and amphibolite gneiss intercalated with granitoid gneiss dominate the rocks of the flanks, and small bodies of metamorphosed mafic and ultramafic rocks occur throughout the sequence. Biotite gneiss and micaceous quartzofeldspathic rocks are also present. These descriptions of the flanks are similar to descriptions of the Dadeville belt.

A strongly contrasting view of the geology of the Inner Piedmont and the Dadeville belt in particular was presented by Higgins and others (1984) for the Atlanta, Geogria area. They mapped the crystalline rocks as two stacks of folded thrust sheets: the Little River and Georgiabama thrust stacks. The Georgiabama stack consists of 11 thrust sheets that collectively contain rock units previously assigned to the Blue Ridge, Inner Piedmont and Pine Mountain window. Map patterns indicate that individual sheets are folded into large, open synforms and antiforms similar in style to the $D_2$ structures seen in the Alabama portion of the Dadeville belt. Recently they (Higgins and others, 1986) extended the thrust sheet model into the Alabama Piedmont.

It is difficult to reconcile the thrust sheet concept with the detailed mapping that has been done in the Alabama Inner Piedmont. For example, Sears and others (1981) showed that the "melange" at West Point Dam on the Chattahoochee River is not fault bound, yet this locality represents the West Point thrust sheet of Higgins and others (1984). In the Tallassee synform, my mapping (this paper, Figure 1) indicates that the thrust contacts shown by Higgins and others (1986, sheet 1) are not sheared, and they are interpreted by me to be either intrusive or depositional contacts. Shear zones within the Dadeville belt are interpreted as late stage extensional faults by Bittner and Cook (1987). An additional discrepancy lies in the relationship of the metaplutonic mafic and ultramafic rocks and the Ropes Creek Amphibolite. Near Atlanta, these metaplutonic rocks comprise the Soapstone Ridge thrust sheet which is structurally above the Ropes Creek Metabasalt, whereas in the Tallassee synform of Alabama, metagabbros, metaorthopyroxenites and metanorites are interpreted as sill-like intrusions into the Ropes Creek Amphibolite (Neilson and Stow, 1986).

## REFERENCES


Allison, C., & Neilson, M. J., 1981, A mafic-ultramafic complex near Easton, Tallapoosa Co., Alabama: Alabama Academy of Science Journal, v. 52, p. 120.

Bentley, R. D, & Neathery, T. L., 1970, Geology of the Brevard fault zone and related rocks of the Inner Piedmont of Alabama: Alabama Geological Society Guidebook, no. 8, p 1-76.

Bentley, R. D, & Neathery, T. L., & Scott, J. C., in press, Geology and Mineral Resources of Lee County, Alabama: Alabama Geological Survey Bulletin 107, 119 pp.

Bittner, E & Cook, R. B., 1987, Sequence and styles of deformation in the

Dadeville Complex of the Alabama Inner Piedmont: Geological Society of America, Abstracts with Programs, v. 19, no. 2, p. 76.
Brown, D. E. & Cook, R. B., 1981, Petrography of major Dadeville Complex rock units in the Boyds Creek area, Chambers and Lee Counties, Alabama: *in* Sears, J. W. ed., "Contrasts in tectonic style between Inner Piedmont terrane and the Pine Mountain window" Alabama Geological Society Guidebook, no. 18, p. 15-33.
Buddington, A. F., 1959, Granite emplacement with reference to North America: Geological Society of America Bulletin, v. 70, p. 671-747.
Clark, J. R., 1973, The petrology and geochemistry of the Seroyer Branch mafic-ultramafic complex, Chambers County, Alabama: M. S. Thesis, The University of Alabama, 85 pp.
Fleming, G., Nunan, A., & Neilson, M. J., 1980, A metamorphosed mafic-ultramafic pluton from the Dadeville Complex, Tallapoosa County, Alabama: Alabama Academy of Science Journal, v. 51, p. 201-202.
Goldberg, S. A., Burnell, J. R., & Fullagar, P. D., 1985, The Farmville Granite: a record of Acadian metamorphism in the Inner Piedmont of Alabama: Geological Society of America Abstracts with Programs, v. 17, no. 2, p. 93.
Griffin, V. S. Jr., 1971, The Inner Piedmont Belt of the Southern Crystalline Appalachians: Geological Society of America Bulletin, v. 82, p. 1885-1898.
Griffin, V. S. Jr., 1974, Analysis of the Piedmont in Northwest South Carolina: Geological Society of America Bulletin, v. 85, p. 1123-1138.
Hatcher, R. D. Jr., 1972, Developmental model for the Southern Appalachians: Geological Society of America Bulletin, v. 83, p. 1123-1138.
Hatcher, R. D. Jr., 1978, Tectonics of the western Piedmont and Blue Ridge, Southern Appalachians: review and speculation: American Journal of Science, v. 278, p. 276-301.
Hatcher, R. D. Jr., Butler, J. R., Fullagar, P. D., Secor, D. T., & Snoke, A. W., 1979, Geologic Synthesis of the Tennessee-Carolinas-northeast Georgia Southern Appalachians: *in* D. R. Wones. ed., "The Caledonides in the USA" I.G.C.P. Project 27, Caledonide Orogen Memoir 2, p. 83-90.
Hatcher, R. D. Jr. & Odom, A. L., 1980, Timing of Thrusting in the southern Appalachians, USA: model for orogeny?: Journal of the Geological Society of London, v. 137, p. 321-327.
Hawkins, J. W. Jr., 1977, Petrologic and Geochemical Characteristics of Marginal Basin Basalts: *in* M. Talwani & W. C. Pitman III eds, "Island Arcs, Deep Sea Trenches and Back-Arc Basins" American Geophysical Union, Maurice Ewing Series 1, p. 355-365.
Higgins, M. W., Atkins, R. L., Crawford, T. J., Crawford, R. F. III, & Cook, R. B., 1984, A brief excursion through two thrust stacks that comprise most of the crystalline terrane of Georgia and Alabama: Georgia Geological Society Guidebook 19th Annual Field Trip. 67 pp.
Higgins, M. W., Atkins, R. L., Crawford, T. J., Crawford, R. F., III, Brooks, R., & Cook, R. B., 1986, The structure, stratigraphy, tectonostratigraphy, and evolution of the southernmost part of the Appalachian orogen, Georgia and Alabamba: United States Geological Survey Open File Report, no. 86-372.
Karig, D. E., 1974, Evolution of arc systems in the western Pacific: Annual

Reviews of Earth and Planetary Sciences, v. 2, p. 51-57.
Knight, S. G., & Burnell, J. R., 1984, The Farmville Granite - an S-type Granite in the Alabama Inner Piedmont: Geological Society of America, Abstracts with Programs, v. 16, no. 3, p. 150.
Neathery, T. L., 1968, Talc and asbestos deposits in Tallapoosa and Chambers counties, Alabama: Geological Survey of Alabama Bulletin 90, 98 p.
Neilson, M. J., 1983, Structure and stratigraphy of the Dadeville Group within the Tallassee synform, Tallapoosa County, Alabama: Geological Society of America Abstracts with Programs, v. 15, no. 2, p. 110.
Neilson, M. J., 1987, The felsic gneisses of the Inner Piedmont: *in* Drummond, M.S. & Green, N.L. eds "Granites of Alabama" Alabama Geological Survey, Tuscaloosa, AL, p. 9-16.
Neilson, M. J., & Stow, S.H., 1986. Geology and geochemistry of the mafic and ultramafic intrusive rocks, Dadeville belt, Alabama: Geological Society of America Bulletin, v. 97, p. 296-304.
Sears, J. W., Cook, R. B., Jr, & Brown, D. E., 1981, Tectonic evolution of the western part of the Pine Mountain window and the adjacent Inner Piedmont Province: *in* Sears, J. W. ed., "Contrasts in Tectonic Style between the Inner Piedmont terrane and the Pine Mountain window.", Alabamba Geological Society Guidebook, no. 18, p. 1-14.
Stow, S. H., Neilson, M. J., & Neathery, T. L., 1984, Petrography, geochemistry, and tectonic significance of the amphibolites of the Alabama Piedmont: American Journal of Science, v. 284, p. 416-436.
Walls, I. A., & Neilson, M. J., 1982, Location of the kyanite-sillimanite isograd in the Tallassee synform, Dadeville complex, Tallapoosa County, Alabamba: Alabama Academy of Science Journal, v. 53, p. 52.
Wampler, J. M., Neathery, T. L., & Bentley, R. D., 1970, Age Relations in the Alabama Piedmont: in Bentley, R. D. and Neathery, T. L. eds, "Geology of the Brevard Fault Zone and related rocks of the Inner Piedmont of Alabama" Alabamba Geological Society Guidebook, no. 8, p. 81-90.
Williams, H., 1978, Tectonic Lithofacies Map of the Appalachian Orogen: Map 1. Memorial University of Newfoundland.
Williams, H., & Hatcher, R. D. Jr., 1983, Appalachian Suspect Terrains: *in* R. D. Hatcher, H. Williams, & I. Zietz, eds. "Contributions to the Tectonics and Geophysics of Mountain Chains" Geological Society of America Memoir 158, p.33-54.

# RE-EXAMINATION OF THE GOLD HILL SHEAR ZONE CABARRUS AND STANLY COUNTY AREA, SOUTHCENTRAL NORTH CAROLINA

GAIL G. GIBSON — *Mathematics and Science Education Center, UNC-Charlotte, Charlotte, NC 28223*

JOHN R. HUNTSMAN — *Department of Earth Sciences, UNC-Wilmington, Wilmington, NC 28403*

## ABSTRACT

The Gold Hill shear zone, extending northward into southcentral North Carolina as the boundary between the Charlotte belt (CB) and the Carolina slate belt (CSB), is characterized by northeast-trending, lenticular zones of highly sheared rocks within more extensive, northeast-trending, less sheared rocks. Lithologic characteristics of CSB strata are generally well preserved in areas of less strain within the shear zone. These characteristics correspond to those of the upper McManus Formation (Floyd Church Member) of the Albemarle Group, and the CSB stratigraphic sequence exposed in the western limb of the New London synclinorium continues essentially unbroken westward across the Gold Hill shear zone into the Charlotte belt.

Finite strain within the shear zone, as recorded by spacing of cleavage domains and changes in domain morphologies, demonstrates an overall, but not everywhere equal, increase in shearing intensity into the shear zone. Based on the reinterpretation of the stratigraphic sequence and the morphological variation in cleavages, the shear zone is interpreted as a localized area of greater strain at the boundary between the infrastructural Charlotte belt rocks and the volcaniclastic units of the Carolina slate belt, with no apparent major stratigraphic displacement across the zone.

## INTRODUCTION

The Gold Hill and Silver Hill faults form the northwestern and southeastern borders, respectively, of the northeast-striking Gold Hill shear zone (GHSZ). The GHSZ extends some 120 km into North Carolina from northern South Carolina and is recognized as the boundary between the igneous rocks and amphibolite-facies grade metamorphic rocks of the Charlotte belt, and the lower greenschist-facies volcaniclastic and sedimentary units of the Carolina slate belt (Figure 1).

Various genetic interpretations of the shear zone have been proposed and include: a) a narrow zone of high metamorphic gradient (Tobisch and Glover, 1971); b) a zone of high-angle reverse faulting (Laney, 1910); and c) a margin of a pull-apart basin (Moye and Stoddard, 1987). Secor and others (1986) suggest that the shear zone is part of the boundary between the infrastructural Charlotte belt (CB) rocks and the genetically related suprastructural sedimentary and

volcanic rocks of the Carolina slate belt (CSB). Williams and Hatcher (1982, 1983) interpreted the GHSZ as an internal feature within the Avalon terrane.

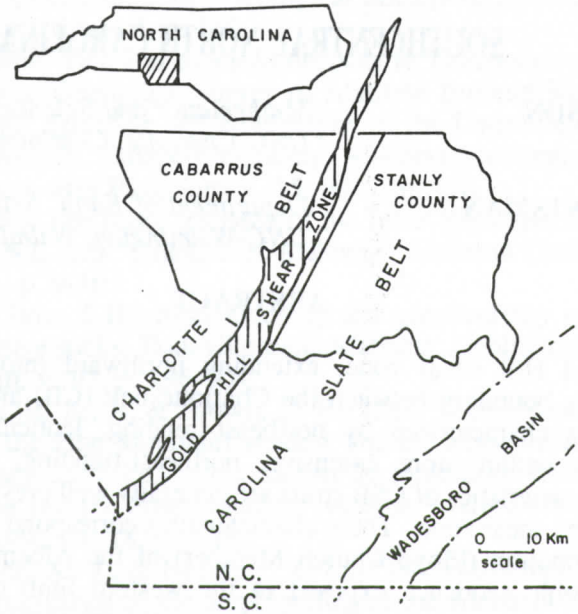


**Figure 1. Location of Gold Hill shear zone.**

Movement along the ductile to semi-brittle GHSZ occurred between 400 and 329 Ma, as constrained by post-faulting gold-bearing quartz veins within the shear zone, and the ages of relatively undeformed discordant plutons (Butler and Fullagar, 1978; Glover and others, 1983).

Discovery of Ediacarian fossils in the sedimentary sequence of the Carolina slate belt (Gibson and others, 1984; Teeter, 1983, 1984), in close proximity to the GHSZ, has spurred detailed stratigraphic analyses of the low-grade metasedimentary and metavolcanic rocks of the Albemarle Group (Gibson and Teeter, 1984; Gibson, 1985). An outgrowth of these studies has been the re-examination of the GHSZ and adjacent areas of the CSB and CB in Stanly and Cabarrus counties. Northwest-southeast transects from relatively undeformed CSB rocks through the central area of the GHSZ into the adjacent CB block not only examined the stratigraphic relationships, but were the basis for description and measurement of cleavage morphologies and cleavage densities within the deformed volcaniclastic strata.

This article presents new stratigraphic and structural data from the GHSZ and suggests additional interpretations of the structural significance of the shear zone.

## STRATIGRAPHY OF THE CAROLINA SLATE BELT, SOUTHCENTRAL NORTH CAROLINA

### Stratigraphic Characteristics of the Albemarle Group

Conley (1962) established mapping units within the CSB of southcentral

North Carolina in his pioneer stratigrahic work in the Montgomery and Stanly county area. Conley and Bain (1965) synthesized earlier geologic data for south-central North Carolina, formally named and described the slate belt units, and suggested a genetic relationship by including them in the Albemarle Group. Later workers have extended this terminology into immediately adjacent areas (Randazzo, 1972), while others have modified the stratigraphic terminology (Stromquist and Sundelius, 1969; Stromquist and others 1971; Sundelius and Stromquist, 1978; Milton, 1984). Several of the proposed stratigraphic terminologies from the CSB of southcentral North Carolina employ similar nomenclature (Figure 2), differing largely in the genetic interpretations and extent of the several lithofacies.

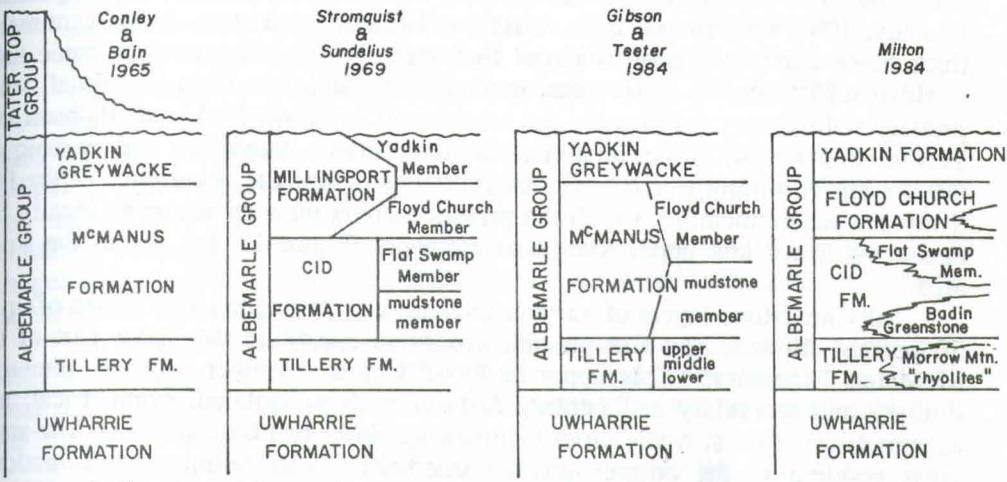


**Figure 2. Stratigraphic terminology for Albemarle Group, North Carolina.**

This discussion adopts the terminology established by Conley and Bain (1965) as modified by Gibson and Teeter (1984), and reflects the present authors' interpretation of the genetic relationships among the several units. This interpretation relates primarily to the McManus Formation, that in the area of the present study can be conveniently subdivided into two members that are in gradational or interfingering contact, and are bounded by the Tillery and Yadkin units. The Albemarle Group thus includes, in ascending order; the Tillery Formation, the McManus Formation, and the Yadkin Graywacke.

**Tillery Formation:** Laterally extensive pairs or couplets of light- and dark-colored laminations of siltstone and claystone characterize the Tillery Formation, which is the oldest of the Albemarle Group units. Many of the light-dark couplets exhibit normal grading. Three informal members are recognized in southcentral North Carolina (Figure 2).

Rippled and crossbedded sandstone, parallel laminated sandstone, and subaqueous debris flows, all with subordinate interbedded laminated claystone and siltstone couplets comprise the lower member of the Tillery Formation. Laminated couplets with minor thin interbeds of grain-supported crystal tuffs dominate the lithologies of the middle unit of the Tillery. This is the "characteristic" Tillery

described in most general works. Thicker and much more common intervals of fine-grained tuffaceous deposits characterize the upper Tillery. The contact between the Tillery and overlying McManus formations is gradational or interfingering.

**McManus Formation:** Two extensive members comprise the McManus formation in Stanly County (Gibson and Teeter, 1984). The lower or mudstone member (Cid Formation of Stromquist and Sundelius, 1969) consists of massively bedded and generally structureless mudstones. Noticeably absent from most of this member are the interbeds and interlaminations of rhythmically layered couplets so common in the Tillery. Other distinctive stratigraphic features of the lower member include extensive zones of volcanic tuffs of varied composition (Conley, 1962; Conley and Bain, 1965), and characteristic two- to six-centimeter thick black bands of denser material that appear to be compacted volcanic tuffs (welded tuffs?) and in some cases seem to have stylolitic textures. Small scale primary sedimentary features are not common in the lower McManus (Gibson and Teeter, 1984). At some localities, Milton (1984), Sundelius and Stromquist (1978), and Stromquist and Sundelius (1969) recognize the occurrence of the Flat Swamp volcanic member, which the present authors view as occurring locally between the lower and upper McManus members (Figure 2), but not in the study area.

Silty mudstone layers of varying thicknesses interbedded with layers of up to 50 percent siltstone and fine-grained sandstone constitute the upper part of the McManus Formation. This upper or Floyd Church Member contains numerous primary and secondary sedimentary features such as isolated, symmetrical, and asymmetrical ripples; ripple-cross laminations; flaser bedding; and very low-angle cross bedding in the coarser grained interbeds. Soft sediment deformational features are also common within this member (Gibson and Teeter, 1984; Gibson, 1985). Volcanic tuff layers within the Floyd Church Member are not as distinctive as those found in the mudstone member. The upper contact of the McManus with the overlying Yadkin Graywacke is gradational over approximately thirty meters.

**Yadkin Graywacke:** Poorly sorted, interbedded volcanic sandstones and siltstones characterize the Yadkin Graywacke. Common primary sedimentary features include ripple-cross laminations, various types of lenticular bedding, concordant and discordant ripples, dessication cracks, and rare bimodal cross laminations (Gibson and Teeter, 1984; Gibson, 1985). These lithologic and structural features distinguish the Yadkin Graywacke from other formations within the Albemarle Group.

**Igneous Units:** Numerous steeply dipping silicic and mafic dike- and sill-like bodies parallel the regional structural trend within the GHSZ (Sundelius and Stromquist, 1978). Igneous bodies with similar structural relationships and lithologic characteristics also occur along the eastern limb of the New London synclinorium (Conley and Bain, 1965). The stratigraphic and structural position and lithologic properties of these bodies suggests the possibility of stratigraphic correlations between the igneous rocks in these two areas.

## STRATIGRAPHY OF THE GOLD HILL SHEAR ZONE

Any interpretation of stratigraphic displacement across the Gold Hill shear zone necessitates identification of the stratigrahic units both within, and in the blocks adjacent to the shear zone. Previous work in the GHSZ by Sundelius and Stromquist (1978) described the host rock lithologies as follows:

> "Chiefly gray, white, pale-green, pink, and lavender thinly layered siltstone, and foliated phyllite and schist. Siltstone and phyllite are composed of quartz, feldspar, sericite and chlorite and lesser amounts of epidote, biotite, pyrite, and leucoxene after sphene. Schist occurs in small interbeds and lenses, composed of fine-grained chlorite, epidote, and plagioclase, that weather pale green and are derived from mafic volcanics; or occur as sericite schist that weathers white and is derived from felsic volcanics. Locally, tiny oval metacrysts occur in the planes of schistosity and probably are remnants of chloritoid."

Sundelius and Stromquist (1978) assigned the strata thus described within the Gold Hill shear zone to the Tillery Formation (Figure 3). East of the shear zone, they mapped lithologies that are here assigned to the Floyd Church Member of the McManus Formation. West of the fault zone, Stromquist and Sundelius (1978) mapped units that they considered equivalent to the lower or mudstone member of the McManus Formation of this report.

The North Carolina Geologic Map (1985) describes the rock units within the GHSZ as "...phyllite and schist — locally laminated and pyritic; includes phyllonite, sheared fine-grained metasediment, and metavolcanic rock." No formational status was assigned to any of these lithologies.

The authors' mapping of the deformed strata within the GHSZ in Cabarrus County reveals a dominance of sedimentologic and stratigraphic features characteristic of the upper or Floyd Church Member of the McManus Formation. None of the outcrops examined by the present authors are dominated by the light-dark colored siltstone and claystone couplets or laminations so characteristic of the Tillery Formation in southcentral North Carolina. Some weakly strained to highly strained massive mudstones within the shear zone exhibit the dark (tuffaceous?) layering characteristic of the lower McManus. However, the majority of recognizable strata within the shear zone, including that with relatively high strain, is composed of silty mudstones of the Floyd Church Member.

## STRUCTURAL FEATURES OF THE GOLD HILL SHEAR ZONE

### Background

Laney (1910) ascertained relative movement on the Gold Hill fault from scattered exposures of slickensides and minor subsidiary faults. Butler and Fullagar (1978) indicated that the average N 25° E trend of the GHSZ and its cleavage truncates earlier major folds and cleavages that strike between N 45° E and N 55° E. Cleavages related to shearing along the GHSZ obliterated earlier fold-related cleavages. Schroeder and Nance (1987) described mylonitic fabrics in a local area within the shear zone in Union County, and interpreted those to be

the result of Acadian discontinuous shearing under low (greenschist facies) metamorphic conditions.

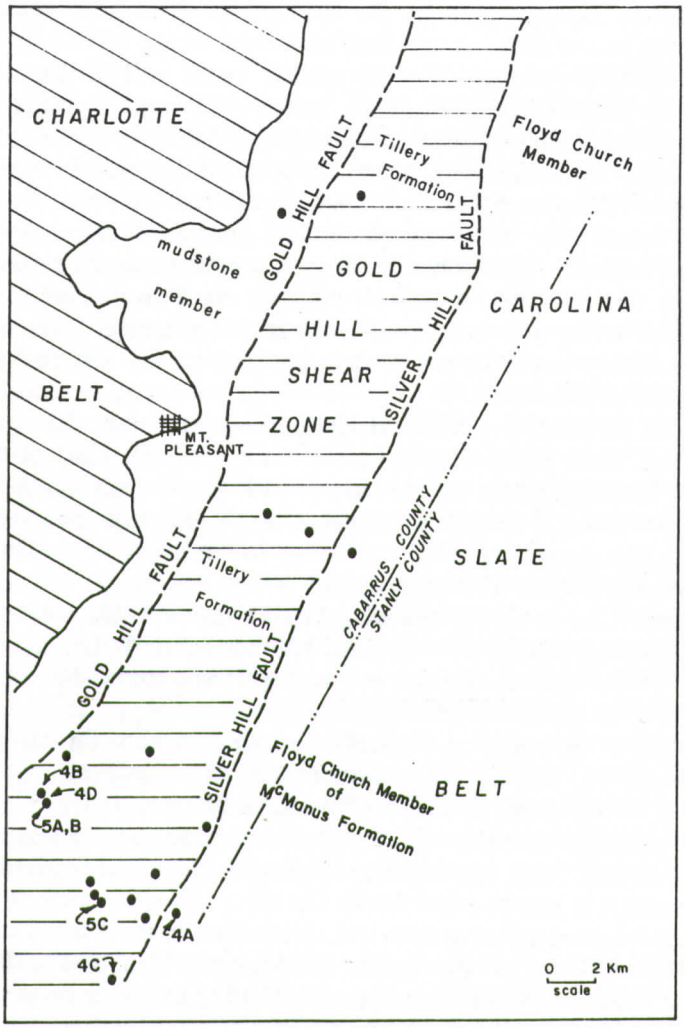


**Figure 3. Generalized geologic map of the Gold Hill shear zone and adjacent areas in Cabarrus and Stanly counties (adapted from Stromquist and Sundelius, 1978). Horizontal line pattern marks area of the shear zone. Slanting line pattern marks area of Charlotte belt igneous and metamorphic lithologies. Areas without line pattern, as well as GHSZ, contain Carolina slate belt, Albemarle Group lithologies; although GHSZ is generally considered as the boundary between and Charlotte belt and Carolina slate belt. *Compare map units with those of Figure 5.* Solid circles represent data points pertinent to this study and numbers refer to photograph locations in Figure 4.**

## Cleavage Data from the Present Study

The GHSZ in Cabarrus County consists of lenses of highly sheared rocks

interspersed within broader areas of less strained strata exhibiting well-preserved sedimentologic and stratigraphic features. All cleavages trend between N 30° E. and N 40° E. Overall, shearing becomes progressively less intense towards the boundaries of the shear zone and grades into adjacent, relatively undeformed country rocks. East of the shear zone, dips of undeformed strata are southeasterly towards the axis of the New London synclinorium. Within the shear zone, dips of strata are steep and variable, maintaining a general northwestward dip direction, in contrast to CSB regional southeasterly dip towards the axis of the New London synclinorium. Large scale folds and discrete fault surfaces are not present within exposures in the area examined.

Spaced cleavages in the CSB and the GHSZ are best described as disjunctive cleavages according to the classification presented by Borradaile and others (1982). Minor crenulation cleavages occur locally within the lenses of the highly strained rocks of the shear zone (Figure 4a). Disjunctive cleavage domains in all lithologies are rough to smooth and exhibit patterns that range from anastomosing (Figure 4b) to sinuous (Figure 4a) to planar (Figure 4c). Tuffaceous units typically have slightly narrower cleavage domains and microlithons than do the siltstones and mudstones.

Cleavage morphologies vary between the lenses of highly strained rock and the areas of lesser deformed host rock that comprise the GHSZ. Disjunctive cleavages within the lower-strained host rocks are zonal with discrete boundaries between domains whose width is relatively constant at one millimeter, and microlithons whose width is generally five to fifteen millimeters (Figure 4b). Disjunctive cleavages of the intensely sheared lenses are nearly continuous microlithons diminished in width to one millimeter or less (Figure 4c).

A pronounced crenulation cleavage transects sinuous to nearly continuous $S_1$ cleavages within the shear zone as discrete, northwest-dipping planar zones (Figure 4a, d). The strike of the crenulation cleavages is essentially parallel to that of the shear zone. In both plan and profile views, the crenulations demonstrate a subtle "S" shape suggestive of dextral shear (Figure 4a).

Outside the GHSZ, cleavage morphologies and densities are similar to those of the lesser-strained rocks within the shear zone. Cleavage spacings become wider with increasing distance away from the shear zone; microlithons approach two centimeters in width in relatively coarse-grained siltstones, and cleavage domains are reduced to discontinuous and overlapping zones of very thin, anastomosing to sinuous selvages (Figure 4b). Lapilli and crystals in tuffaceous units undergo a change in shape from subequant grains outside the GHSZ to flattened/sheared forms with length to width ratios of at least 10:1 inside the zone.

Characteristic changes in cleavage spacings and morphologies across the area examined in this study reflect an overall increase in strain from the CSB towards the GHSZ. Stratigraphic and sedimentologic features of the volcaniclastic rocks are preserved throughout the study area, except in those localized and discontinuous lenses of rock that contain the greatest strains within the shear zone; i.e., rocks that superficially resemble Tillery lithologies. Crenulation cleavages with strikes subparallel to the shear zone boundaries transect earlier cleavages with a dextral offset.

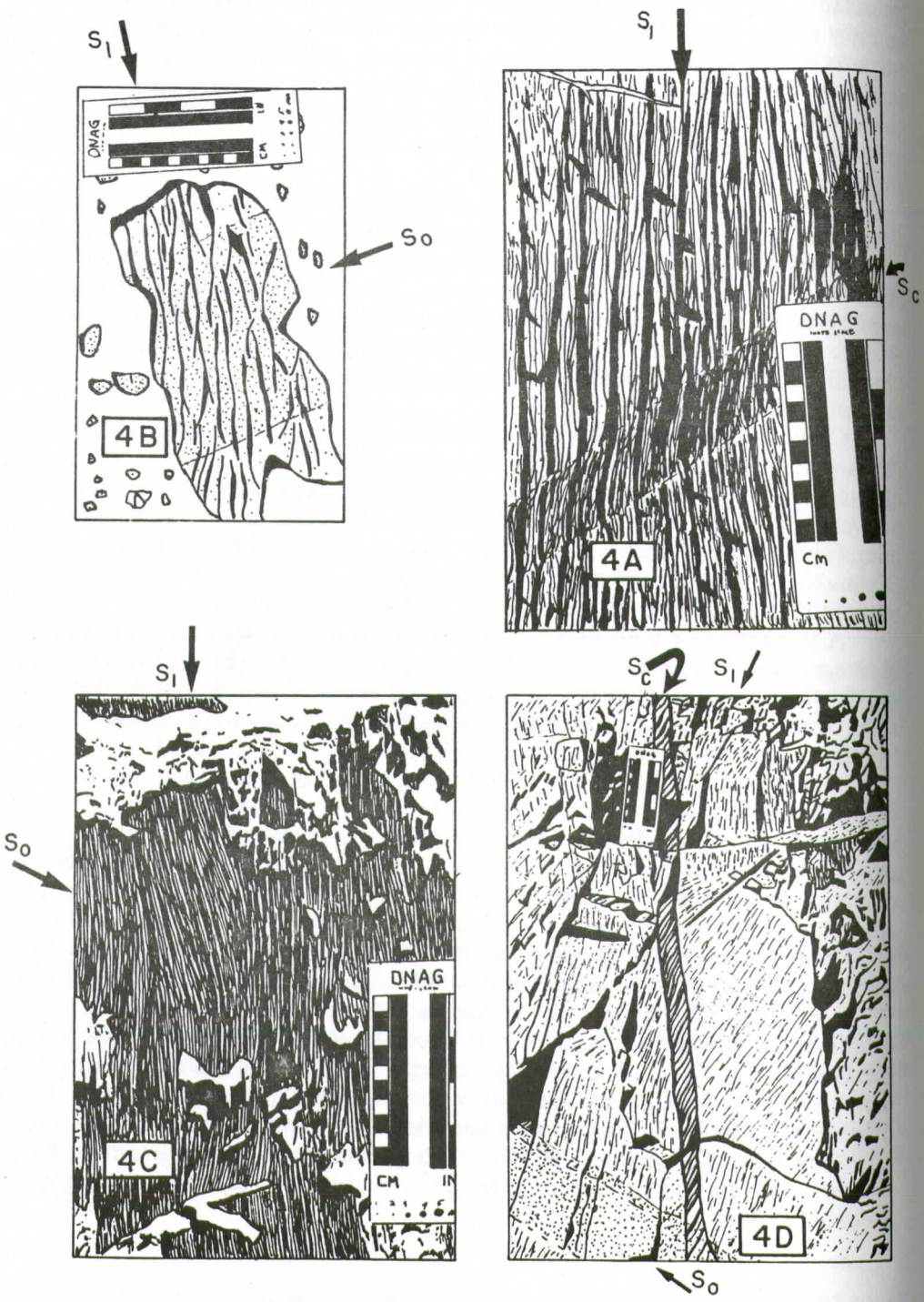
S1
So
4B
S1
Sc
4A
DNAG
Cm
S1
So
4C
DNAG
CM
IN
Sc
S1
4D
So

## DISCUSSION

Recognition of similar McManus lithofacies both within the GHSZ and in adjacent blocks (Figure 5) places constraints on the amount of stratigraphic displacement across the shear zone. This is in opposition to the Sundelius and Stromquist (1978) interpretation of a tectonically-emplaced sequence of stratigraphically lower Tillery lithologies between adjacent fault block units of upper McManus to the southeast and lower McManus to the northwest. This geometry would require a significant amount of stratigraphic throw across the zone. Laney (1910) concluded that the northwest side, i.e., Charlotte belt, was upthrown. This was based on available evidence from slickensides, attitudes of subsidiary faults, and the relatively higher regional metamorphic grade of the Charlotte belt.

However, our reinterpretation of the stratigraphic units, both within and adjacent to the shear zone, as McManus Formation along with the recognition of cleavage variability across the GHSZ suggests a different interpretation. Reconnaissance work immediately northwest of the shear zone has revealed sedimentary units with characteristics of the upper or Floyd Church Member of the McManus, rather that those of the lower or mudstone member. Thus, the stratigraphic succession across the GHSZ appears to represent a logical continuation of that on the western limb of the New London synclinorium-Denton anticlinorium, locally modified by cleavage. Regional mapping of the Tillery Formation in eastern Stanly and adjacent Montgomery counties further substantiates the hypothesis that the GHSZ corresponds to the deformed western limb of a northeastward-plunging anticline.

Relatively little vertical stratigraphic displacement is required to explain relationships present across the zone. The extension of McManus lithologies from the CSB into the GHSZ and westward into the immediately adjacent part of the Charlotte belt, with no apparent significant break in stratigraphic continuity, supports the Secor and others (1986) interpretation that the CSB is the suprastructural extension of the Charlotte belt.

**Figure 4. Representative cleavages from the GHSZ and CSB of Cabarrus County: 4a) Vertical profile (looking 'down-plunge' towards the northeast) of a crenulation cleavage band ($S_c$) transecting very closely spaced sinuous cleavage ($S_1$) in McManus Formation within GHSZ. Note dextral offsets of $S_1$ by $S_c$. Strike of $S_c$ is subparallel to the strike of the GHZS. Locality 4B, Fig. 3, 5. Ink tracing of photograph. 4b) Discontinuous and widely spaced, sinuous to anastomosing cleavage ($S_1$) transecting bedding ($S_0$) in coarse-grained siltstone of the McManus Formation southeast of the GHSZ. Locality 4A, Figure 3, 5. Ink tracing of photograph. 4c) Vertical profile (towards the northeast) of continuous, very closely spaced and nearly planar cleavage ($S_1$) transecting bedding ($S_0$) of McManus Formation within the GHSZ. Note the more continuous character of the cleavage and the thinning of the microlithons between the cleavage selvages as compared to 4a (above). Locality 4D, Figure 3, 5. Ink tracing of photograph. 4d) Vertical profile (towards the southwest) of narrow band of crenulation cleavage ($S_c$) transecting bedding ($S_0$) and sinuous cleavage ($S_1$) in McManus Formation. Sense of relative offset along crenulation band is similar to that of 4b (above). Locality 5C, Figures 3, 5. Ink tracing of photograph.**

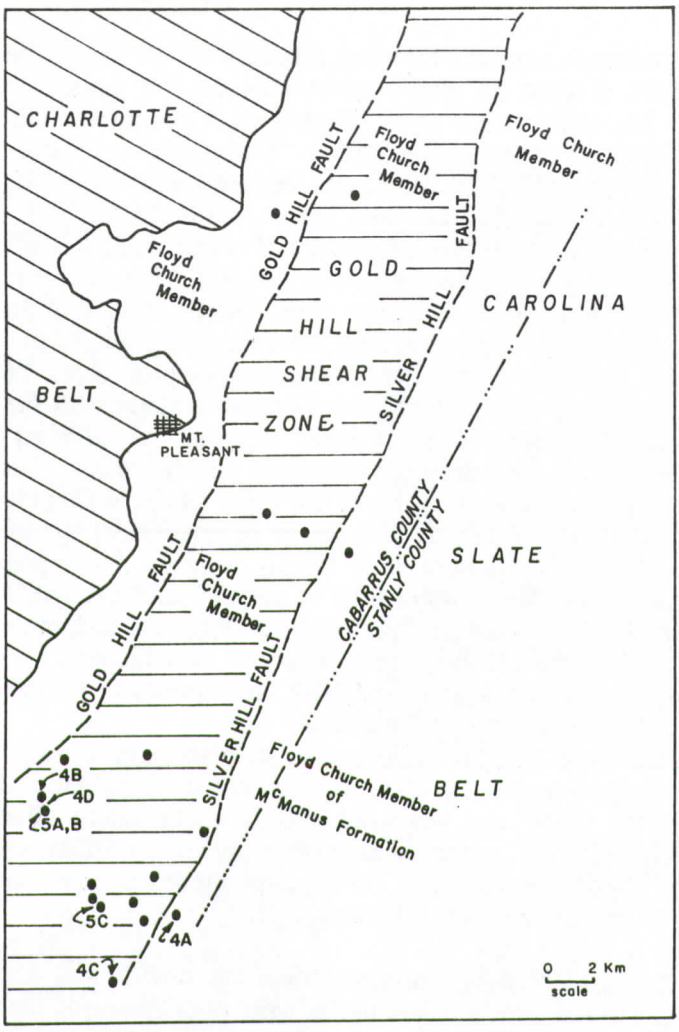


**Figure 5. Generalized geologic map of the Gold Hill shear zone and adjacent areas of Cabarrus and Stanly counties, illustrating recently recognized stratigraphic relationships. Horizontal line pattern marks area of shear zone. Slanting line pattern marks area of Charlotte belt igneous and metamorphologic lithologies. Areas without line patterns, as well as GHSZ, contain Albemarle Group McManus Formation facies. *Compare map units with those of Figure 3.* Solid circles represent locations of data points pertinent to this study, and numbers correspond to photographs in Figure 4.**

The structural fabric of the GHSZ and adjacent parts of the Cabarrus and Stanly county areas reflects that of a relatively high-angle dextral shear zone (Figure 6). A similar interpretation was made by Schroeder and Nance (1987) based on mylonites in the GHSZ of Union County, to the south.

Given the apparent lack of major stratigraphic displacement across the shear zone, we concur with the interpretation that the GHSZ represents a localized area

relatively steeper metamorphic gradient and marks the border between the Charlotte and Carolina slate belts in this region. The GHSZ may represent an outermost region of a terrane(?) that accommodated Acadian ductile shear within the Piedmont of the Carolinas (Glover and others, 1983).

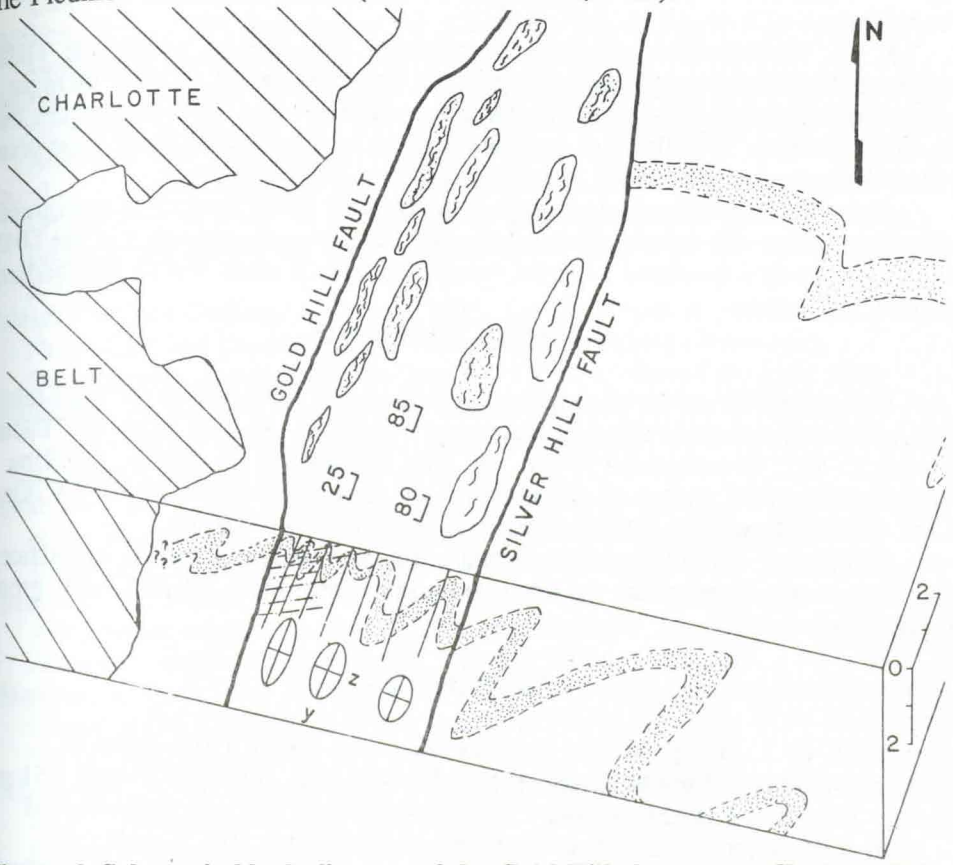


**Figure 6. Schematic block diagram of the Gold Hill shear zone. Charlotte Belt — diagonally ruled; Carolina slate belt — blank; hypothetical marker within the Floyd Church — stippled. Strain ellipses in profile view oriented with Y axis vertical and Z axis horzontal; orientation of Y tentatively supported by highly weathered linear fabrics. Wavy lines in podiform areas of plan view indicate areas of anomalous strain. NOTE: Steep $S_1$ cleavage overprinted by gently-dipping $S_2$ cleavage near the western border of the shear zone. Age of $S_1$ cleavage is 455- 465 Ma (Noel and others, 1988). Vertical and horizontal scales in kilometers. Strike and dip symbols indicate representative attitude values of higher angle $S_1$ cleavage and lower angle $S_2$ overprint cleavage.**

## CONCLUSIONS

Several conclusions can be drawn from the data presented above:

1. — The stratigraphic units *within* the GHSZ in Cabarrus County belong primarily to the Floyd Church Member of the McManus Formation, and not the stratigraphically lower Tillery Formation as proposed by Sundelius and Stromquist

(1978). Lithologic similarities between the units cropping out in the GHSZ and the Tillery Formation of eastern Stanly County do not exist;

2. — Exposed CSB lithofacies west of the GHSZ are characteristic of the upper McManus rather than of the lower or mudstone member of the McManus Formation;

3. — Variations in cleavage morphology and density within the GHSZ delineate distinct zones of intensely cleaved material, and a relative increase in strain towards the central part of the zone, from undeformed strata in adjacent fault blocks (Figure 6). Locally high densities of cleavages within the shear zone create Tillery-like appearances in the massive McManus lithologies; and

4. — Given the present stratigraphic interpretation, the amount of stratigraphic separation across the shear zone is relatively insignificant, requiring that the GHSZ be interpreted as a localized zone (of Acadian?) dextral shear within the Piedmont of the Carolinas.

## ACKNOWLEDGMENTS

JRH gratefully acknowledges partial defrayment of expenses for field-related research in this region through Research Grant No. 85-017 from the Faculty Research and Development Fund of the University of North Carolina at Wilmington. GGG wishes to acknowledge the financial support from NSF (Grant EAR 84-02903) and the UNCC Faculty Research Grant Program.

In addition, the authors wish to thank Mr. Steven Teeter for his assistance in the field. The comments of the reviewers were most helpful and greatly appreciated.

## REFERENCES

Borradaile, G. J., Bayly, M. M., and Powell, C. M. (eds.), 1982, Atlas of deformational and metamorphic rock fabrics: Berlin, Springer-Verlag, 551 p.

Butler, J. R., and Fullagar, P. D., 1978, Petrochemical and geochronological studies of plutonic rocks in the southern Appalachians: III. Leucocratic adamellites of the Charlotte belt near Salisbury, North Carolina: Geological Society of America Bulletin, v. 89. p. 460-466.

Conley, J. F., 1962, Geology of the Albemarle quadrangle, North Carolina: North Carolina Department of Conservation and Development, Division of Mineral Resources Bulletin 75, 26 p.

Conley, J. F., and Bain, G.L., 1965, Geology of the Carolina slate belt west of Deep River-Wadesboro Triassic basin, North Carolina: Southeastern Geology, v. 6, p. 117-138.

Gibson, G. G., 1985, Sedimentary structures of the Late Precambrian Albemarle Group, Carolina slate belt, southcentral North Carolina: Geological Society of America Abstracts with Programs, v. 17, p. 92.

Gibson, G. G., and Teeter, S. A., 1984, A stratigrapher's view of the Carolina slate belt, southcentral North Carolina: Carolina Geological Society 1984 Fieldtrip Guidebook, 43 p.

Gibson, G. G., Teeter, S. A., and Fedonkin, M. A., 1984, Ediacarian fossils from the Carolina slate belt, Stanly County, North Carolina: Geology, v. 12, p. 387-390.

Glover, L., III, Speer, J. A., Russell, G. S., and Farrar, S. S., 1983, Ages of regional metamorphism and ductile deformation in the central and southern Appalachians: Lithos, v. 16, p. 223-245.

Laney, F. B., 1910, The Gold Hill mining district of North Carolina, North Carolina Geological and Economic Survey Bulletin 21, 137 p.

Milton, D. J., 1984, Revision of the Albemarle Group, North Carolina: U. S. Geological Survey Bulletin 1537-A, p. A69-A72.

Moye, R. J., Jr., and Stoddard, E. F., 1987, The Albemarle basin: a wrench fault pull-apart in the slate belt of North Carolina: Geological Society of America Abstracts with Programs, v. 19, p. 119-120.

Noel, J. R., Spariosu, D. J., and Dallmeyer, R.D., 1988, Paleomagnetism and $_{40}Ar/_{39}Ar$ ages from the Carolina slate belt, Albemarle, North Carolina: Implications for terrane amalgamation with North America: Geology, v. 16, p. 64-68.

North Carolina Geological Survey, 1985, Geologic map of North Carolina: North Carolina Department of Natural Resources and Community Development, Raleigh, North Carolina, 1 Sheet, colored geologic map.

Randazzo, A. F., 1972, Petrography and stratigraphy of the Carolina slate belt, Union County, North Carolina: North Carolina Division of Mineral Resources Special Publication 4, 38 p.

Schroeder, K. E., and Nance, R. D., 1987, Mylonite-hosted gold mineralization at the Howie mine, Union County, North Carolina: Geological Survey of America Abstracts with Programs, v. 19, p. 128.

Secor, D. T., Snoke, A. W., and Dallmeyer, R.D., 1986, Character of the Alleghanian orogeny in the southern Appalachian: III. Regional tectonic relations: Geological Society of America Bulletin, v. 97, p. 1345-1353.

Stromquist, A. A., and Sundelius, H. W., 1969, Stratigraphy of the Albemarle Group of the Carolina slate belt in central North Carolina: U. S. Geological Survey Bulletin 1274-B, p. 1-22.

Stromquist, A. A., Choquette, P. W., and Sundelius, H. W., 1971, Geologic map of the Denton quadrangle, central North Carolina: U. S. Geological Survey Geologic Quadrangle Map GQ-872.

Sundelius, H. W., and Stromquist, A. A., 1978, Interpretative geologic map of the bedrock, Mount Pleasant quadrangle, Cabarrus and Stanly Counties, North Carolina: U. S. Geological Survey Miscellaneous Investigations Series Map I-1082.

Teeter, S. A., 1983, New trilobite(?) locality from the Carolina slate belt, Stanly County, North Carolina: Journal of the Elisha Mitchell Scientific Society, v. 99, p. 178.

Teeter, S. A., 1984, *Pteridinium* from the Carolina slate belt, Stanly County, North Carolina: Geological Society of America Abstracts with Programs, v. 16, p. 66.

Tobisch, O. T., and Glover, L., III, 1971, Nappe formation in part of the southern Appalachian Piedmont: Geological Society of America Bulletin, v. 82, p. 2209-2230.

Williams, H., and Hatcher, R. D., Jr., 1982, Suspect terranes and accretionary history of the Appalachian orogen: Geology, v. 10, p. 530-536.

Williams, H., and Hatcher, R. D., Jr., 1983, Appalachian suspect terranes: *in*,

Hatcher, R.D., Jr., Williams, H., and Zietz, I. (eds.), Contributions to the Tectonics and Geophysics of Mountain chains, Geological Society of America Memoir 158, p. 33-54.